# A Novel Perfusion Imaging Strategy for the Ischaemic Limb

Bajwa, Adnan Ahmad

*Awarding institution:*
King's College London

# A Novel Perfusion Imaging Strategy for the Ischaemic Limb

**Adnan Ahmad Bajwa**

**Thesis submitted for the degree of**
**Doctor of Philosophy**
**2018**

**Academic Department of Surgery**
**King's College London**
**School of Medicine**
**Cardiovascular Division**
**St Thomas' Hospital**
**1st Floor North Wing**
**Westminster Bridge Road**
**London, SE1 7EH**

**In memory of Nadim**

# Statement of originality

The work contained in this thesis is my own original work, except where acknowledged in the text.

# Acknowledgments

I would like to thank my supervisors, Mr Bijan Modarai and Professor Alberto Smith, for their unrivalled support and guidance throughout my research. I am indebted to them for their advice and encouragement in pursuing an academic path and for the skills and expertise that I have gained. They have shown true kindness and professionalism when I have needed it most, and encouraged me to achieve more than I could have ever imagined before starting on this journey.

I am extremely grateful for the assistance, advice and guidance of our collaborators, Professor Eike Nagel and Dr Roman Wesolowski. Their expertise in perfusion MRI was invaluable for this project. Professor Nagel provided expert opinion on how to develop this project. Roman, I am so grateful for the long days and nights you spent helping develop the different MRI sequences, and also you expertise in MATLAB to develop and write the analysis software.

The staff in the Academic Department of Vascular Surgery were vital in helping me develop the project. I am particularly indebted to Ashish Patel, Prakash Saha and Mohammad Ikram for answering my stupid questions and showing me the ropes in research. I would also like to thank the Vascular Surgery Unit at Guy's & St Thomas' Hospital, for allowing me to recruit the patients under their care and for letting me continue my clinical training.

I would like to thank the all the people who agreed to participate in this study, allowing me to search for the answers to an ever-increasing clinical problem.

I am extremely grateful for the invaluable financial support from the British Heart Foundation and the Circulation Foundation, without whom this project would not have been possible.

I would like to thank my parents for raising me and providing me an education that has allowed me to achieve so much more then I could have ever thought possible. You raised 4 boys, and showed them love, patience, kindness and the desire to never rest on our laurels.

My wife Farrah, and the twins, Zakariya and Aleena have had to endure the biggest sacrifice. They have had to do without me when I worked the long hours; they had to support each other and me. This is all for you and without you this would mean nothing.

Finally, this thesis is dedicated to my brother and best friend Nadim, who passed away at a young age from cardiovascular disease. You showed me drive and determination; you showed my happiness and joy; you showed me kindness and patience; you made sure I enjoy everyday to the most. Rest in peace.

# Abstract

Current assessment of peripheral arterial disease (PAD) is focused on delineating luminal narrowing or obstruction in the major lower limb blood vessels. The imaging modalities used do not provide information on the microcirculation or muscle perfusion in the affected limb, the most important determinants of limb salvage in patients with PAD. An objective, non-invasive method for measuring and mapping muscle perfusion would aid diagnosis in PAD. It would may also inform planning of revascularisation strategies and better determine success after revascularization, ultimately improving limb salvage.

Blood Oxygenation Level Dependent Magnetic Resonance Imaging (BOLD-MRI) is a technique that has been used to measure perfusion in the brain, kidneys and heart. The utility of BOLD-MRI in the lower limb musculature has, to date, been limited by a lack of sensitivity and reproducibility.

The present study aimed to develop BOLD-MRI as an objective and reproducible tool for measuring perfusion in the calf musculature. The calf was imaged at 3 Tesla in young healthy controls, age-matched controls, and patients with critical limb ischaemia (CLI). A cuff placed around the thigh was used during the scan to provoke hyperaemia. T2* Signal intensity time curves were generated for each muscle group and curve parameters, including signal

reduction during ischemia (SRi) and gradient during reactive hyperaemia (Grad). BOLD-MRI was also used to assess changes in perfusion following revascularization in CLI patients. Muscle biopsies, obtained at the level of BOLD-MRI measurement and from healthy proximal muscle of patients undergoing lower limb amputation were analysed for capillary:fibre (C:F) ratio.

Good interuser and interscan reproducibility was found for Grad and SRi. The ischaemic limb had lower Grad and SRi compared with the contralateral asymptomatic limb, age-matched controls, and young controls. Successful revascularisation consistently resulted in significant improvement in both Grad and SRi. There was a significant correlation between C:F ratio in muscle biopsies from amputated limbs and Grad measured preoperatively at the corresponding level.

These data suggest that BOLD-MRI holds promise as a reliable tool for assessing perfusion in the lower limb and may allow refinement of current treatment algorithms. Its utility merits further investigation in a multi-centre clinical trial.

# Table of Contents

## Index of Figures

### CHAPTER 1



### CHAPTER 2



### CHAPTER 3

**CHAPTER 4**



**CHAPTER 5**



**CHAPTER 6**

## Index of Tables

### CHAPTER 1



### CHAPTER 4



### CHAPTER 5

**List of Abbreviations**

| | |
|---|---|
| ABPI | Ankle Brachial Pressure Index |
| AIF | Arterial Input Function |
| AKA | Above Knee Amputation |
| ASL | Arterial Spin Labelling |
| BKA | Below Knee Amputation |
| $B_0$ | External Magnetic Field |
| BOLD | Blood Oxygenation Level Dependent |
| BP | Blood Pressure |
| BSA | Bovine Serum Albumin |
| CASL | Continuous Arterial Spin Labelling |
| CEUS | Contrast Enhanced Ultrasound |
| C:F | Capillary:Fibre Ratio |
| CFA | Common Femoral Artery |
| CIA | Common Iliac Artery |
| CIN | Contrast Induced Nephropathy |
| CLI | Critical Limb Ischaemia |
| CT | Computed Tomography |
| CTA | Computed Tomography Angiography |
| DCE | Dynamic Contrast Enhanced |
| EIA | External Iliac Artery |
| EPI | Echo Planar Imaging |
| ETL | Echo Train Length |

| | |
|---|---|
| FA | Flip Angle |
| FCS | Foetal Calf Serum |
| FFR | Fractional Flow Reserve |
| FOV | Field of View |
| GE-EPI | Gradient Echo – Echo Planar Imaging |
| Grad | Gradient |
| GRE | Gradient Echo |
| IADSA | Intra-arterial Digital Subtraction Angiography |
| IC | Intermittent Claudication |
| ICC | Interclass Correlation Coefficient |
| ICGA | Indocyanine Green Fluorescence Angiography |
| IIA | Internal Iliac Artery |
| LDF | Laser Doppler Flowmetry |
| LDI | Laser Doppler Imaging |
| MRA | Magnetic Resonance Angiography |
| MRI | Magnetic Resonance Imaging |
| NHS | National Health Service |
| NICE | National Institute for Clinical Excellence |
| NSF | Nephrogenic Systemic Fibrosis |
| PASL | Pulsed Arterial Spin Labelling |
| PAD | Peripheral Arterial Disease |
| PBS | Phosphate Buffered Saline |
| pCASL | Pseudo-Continuous Arterial Spin Labelling |
| PET | Positron Emission Tomography |
| PHF | Peak Hyperaemic Flow |

| | |
|---|---|
| PSV | Peak Systolic Velocity |
| PTA | Percutaneous Transluminal Angioplasty |
| PTFE | Polytetrafluroethylene |
| RF | Radiofrequency |
| ROI | Region of Interest |
| SD | Standard Deviation |
| SE | Spin Echo |
| SFA | Superficial Femoral Artery |
| SPECT | Single Positron Emission Computed Tomography |
| SRi | Signal Reduction during Ischaemia |
| TcPO2 | Transcutaneous Oxygen Pressure |
| TASC | Trans-Atlantic Inter-Society Consensus |
| TE | Time to Echo |
| THIM | Time to Half Ischaemia |
| TR | Time to Repeat |
| TTP | Time to Peak |
| T2*Max | Maximum T2* |
| T2*Min | Minimum T2* |
| VOP | Venous Occlusion Plethysmography |
| XMR | Interventional Magnetic Resonance |
| 2D | 2-Dimensional |
| 3D | 3-Dimensional |

# CHAPTER 1

# General Introduction

## 1.1 Peripheral arterial disease

### 1.1.1 Natural History, Epidemiology and Risk Factors

Peripheral arterial disease (PAD), most commonly caused by atherosclerosis, is a condition that can lead to a severe restriction of blood flow in the arteries to the lower limb[1] (Figure 1.1). Most individuals with PAD are asymptomatic[2] with the remainder developing intermittent claudication (IC) or critical limb ischaemia (CLI). The former refers to a condition characterised by pain in the limb that the patient experiences when walking, and is relieved by rest. The latter produces pain at rest, ulceration or gangrene and is associated with high morbidity and mortality. Up to 25% of patients eventually lose a limb[3]. Patients with PAD, irrespective of symptoms, have an increased risk of myocardial infarction and stroke, and are 6-times more likely to die within 10years[4]. This condition represents a growing global healthcare problem, and is estimated to affect 27 million people in Europe and North America[5]. The burden of PAD is likely to increase over the coming years as a result of ageing and increased life expectancy, improved treatment of coronary artery disease and increasing prevalence of diabetes.

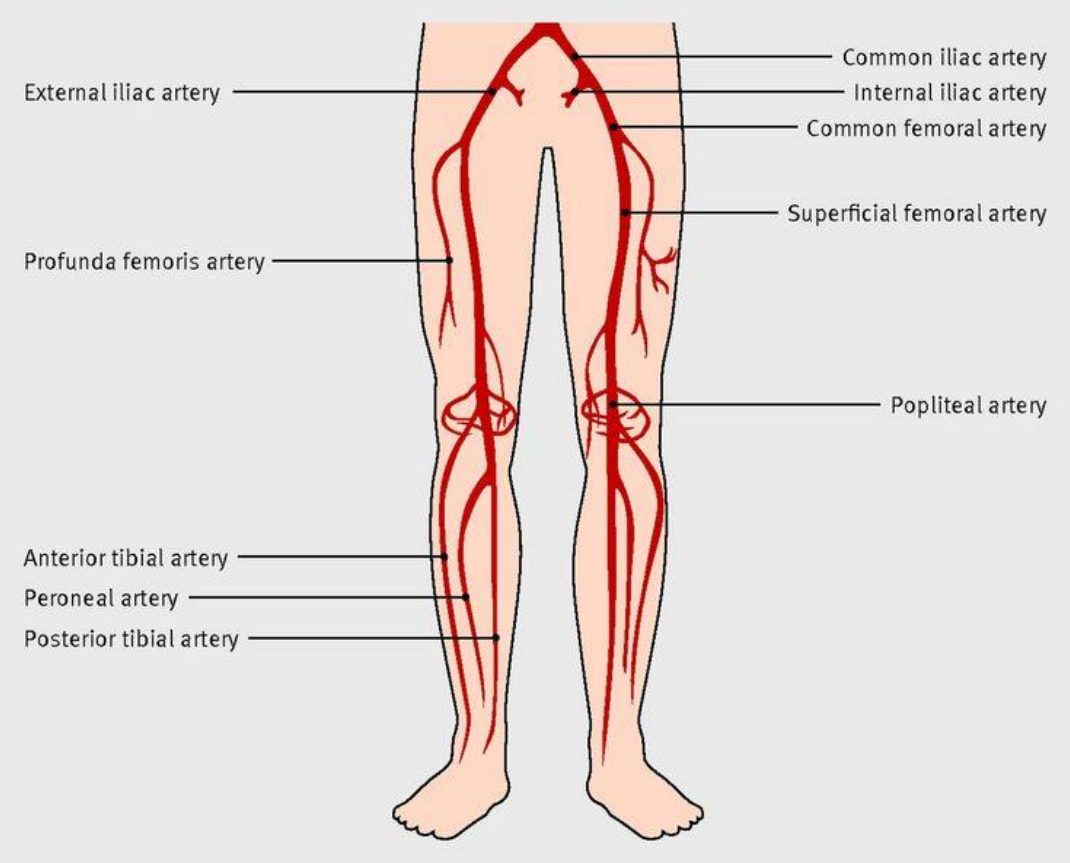


**Figure 1.1: Anatomy of the arteries supplying the lower limb (from Peach et al.[6])**

### *Natural History*

PAD is a progressive disease presenting with a spectrum of signs and symptoms. Most individuals with PAD are asymptomatic[2,7] with the remainder developing IC or CLI. It is estimated that up to one third of patients with PAD present with IC. Most patients with IC remain stable with only 5-10% deteriorating to CLI. CLI is associated with poor outcomes with nearly a quarter of patients dead at 1 year and up to 30% of patients losing a limb[1,3].

Atherosclerosis affects any arterial territory, including the coronary and cerebral circulation, and therefore these patients also have increased risk of coronary

artery and cerebrovascular morbidity and mortality[1,3–5,8,9]. Therefore patients with PAD, irrespective of symptoms, have an increased risk of myocardial infarction and stroke, and are 6-times more likely to die within 10years[4]. The natural history and outcomes in patients with PAD are highlighted in figure 1.2.

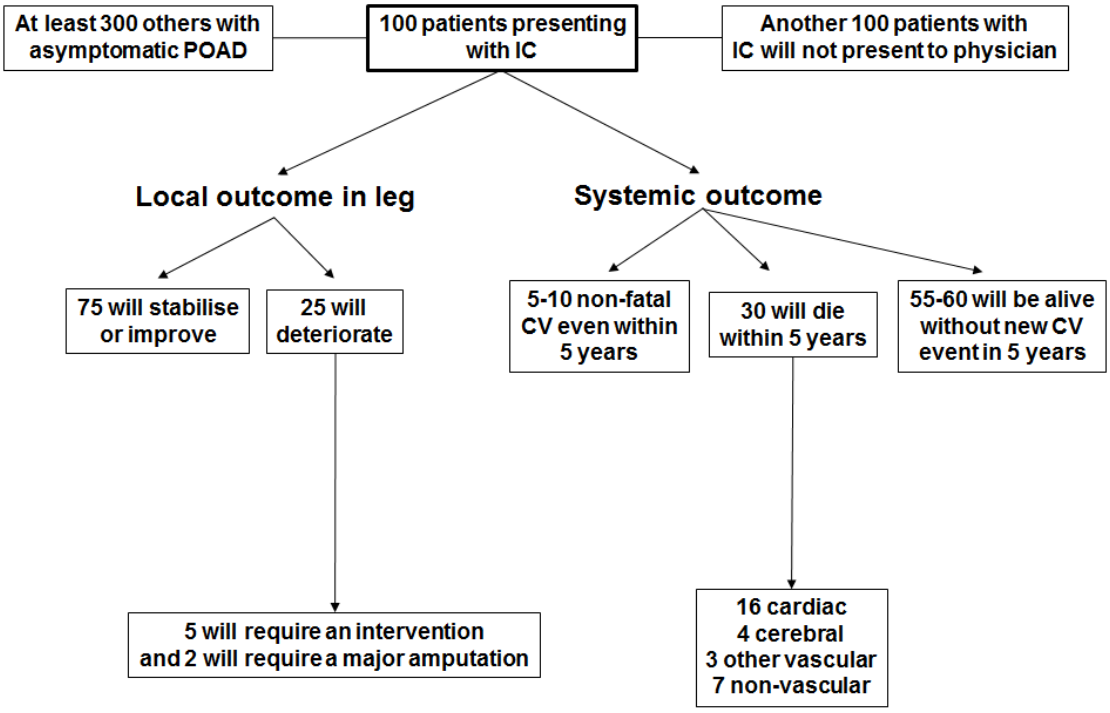


**Figure 1.2: Five-year fate of patients with intermittent claudication (modified from Norgren et al.[3]).**

### *Epidemiology*

Several epidemiological studies have attempted to define the incidence and prevalence of PAD in the general population. The difficulty has been in recruiting a true representative cohort of the general population to be able to define the incidence and prevalence. It is estimated that the prevalence of asymptomatic PAD is in the region of 7-15%[7,10], however, given the difficulties in investigating a truly representative population the incidence and prevalence is likely to be to higher. One aspect that seems certain is that the prevalence of PAD increases with age (Figure 1.3).

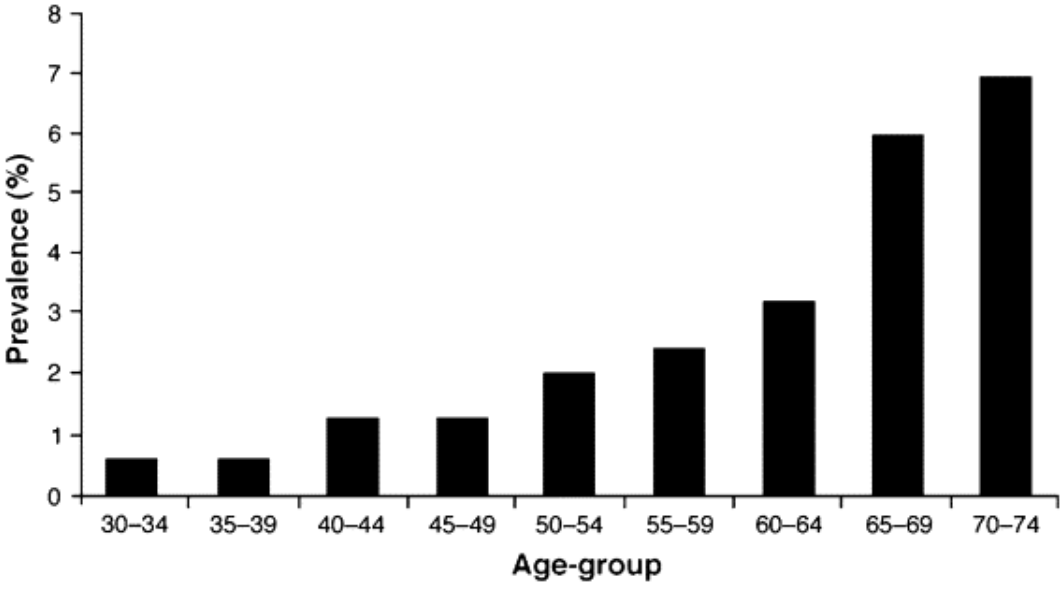


**Figure 1.3: Mean prevalence of intermittent claudication in large population based studies (from Norgren et al.[3]).**

### *Risk Factors*

Atherosclerotic plaque formation in the arteries most commonly causes PAD. Factors that have been identified that accelerate plaque formation include older age (>40 years), hyperlipidaemia, hypertension, diabetes mellitus, race, gender, cigarette smoking and positive family history[1,3,10,11] (Figure 1.4). Addressing these risk factors plays an important role in the management of this group of patients and there is a low threshold for secondary prevention treatment including anti-platelet therapy, anti-hypertensive medications, smoking cessation, statin therapy and strict glycaemic control in diabetics. Despite the acknowledged risks of cardiovascular morbidity and mortality in PAD patients the instigation of risk factor modification remains poor compared to patients with coronary or cerebrovascular disease[12].

## 1.1.2 Classification of PAD

PAD is commonly categorised using the Fontaine[13] or Rutherford[14] classifications (Table 1.1). Both systems grade severity of disease based on symptoms. The Rutherford classification was updated in 1997 to include criteria for designating clinical improvement which require an upward shift by at least one clinical category or in the case of tissue loss an improvement of at least 2 categories and at least reach the level of claudication[15].

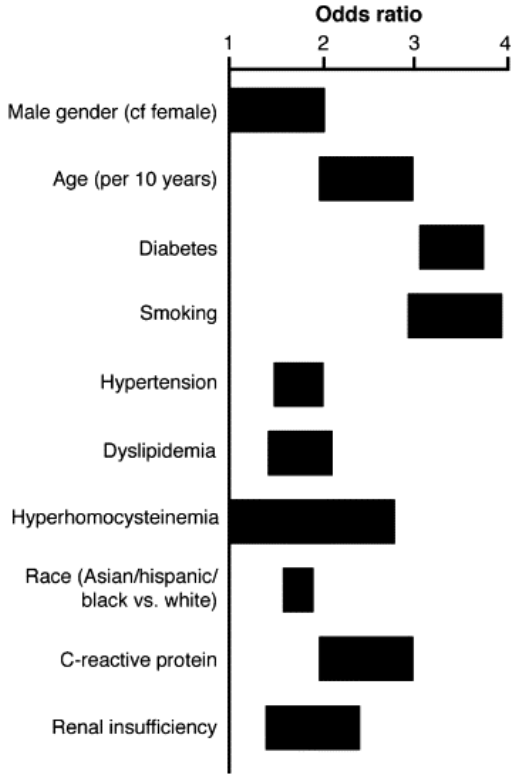


**Figure 1.4: Odds ratio for risk factors associated with PAD (from Hirsch et al.[1]).**

**Table 1.1: Fontaine and Rutherford classification PAD[13,14]**

| Fontaine | | Rutherford | | |
|---|---|---|---|---|
| Stage | **Clinical** | **Grade** | **Category** | **Clinical** |
| **I** | Asymptomatic | 0 | 0 | Asymptomatic |
| **IIa** | Mild Claudication | I | 1 | Mild Claudication |
| **IIb** | Moderate/Severe Claudication | I | 2 | Moderate Claudication |
| | | I | 3 | Severe Claudication |
| **III** | Ischaemic Rest Pain | II | 4 | Ischaemic Rest Pain |
| **IV** | Ulceration/Gangrene | III | 5 | Minor Tissue Loss |
| | | III | 6 | Major Tissue Loss |

### 1.1.3 Current Diagnostic Methods in PAD

A variety of simple diagnostic tests and imaging modalities are utilised in confirming the diagnosis of PAD and planning revascularisation. Ankle: Brachial pressure index (ABPI) is usually the first investigation performed to confirm the diagnosis and severity of PAD. If clinical history and examination, along with a reduced ABPI suggests PAD, then commonly an imaging modality is utilised to confirm the diagnosis and also to plan intervention.

***Ankle: Brachial Pressure Index (ABPI)***

ABPI is currently the standard practice in the initial evaluation of patients with PAD and represents a ratio between the highest systolic pressure from either pedal arteries (dorsalis pedis or posterior tibial) and the highest systolic pressure from either arm measured at the brachial artery. A continuous-wave Doppler ultrasound probe is used to measure the systolic pressure[16]. The ABPI can also provide an indication of the severity of the PAD by virtue of the values obtained. Furthermore, in cases where the diagnosis of PAD is unsure and other differentials are considered (such as spinal claudication or osteoarthritis) the ABPI can be a useful aid. An ABPI of between 0.9-1.3 is deemed to be normal, whereas patients with IC typically have values of between 0.4-0.9. Patients with CLI typically have values <0.4. An ABPI >1.3 is indicative of calcified, non-compressible arteries, commonly seen in patients with diabetes or chronic renal disease, and limits its use in these groups of patients[1,3]. To overcome this limitation, toe: brachial pressure index (TBPI) has been used where pressures are measured in the digital arteries of the 1$^{st}$ or 2$^{nd}$ toe, with a

small cuff used on the proximal part of the toe. A TBPI of >0.7 is considered normal, with values of <0.25 seen in patients with CLI[1,3]. However, ABPI and TBPI provide an indication of the inflow to the limb, with no information on segmental muscle/tissue perfusion. Nevertheless, ABPI has been shown to have a good sensitivity (80-95%) and specificity (95-100%) in detecting angiogram positive PAD[1].

A variety of imaging modalities are used to confirm the presence of PAD, evaluate its severity and to plan interventions.

***Duplex Ultrasonography***

Duplex Ultrasound uses a combination of B-mode ultrasound, to visualise structures, and colour Doppler ultrasound, to image flow. Duplex is able to visualise and grade severity of arterial disease by assessing the haemodynamic changes in the peak systolic velocity (PSV) across a lesion[1,3,17]. A PSV ratio is measured by comparing the velocities across a lesion to the PSV in the artery proximal to it. The ratio can grade severity of arterial stenosis. A PSV ratio greater than 2:1 indicates a >50% stenosis, greater than 4:1 a >75% stenosis and greater than 7:1 indicating a >90% stenosis[17].

Duplex is a non-invasive imaging modality, and is relatively cheap to perform, making it ideal as a first line modality for assessing severity of PAD. It is however operator dependent and, for supra-inguinal lesions, it can be hampered by patient habitus and bowel gas. Duplex ultrasound only images the major blood vessels in the lower limb, and its utility in assessing in very

distal tibial arteries and collaterals are limited. Its use is also further limited in the presence of calcification where full examination of the arterial tree may not be possible. Nevertheless, duplex is often used for decision-making prior to intervention and for surveillance after revascularisation of endovascular stents and bypass grafts.

***Computed Tomography Angiography***

Computed tomography angiography (CTA) provides high spatial resolution imaging (figure 1.5) of peripheral arteries and has a sensitivity and specificity of 95% and 96% respectively[18]. The rapid technical developments in CTA technology with multidetector scanners means that it is now possible to perform angiography of the whole peripheral arterial tree with short acquisition times, providing 3-dimensional (3D) high resolution images. This makes CTA a very attractive modality to use to plan interventions and survey post-intervention patients. Its availability 24 hours a day, 7 days a week makes it particularly useful in the acute settings, where experienced Duplex ultrasonography operators may not be available.

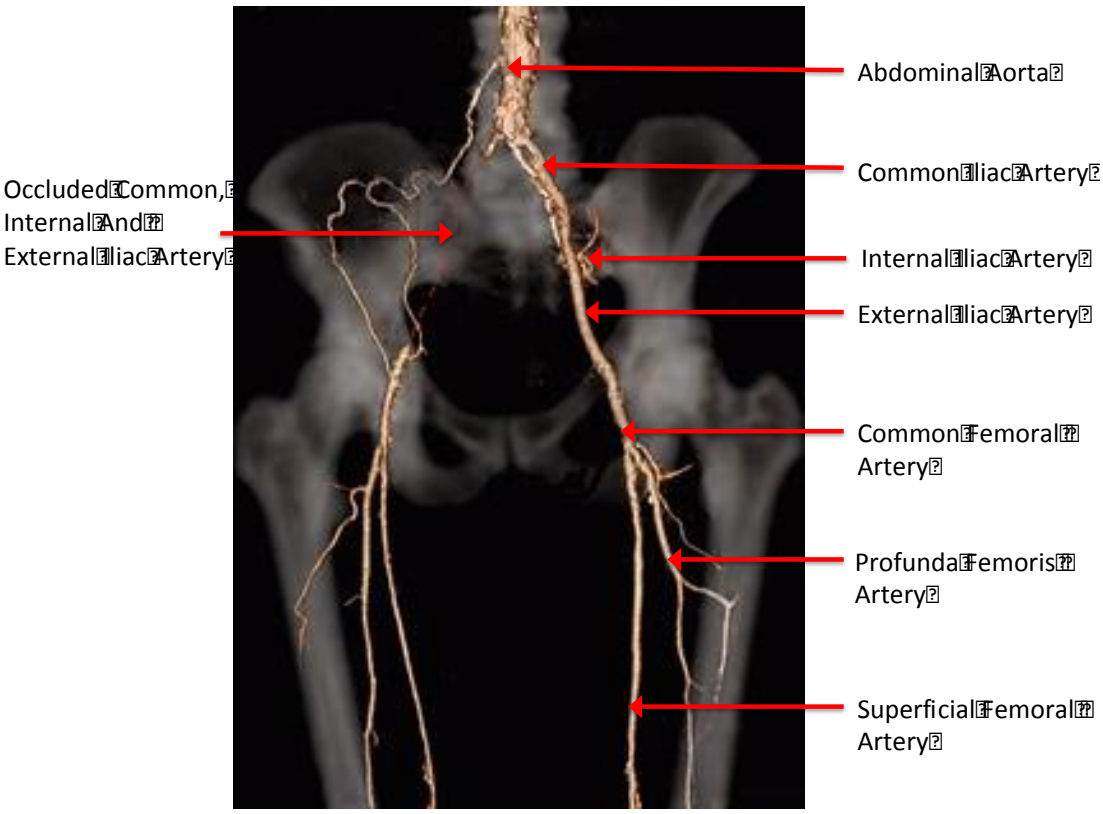


**Figure 1.5: Computed Tomography Angiogram (CTA) reconstruction in a patient with PAD demonstrates occlusion of the right common iliac, internal iliac and external iliac arteries (red dotted line). This imaging can be used to plan revascularisation.**

CTA does require the administration of iodinated contrast agents with inherent risks of contrast-induced nephropathy (CIN) in high-risk patients (such as those with underlying renal impairment). It is estimated that up to 17% of these high risk patients suffer with CIN after administration of iodinated contrast agents[19]. Although <1% of patients who develop CIN need renal replacement therapy[17], there is a 5 fold increase in in-hospital mortality in patients with renal failure compared to those with patients who do not develop CIN (7% versus 34%)[20].

Another factor that needs to be considered when imaging with CTA is exposure to ionising radiation. It is estimated that the average radiation dose from CTA is

7.47 mSv[21], compared to the average annual background radiation exposure of between 2-3 mSv. In most patients with advanced PAD the life expectancy is significantly less than the latent period of a radiation-induced malignancy, however in younger patients this exposure risk is more pertinent and dosing should be minimised as much as possible.

Calcification can make interpretation of CTA image difficult and the true extent of arterial disease can be difficult to quantify. This becomes more problematic in the crural vessels of the leg.

***Magnetic Resonance Angiography***

Different techniques for magnetic resonance angiography (MRA) are available, but most commonly 3D contrast enhanced MRA is used for the assessment of PAD. MRA has been shown to have a high sensitivity and specificity for the detection of arterial lesions (95% and 97% respectively)[22], which is greater than CTA and duplex ultrasonography. MRA is not affected by vessel calcification and is more accurate in assessing the crural vessels in the leg. It avoids exposure to radiation and the gadolinium based contrast agents used have a lower risk of anaphylaxis compared to iodinated contrast agents[17]. CIN is not an issue with MRA, however it is relatively contraindicated in patients with glomerular filtration rate of <30 ml/min due to the risk of nephrogenic systemic fibrosis (NSF), a condition characterised by fibrosis of the skin and internal organs resulting in contractures and reduced mobility[23]. NSF is associated with increased long term morbidity and mortality[24].

Not all patients are suitable for MRA, with the presence of metallic implants, such as cardiac pacemakers and cochlear implants contraindicated. Even if the presence of metallic objects is not deemed a contraindication to MRA (for example MRA compatible arterial stents), artefacts can lead to signal loss if they are in close proximity to the arterial tree. MRA does have the tendency to overestimate arterial stenosis, and venous contamination may make interpretation of extent of disease difficult, particularly below the knee[17]. Nevertheless the safety and high sensitivity and specificity means that the National Institute for Clinical Excellence (NICE) recommends that's patients with PAD being considered for intervention undergo MRA for planning revascularisation.

***Intra-Arterial Digital Subtraction Angiography***

The gold standard for imaging in PAD is still considered to be intra-arterial digital subtraction angiography (IADSA)[1](Figure 1.6). The added advantage of IADSA is the ability to perform endovascular revascularisation at the same time and the ability to measure pressure gradients allowing for assessment of haemodynamic significance of lesions to guide interventions.

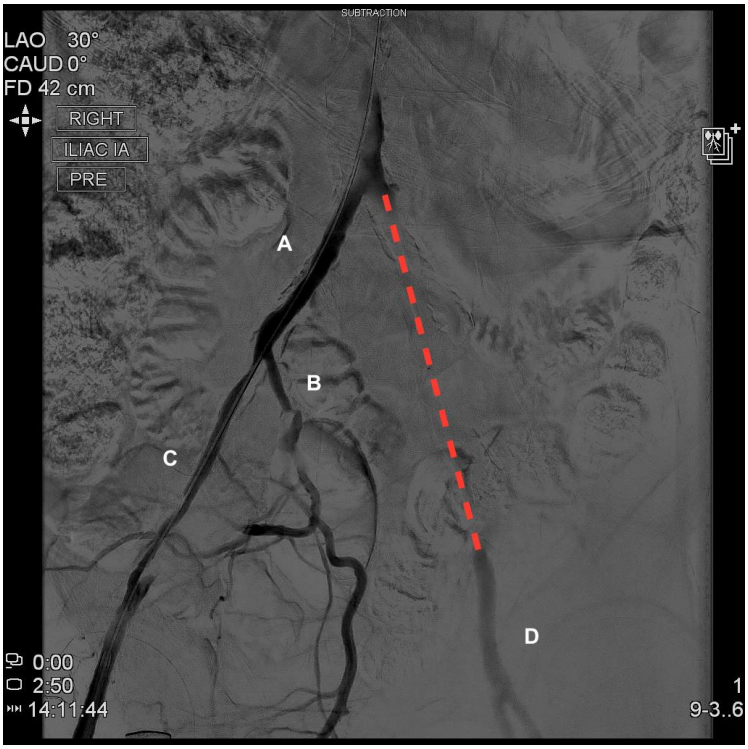


**Figure 1.6: Inter-Arterial Digital Subtraction Angiogram (IADSA) in a patient showing a patent right common iliac (A), internal iliac (B) and external iliac (C) artery. Occlusion of the left common iliac, internal iliac and external iliac arteries is seen (Red Dotted Line), with reconstitution of the left common femoral artery (D).**

IADSA is an invasive procedure, which is more costly than other imaging modalities and exposes the patient to both ionising radiation and iodinated contrast-agents. Carbon dioxide has been used as an alternative contrast agent in patients with renal impairment to avoid CIN. It is estimated that IADSA carries a 0.1% risk of severe reaction to iodinated contrast agents, a 0.7% risk of severe complications, and 0.16% mortality risk[3]. IADSA images are also only 2-Dimensional (2D) and can underestimate the severity of a lesion unless projections are undertaken in more then 1 plane, or pressure gradients measured.

### 1.1.4 Treatment of PAD

***Non-surgical Management***

The overriding management strategy in patients with PAD is the modification of risk factors associated with atherosclerosis. These patients are at increased risk of morbidity and mortality from cardiovascular pathology affecting not only the peripheral circulation, but also the coronary and cerebral circulation[12]. It is important to address risk factors such as smoking, hypertension, hyperlipidaemia and diabetes mellitus in this group of patients.

Antiplatelet therapy, usually with aspirin and/or clopidogrel, is indicated in patients with PAD for secondary prevention from cardiovascular morbidity and mortality[1,3]. The antithrombotic trialists' collaboration meta-analysis showed a 23% reduction in serious vascular events in patients with PAD treated with antiplatelet therapy[25]. Low dose aspirin (75-325mg) is most commonly used, as no benefit has been found with higher doses, but an increased risk of bleeding is associated[26]. The CAPRIE trial investigated the cardiovascular outcomes showing a moderate benefit of clopidogrel over low dose aspirin, with a similar side effect profile for both medications[27]. There is some emerging evidence for the combination of aspirin and clopidogrel in reducing cardiovascular morbidity and mortality, at the expense of an increase in bleeding risk[28], however this benefit seems to only last for the short term and that extended duration dual anti-platelet therapy has no advantage over monotherapy[29].

Smoking is perhaps the most important risk factor that needs addressing in patients with PAD. The extent of tobacco intake correlates with incidence of PAD, severity of disease, lower limb amputation rates, occlusion of bypass grafts after revascularisation and mortality[3,30–32]. Patients with PAD should be advised regarding the risks of continued smoking along with the benefits or giving up. Patients enrolled on formal smoking cessation programmes along with nicotine replacement therapy are more likely to refrain from tobacco use in the long term with studies showing a 22% cessation rate out to 5 years, compared to 5% in groups not in a formal programme[30], along with a significant survival benefit. A Cochrane review concluded that the use of nicotine replacement therapy increased the odds of successfully stopping smoking by 50-70%[33].

Patients with PAD should, along with an anti-platelet agent, be prescribed a statin. The Heart Protection Study assessed the impact of statins on mortality and cardiovascular events and showed a significantly reduced all cause and cardiac mortality in patients taking statins, irrespective of their cholesterol level[34]. More importantly the study found that in a subgroup of patients with PAD, a 22% reduction in major cardiovascular events. A Cochrane review, including 18 randomised controlled trials with over 10,000 patients, scrutinised the effects of statins in PAD patients and found a significant reduction in cardiovascular events[35].

Attention needs to be paid to controlling blood pressure in patients with PAD. All drugs capable of reducing blood pressure should be considered in treating hypertension in theses patients. The treatment goal for antihypertensive

therapy should aim for a blood pressure (BP) of below 140/90mmHg, and below 130/80mmHg in patients with diabetes mellitus and/or renal insufficiency[31].

Diabetes mellitus increases the risk of PAD by approximately three- to four-fold[3]. Diabetes is also associated with neuropathy and decreased resistance to infection, all of which lead to increased risk of tissue loss and ulceration in the limb and ultimately amputation. It has not been determined as yet whether strict diabetic control yields improvement in outcomes such as limb salvage or freedom from repeated revascularisation in patients with PAD. Nevertheless, in diabetic patients, the haemoglobin A1c should be kept <7% and expert foot care is essential to minimise the risk of developing diabetic foot complications.

The primary management strategy for PAD patients with IC is a supervised exercise program. If an exercise programme is supervised (minimum 6 months) then an increase in walking time and distance, with lower severity claudication pain is seen in patient with IC compared to usual medical care or unsupervised/unstructured exercise[1,3]. The main problem arises in the lack of availability of suitable supervised exercise programme for PAD patients to enrol in. There is no role for exercise therapy in patients with CLI. These patients are at high risk of limb loss and therefore require urgent revascularisation

Although the majority of non-surgical management if patients with PAD is aimed at addressing risk factors and reducing morbidity and mortality from secondary cardiovascular events, there are a range of ‘vasoactive’ drugs now available for use in patients with IC to try to improve walking. The two most common drugs used in patients with stable PAD are cilostazol and naftidrofuryl oxalate.

Cilostazol is a phosphodiesterase III inhibitor with vasodilator, metabolic and antiplatelet activity. A meta-analysis of it's use in claudicants concluded cilostazol usage improved walking distance and quality of life compared to placebo[36]. Naftidrofuryl oxalate is a 5-hydroxytryptamine antagonist, which is thought to improve muscle metabolism along with reducing platelet aggregation. In a meta-analysis it was shown that it improved walking distance by 26% compared to placebo alone[37]. Currently NICE is the UK only recommends the use of naftidrofuryl oxalate in patients with IC.

In patients with CLI the use of these vasoactive drugs is contraindicated, as they will not alter the outcome for these patients. The only pharmacological therapy to have any benefit in CLI patients is prostanoids (such as iloprost). A meta-analysis of the use of iloprost compared to placebo has shown significant benefit in ulcer healing, pain relief and in patients avoiding major amputation[38]. It has to be remembered that prostanoids are only indicated in CLI patients not suitable for revascularisation and is not available in all countries.

More recently angiogenic cell therapies have been used to promote neovascularisation in an attempt to treat patients with PAD. Early studies concentrated on the use of angiogenic proteins such as vascular endothelial growth factor[39] and fibroblastic growth factor[40], but more recently research involving stem cells[41] and circulating monocytes[42] have identified new avenues for promoting neovascularisation. Cell therapy is, however, still in its infancy for the treatment of PAD and it use as such is limited to clinical trials.

### *Surgical Management*

The aim of surgical treatments for PAD is to improve blood flow to the affected limb. This can be achieved by a minimally invasive endovascular approach, open surgery, or a 'hybrid' approach incorporating both endovascular and open surgical techniques. The Trans-Atlantic Inter-Society Consensus (TASC) document published guidelines for classifying the severity of PAD based on angiograms, along with recommendation on open surgical versus endovascular treatment strategies in 2000[43], with an update in 2007[3] (TASC II). The principles behind which treatment strategy is considered is based on long term durability compared with relative risk of the procedure to patients. The TASC classification is divided in to anatomical regions of the lower limb arterial circulation, with the classification for the aorto-iliac segment summarised in table 1.2 and for the femoral-popliteal segment in table 1.3. TASC 'A' lesions are considered to most amenable to treatment by endovascular techniques. TASC 'B' lesion are also considered generally suited to an endovascular approach, unless open surgery is also required (such as femoral endarterectomy). TASC 'C' lesion should be treated with open surgical revascularisation, unless the risk to the patient is deemed to great, where endovascular treatment can be considered. TASC 'D' lesions do not yield adequate results from an endovascular method to justify then as first-line treatment.

**Table 1.2: TASC II classification of aorto-iliac disease**
CIA – common iliac artery; EIA – external iliac artery; CFA common femoral artery; IIA – internal iliac artery; AAA – abdominal aortic aneurysm. Adapted from Norgren et al.[3]

| Lesion Type | Characteristic |
|---|---|
| A | • Unilateral or bilateral CIA stenosis<br>• Unilateral or bilateral single EIA stenosis <3cm |
| B | • Stenosis of infrarenal aorta <3cm<br>• Unilateral CIA occlusion<br>• Single/multiple stenosis 3-10cm involving EIA but not extending into CFA<br>• Unilateral EIA occlusion not involving IIA or CFA |
| C | • Bilateral CIA occlusion<br>• Bilateral EIA stenosis 3-10cm long but involving CFA<br>• Unilateral EIA stenosis extending into CFA<br>• Unilateral EIA occlusion involving IIA and/or CFA<br>• Heavily calcified unilateral EIA occlusion with or without involvement of IIA and/or CFA |
| D | • Infrarenal aortic occlusion<br>• Diffuse disease involving the aorta and both CIA/EIA<br>• Diffuse multiple stenoses involving unilateral CIA, EIA and CFA<br>• Unilateral occlusion of CIA and EIA or bilateral EIA occlusion<br>• Iliac stenosis in AAA not amenable to endovascular repair requiring treatment |

**Table 1.3: TASC II classification of femoral-popliteal disease**
CFA – common femoral artery; SFA – superficial femoral artery. Adapted from Norgren et al.[3]

| Lesion Type | Characteristic |
|---|---|
| A | • Single stenosis <10cm<br>• Single occlusion <5cm |
| B | • Multiple lesions (stenosis or occlusions), each <5cm<br>• Single stenosis or occlusion <15cm not involving below knee popliteal artery<br>• Single or multiple lesions in the absence of continuous tibial vessels to improve inflow for a distal bypass<br>• Heavily calcified occlusion <5cm<br>• Single popliteal stenosis |
| C | • Multiple lesions totalling >15cm<br>• Recurrent lesions needing treatment after 2 endovascular interventions |
| D | • Chronic total occlusions of CFA or SFA (>20cm involving the popliteal artery)<br>• Chronic total occlusion of popliteal artery and trifurcation vessels |

In formulating a management plan for patients with PAD multiple factors need to be considered not just the extent and anatomical location of disease, such as patient co-morbidity, life expectancy and local expertise in both open surgical and endovascular revascularisation.

The division of the TASC classification into anatomical regions highlights it weakness as a method for determining revascularisation strategies as most patients with PAD do not present with arterial disease confined to a single anatomical region, but rather have disease affecting multiple levels of the arterial tree. The principles behind revascularisation are to work from proximal to distal anatomical regions and to improve both the inflow and outflow of blood across a lesion in an attempt to improve the blood supply to the limb and the durability of the intervention. For example, revascularising a tibial vessel in a patient with CLI is unlikely to successful if the femoral-popliteal segment proximally is significantly diseased, and distal to the revascularisation the artery is occluded.

Blood supply below the knee is via 3 blood vessels, the anterior tibial artery, the peroneal artery and the posterior tibial artery. When revascularising to below knee vessels, most commonly in the context of CLI, the artery with the least amount of disease and best continuous flow to the ankle and foot is usually chosen. When the patient has tissue loss associated with their CLI, there are some clinicians who believe in targeted revascularisation to the blood vessel directly supplying the area of tissue loss leads to better outcomes (angiosome concept). This so called “angiosome concept” was first devised by anatomic studies that identified 3D blocks of tissue fed by a single artery[44]. The foot has

6 angiosomes originating from the 3 below knee arteries and their branches. Some studies have shown that revascularisation targeted to the angiosome associated directly with the area of tissue lost leads to improved tissue healing and limb salvage rates[45,46]. However no randomised controlled trial has been performed to compare whether direct or indirect revascularisation has an impact on healing and limb salvage rates.

Open surgical techniques for revascularisation comprise of bypass surgery (anatomical and extra-anatomical) and endarterectomy. Endovascular interventions include percutaneous transluminal angioplasty (PTA) with balloon dilatation, stenting and atherectomy devices. Open surgical techniques are well established, whereas the technology and devices available for endovascular interventions are continuing to develop and improve. Advances in balloon and stent technology, such as cutting balloons, and catheter and guidewires, such as re-entry devices and guidewires for crossing long occlusions[47],means that durability and indications for endovascular revascularisation continue to improve. More recently drug eluting technology, for example using the antineoplastic agent paclitaxel, have been used in an attempt to reduce re-stenosis in treated lower limb arteries[48–50]. Paclitaxel is an inhibitor or vascular smooth muscle proliferation[51], and is highly lipophilic promoting rapid tissue uptake even with brief exposure of the drug to the vessel wall. The reduction in re-stenosis with drug eluting stents and balloons has resulted in greater primary and secondary patency in patients undergoing endovascular revascularisation.

Surgical revascularisation is usually not indicated in patients with IC, unless there is significant deterioration in symptoms during a surveillance period whilst

undergoing non-surgical management or there is significant impact on the patient's quality of life. Revascularisation for claudicants is usually only considered if the arterial anatomy is favourable for intervention with the least amount of risk to the patient. For example it would be extremely unusual for a IC patient to undergo a distal bypass, but if their disease was confined to iliac region and anatomically suitable then iliac angioplasty, which has been shown to have a good technical success rate (96%) and long term patency (5 years 71%)[3], may be considered appropriate.

Arterial bypass surgery is performed by anastomosing a graft proximal and distal to the diseased segment of the artery. For long-term durability bypass grafts should be kept as short as possible and there should be minimal disease both proximal and distal to bypassed artery. Anatomical bypasses tend to have greater long term patency than extra-anatomical bypass, for example aortobifemoral bypass has a 5 year patency of >90% compared with axillo-bi-femoral bypass which has a patency of 71%[3].

The conduit for bypass surgery can be either autologous vein or prosthetic, for example Dacron or polytetrafluroethylene (PTFE). Prosthetic bypass grafts are typically used when performing long bypasses, for example axillo-femoral bypass, bypasses involving the aorto-iliac vessels where long-term patency is good, and in cases of infra-inguinal bypasses where a suitable vein conduit is not available. Venous bypass grafts have been shown to have a much better long-term patency (74-76% 5 year patency) compared to prosthetic grafts (39-52%)[3].

The introduction of hybrid operating theatres with fully equipped radiological and surgical equipment, along with principles of surgical revascularisation (ensuring good inflow and outflow, keeping bypasses as short as possible especially if suitable vein conduit is limited) has allowed combined endovascular and surgical techniques to be performed. This allows attempts of dealing with multilevel disease in one sitting and may in the future lead to improved outcomes for patients, particularly with CLI.

## 1.2 Anatomy of the Lower Limb

At the level of the calf the lower limb consists of 4 muscle compartments (Figure 1.7). The anterior compartment is composed mainly of the tibialis anterior muscle with the long extensors of the foot. The main arterial supply to the anterior compartment is via the anterior tibial artery. The lateral compartment usually represents the smallest compartment in the calf and consists of the peroneus longus and brevis muscle. Blood supply to this compartment is from peroneal artery. The posterior compartment of the lower leg is divided into a large superficial and a deep compartment. The superficial compartment comprises the soleus and gastrocnemius muscles. Both muscles represent the largest muscle mass in the calf and whereas in the other muscle compartments it can be difficult to distinguish individual muscles, these two muscles are readily identifiable. The deep posterior compartment

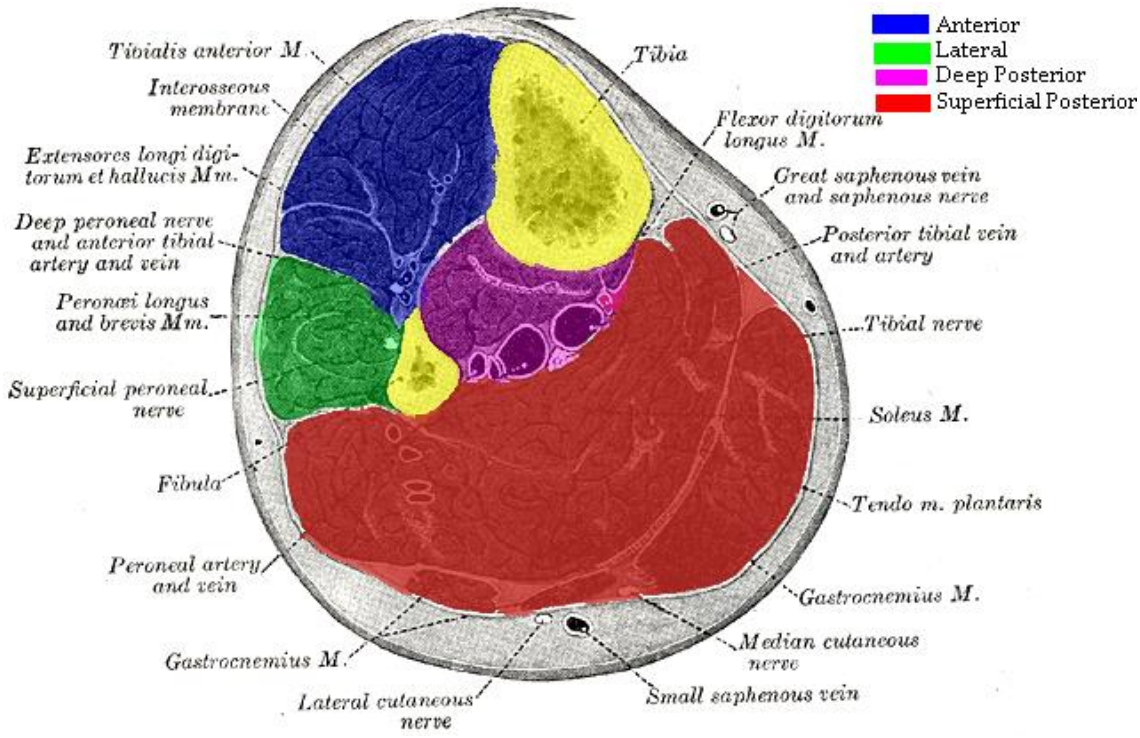


**Figure 1.7: Compartments of the lower leg at the level of the calf showing the different muscle compartments.**

consists of the long flexors of the foot, the tibialis posterior and popliteus muscle. The blood supply to the superficial and deep posterior compartment is mainly from the posterior tibial artery although collateral branches from the popliteal artery also contribute more proximally. From the anatomy of the lower leg it can be seen that the calf can be divided into 5 distinct muscle groups; the anterior muscle compartment, the lateral muscle compartment, the soleus muscle, the gastrocnemius muscle and the deep posterior muscle compartment

## 1.3 Perfusion imaging

At present there are no reliable methods for assessing limb perfusion. The imaging modalities mentioned earlier (duplex, CTA, MRA, IADSA) all allow accurate assessment of the larger vasculature but provide no information about the microcirculation or perfusion at the tissue level. ABPI can predict significant arterial stenosis or occlusion with a high specificity and sensitivity[1], but again this is does not provide assessment of tissue perfusion.

An accurate, non-invasive method of mapping and measuring muscle perfusion would aid diagnosis and treatment of CLI and may increase limb salvage rates. If the angiosome concept is believed to improve limb salvage rates, then accurate assessment of segmental tissue perfusion, would help to delineate areas of ischaemia, accurately guide interventions on the limb and provide an objective means of measuring improvement[52].

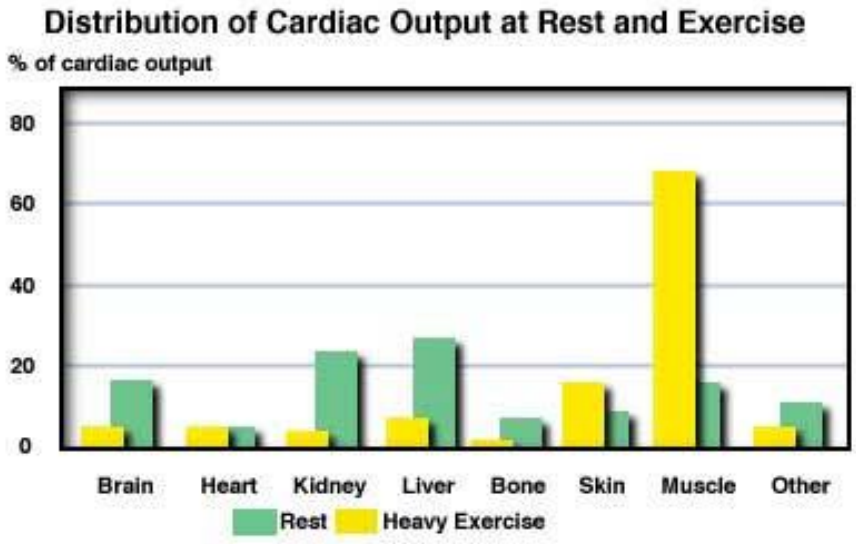


**Figure 1.8: Distribution of cardiac output to various organs at rest and changes with exercise (adapted from[53]).**

Methods for assessment of perfusion in organs such as the heart and brain have progressed rapidly, however muscle perfusion measurements in the lower limb have proven to be more difficult. The biggest challenge to skeletal muscle perfusion imaging is the low basal perfusion at rest. Skeletal muscle represents the largest tissue mass in the human body and at rest receives around 20% of the cardiac output, but this can be increased to up to 80% during exercise. A 20-50 fold increase in blood flow has been measured in muscle after exercise[54,55]. Comparatively, brain and cardiac perfusion are constantly well maintained by auto regulation and receive around 10-20% of the cardiac output (Figure 1.8). Measurement shows resting blood flow to be between 1-2.2ml/min/100g muscle[54,56] with no difference seen between normal subjects and patients with PAD[55]. However during hyperaemia, e.g. from exercise or vasodilation, skeletal muscle perfusion can increase dramatically up to 80-100ml/min/100g muscle[57]. When this is compared with resting perfusion of 60-100ml/min/100g in the heart and brain it is understandable why perfusion imaging in the resting lower limb has been difficult to achieve.

This wide variability in skeletal muscle perfusion makes assessment of this problematic and challenging due to the high sensitivity that would be needed to measure such low blood flow. To be able to detect measurable changes in muscle perfusion in the lower limb, most modalities require a setup where blood flow to the tissues is increased, i.e. hyperaemia. A number of methods have been utilised to achieve this, such as: (i) arterial occlusion, typically with a cuff inflated to suprasystolic pressures to induce ischaemia and subsequently deflated evoking a reactive hyperaemia; (ii) exercise resulting in a functional

hyperaemia, or; (iii) the use of vasodilators to increase blood flow, a pharmacological hyperaemia. The use of hyperaemia results in an increase in blood flow to the tissue, particularly muscle and can be used to assess perfusion as well as physiological reserve, much in the same way as vasodilators and treadmill testing is used in patients to measure cardiac perfusion.

A number of methods have been used in the past to measure lower limb perfusion, with newer techniques being developed to allow accurate measurement of muscle perfusion.

### 1.3.1 Current Methods of Measuring Lower Limb Perfusion

#### Venous Occlusion Plethysmography

Venous Occlusion Plethysmography (VOP) was first described at the beginning of the 20$^{th}$ century[58] but it was only after the introduction of mercury-in-silastic strain gauges in the 1950's and 1960's that it was regularly used to evaluate PAD[59,60]. VOP relies on the principle that when cuffing occludes venous drainage from a limb, the volume of the limb is dependent on the arterial blood which can flow into the limb but is unable to escape. In the lower limb this is achieved by inflating a cuff around the thigh to 50mmHg to occlude venous drainage without obstructing arterial inflow. A strain gauge is applied to the calf to measure the change in volume in the limb. An increase in limb volume following cuff inflation is recorded via a strain gauge applied to the calf as changes in its electrical resistance. If the strain gauge length is made equal to

the limb circumference then changes in limb circumference are directly proportional to change in electrical resistance and this can be calibrated to quantify limb blood flow[61]. Under resting conditions it is estimated that up to 70% of blood flow in to the limb is directed to skeletal muscle with the remainder accounted for by skin circulation[58]. The change in limb volume can, therefore, be considered to be directly related to arterial perfusion of the limb.

VOP has only been shown to correlate well with ABPI[62,63]. One of the limitations of VOP is that it provides a global indication of perfusion of the limb without any anatomical information and, therefore, cannot be used to delineate segmental muscle perfusion. VOP is influenced by numerous factors, such as ambient temperature, arterio-venous shunting, which may lead to erroneous readings.

**Laser Doppler**

Laser Doppler Flowmetry (LDF) and Laser Doppler Imaging (LDI) measure the speed and concentration of blood cells[64] (blood flux, not blood flow, Figure 1.9) and therefore cannot be used to compare perfusion in different individuals[65].

LDF requires direct contact and is only effective over a relatively limited area (~1mm$^3$). LDI assesses a larger area of skin from a distance using a scanning motion that incorporates the entire lower limb and foot[66]. The wavelength of laser, speed of scanning and distance between the scanner and the leg affect tissue penetrance and must be kept constant to allow meaningful comparison of serial measurements[65].

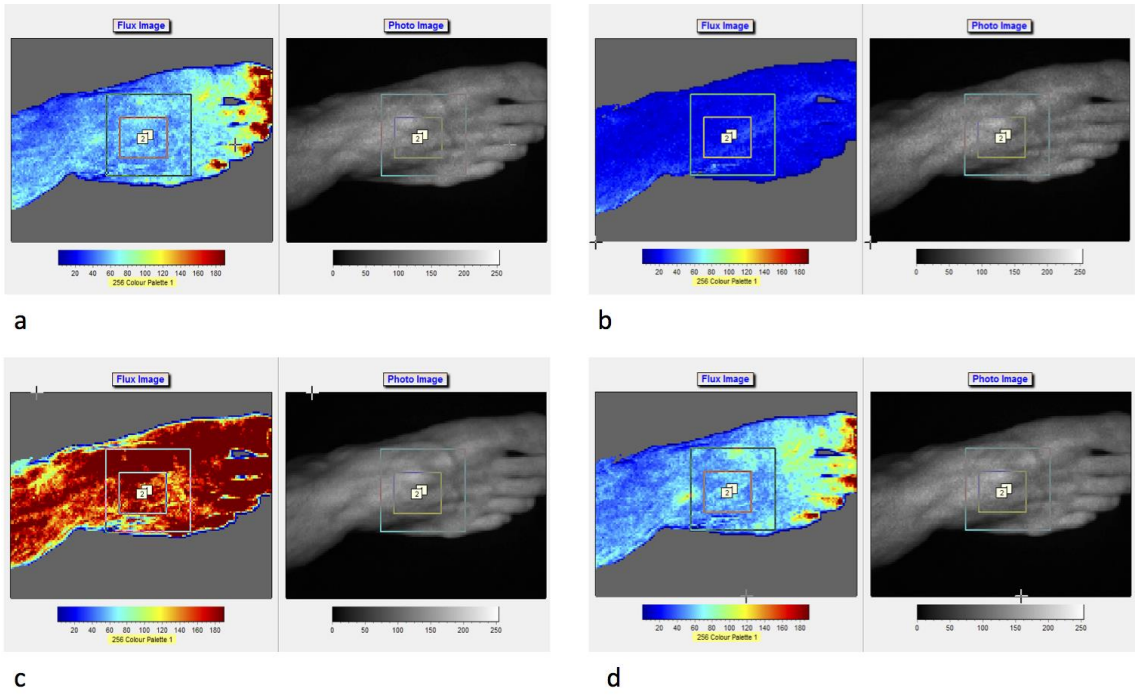


**Figure 1.9: Laser Doppler imaging of the foot at baseline (a). Suprasystolic cuffing induces an ischaemic phase (b) with a decrease in flux in the foot. Reactive hyperaemia after cuff deflation shows an increase in flux (c) with subsequent return to baseline (d). Pictures courtesy of Moor Instruments, Devon, UK**

LDF/LDI was first used in the 1980s to assess the severity of ischaemia in PAD, but these modalities only identify ischaemic compared with normal limbs and cannot quantify the severity of perfusion deficit[67]. More recent studies show that LDF is a good discriminator of skin flap perfusion and can predict the likelihood of healing after limb amputation[68]. LDI is used in preclinical animal models of limb ischaemia (e.g. the murine hindlimb ischaemia model) for high throughput testing of interventions including angiogenic therapies. The technique allows longitudinal acquisition of data, but is limited by motion artefact, ambient temperature variations and “perfusion” measurements weighted toward the

larger vessels that are shallow and reside on the surface of the limb musculature[42].

**Transcutaneous oxygen pressure (TcPO2)**

The measurement of TcPO2 is a non-invasive technique that allows longitudinal assessment of local oxygen diffusion from the capillary bed through the skin epidermis and provides an indication of the amount of oxygen delivered to the tissue. TcPO2 measurements can reflect the severity of PAD[69], assess ulcer healing potential[70] and determine the optimal level for limb amputation[71]. A TcPO2 lower than 20-30mmHg is consistent with CLI[3,69,72] and levels below 40mmHg are associated with poor healing following amputation[72]. Inhalation of 100% oxygen would normally result in TcPO2 >100mmHg, but in patients with CLI the TcPO2 does not rise above 30mmHg[72]. Oxygen therapy resulting in <10mmHg rise in limb TcPO2 is associated with an over 60% chance of an amputation at that level not healing[72]. A rise of >40mmHg in TcPO2 after limb revascularization is considered significant and increases the chances of tissue healing[69,72].

TcPO2 measurements vary in different tissues and under different physiological conditions. Barriers to diffusion such as oedema, increased oxygen consumption secondary to inflammation, and vasoconstriction may lead to falsely low TcPO2 readings. Readings are also affected by temperature, with a 1°C reduction in the thermistor temperature resulting in a 2-3% lower TcPO2 reading[72].

**Indocyanine Green Fluorescence Angiography (ICGA)**

This technique has been used for many years to image retinal vessels[73], and more recently in the assessment of microanastomoses in surgical flap reconstruction surgery, detection of arteriovenous malformations, and measurement of hepatic blood flow[74].

Indocyanine green is a fluorescent dye that is activated by near infrared laser light at ~780nm[75] . This allows a penetrance of 3mm from the surface of the skin to assess the subdermal microcirculation[74,76]. A semi-quantitative measure of perfusion is obtained by measuring pixel fluorescence intensity in different areas of the image from the limb. Perfusion measured by ICGA correlates with LDI in the hind limb ischaemia model[77] and predicts the likelihood of amputation healing in man[75]. This technique can identify patients with peripheral arterial occlusions who have extensive collateralization[76]. Lack of differences between the two groups when ABPI has been used as the discriminator, suggests that ICGA may be a more sensitive method for assessing perfusion in the limb than ABPI.

The main limitation of all of these techniques is that they only provide information on perfusion in superficial tissues. Analysis of skin perfusion misses the muscle compartments, which determines symptomatic and functional limitations in PAD. Changes in skin perfusion in PAD are only reliably detected in the later stages of limb ischaemia whereas disturbances in muscle microcirculation is seen much earlier[78]. Muscle perfusion in end stage CLI patients requiring amputation correlates well with skin perfusion measured by

TcPO2 and LDF[79]. Reliable measurement of muscle perfusion may therefore allow intervention at an earlier stage where a more positive outcome in terms of limb salvage is achievable. Cutaneous blood flow is highly variable and, therefore, is a poor marker of limb perfusion. Autonomic neural dysfunction, as seen in diabetes, and the presence of infection, for example, can significantly alter skin perfusion.

### 1.3.2 Emerging Techniques for Perfusion Imaging

#### Positron Emission Tomography (PET)

This imaging modality was originally used to measure perfusion and absolute blood flow to the brain[80] and heart[81,82], but has also been used to quantify blood flow to the musculature of the leg[54,55,83]. Myocardial perfusion, assessed by PET, correlates extremely well with measurements made using radiolabeled microspheres in animals, a technique that is considered the gold standard in the laboratory setting[82].

$^{15}$Oxygen, in water for injection or mixed with air/$CO_2$ for inhalation, is currently used in man for imaging perfusion using PET[80,83]. A small number of PET studies have assessed blood flow, oxygen consumption and oxygen extraction in the lower limb[54,55,83] and shown that patients with PAD have decreased blood flow and oxygen consumption in the affected limb after exercise compared with the contralateral “control” leg[83]. After stimulation with exercise or intra-arterial administration of vasodilators, the increase in blood flow (hyperaemia) is less

pronounced in patients with PAD compared with young healthy volunteers[55,83,84] (Figure 1.10).

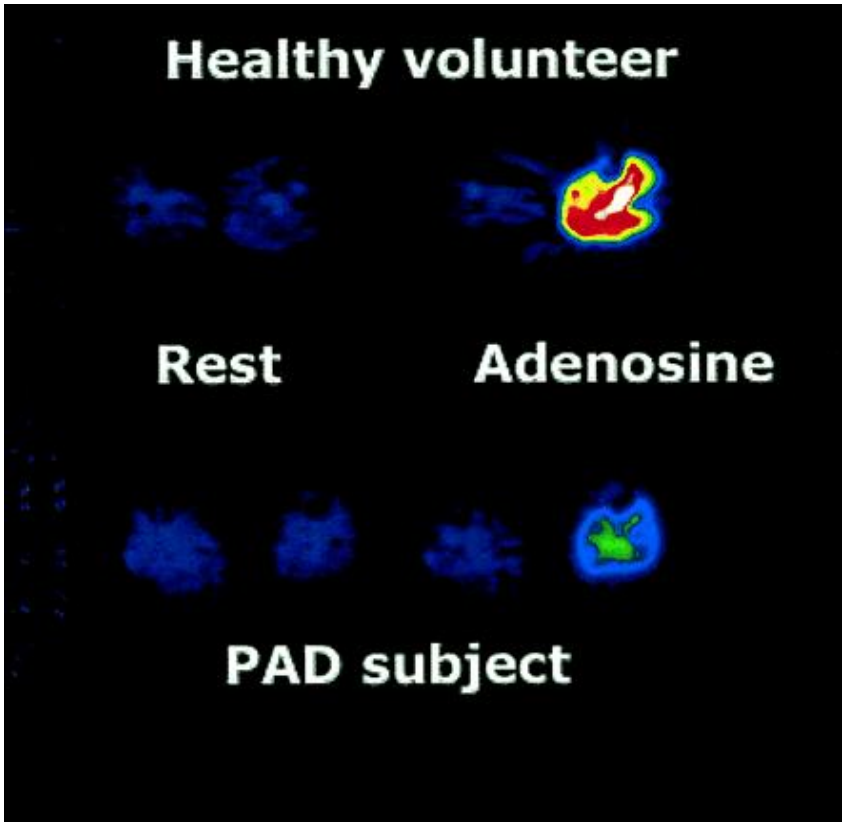


**Figure 1.10: Positron emission tomography (PET) of the calf using $^{15}$Oxygen-labelled water in healthy volunteers and patients with PAD. At rest little difference is seen between the 2 groups. Reactive hyperaemia provoked with intra-arterial adenosine shows a lower response in PAD patients (from Schmidt et al.[84]).**

These studies must, however, be interpreted with caution because they do not use age matched controls, nor do they re-measure perfusion after limb revascularisation. PET does not offer the same spatial and temporal resolution as MR imaging, but its close correlation with microsphere derived perfusion measurements in mouse[85] and canine[86] models of ischaemia renders it the gold standard in perfusion imaging. PET requires a lengthy scan time and exposure

to ionising radiation precluding serial investigations. $^{13}$Nitrogen-ammonia has been used extensively as a PET agent for assessment of cardiac perfusion[87] but not for the measurement of muscle perfusion in the lower limb. $^{13}$Nitrogen-ammonia and $^{15}$Oxygen both have relatively short half-lives of 10mins and 2mins, respectively, which limits their versatility. $^{15}$Oxygen is better suited as a perfusion probe in the lower limb because it is freely diffusible and not affected by metabolism.[18]Fluorine flurpiridaz tracer is an alternative, versatile radioisotope for measuring perfusion because of its longer half-life (110mins) and high extraction rate but its utility in the clinical setting is still under investigation[88].

**Contrast-enhanced ultrasound (CEUS)**

CEUS with microbubble contrast agents (measuring 2.5μm in size) can assess muscle perfusion[89–91]. These contrast agents consist of a shell and a gas core, the latter endowing echogenicity to the structure. The outer shell is broken down by the acoustic energy of the ultrasound and eventually metabolized by the body. The composition of the shell determines how long the contrast agent remains in the circulation.

Assessment of perfusion in skeletal muscle by CEUS is performed with a linear ultrasound transducer probe placed around the calf and a region of interest (ROI) selected in which only muscle is seen and bone is excluded. The probes used usually have a depth of 4cm beneath the skin and are held in place by hand, keeping the ROI in view[89]. Microbubble contrast is administered intravenously, either as a bolus injection[89] or by slow continuous infusion[91] with

the assumption that signal intensity is a direct measure of microbubble contrast concentration in the ROI. It is not known which method of administration is superior.

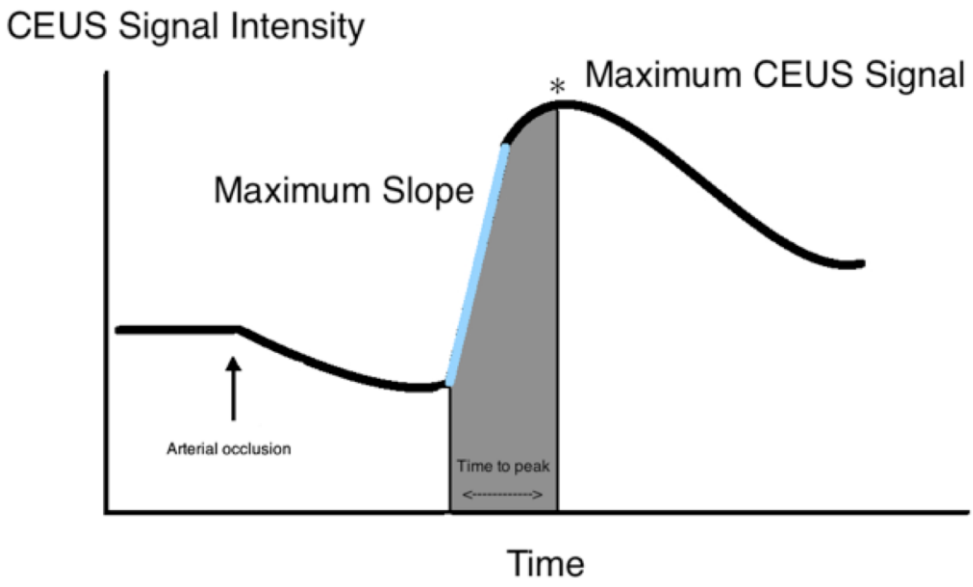


**Figure 1.11: Contrast enhanced ultrasound (CEUS) signal intensity time curve highlighting difference parameters for the assessment of perfusion. Parameters including time to maximum signal, maximum signal intensity and slope of the curve during reactive hyperaemia can be analysed to assess muscle perfusion**

Changes in muscle perfusion are provoked to help assess perfusion and flow reserve. This can be done using a cuff inflated around the thigh to supra-systolic pressure to occlude the arterial circulation. The cuff is subsequently deflated producing a reactive hyperaemia; alternatively the subject exercises to induce functional hyperaemia in the muscle and changes in perfusion. In both scenarios, signal intensity can be used to quantify perfusion (Figure 1.11), but the stressors to increase muscle blood flow in the lower limbs are more difficult

to achieve in CLI patients compared with claudicants. Parameters such as time to peak (TTP) contrast, maximal contrast, areas under time-signal intensity curves and gradients have been used to assess perfusion[89,91]. TTP, maximal signal intensity and area under the time-signal intensity curves are lower in patients with PAD compared with healthy controls[89–91].

CEUS has been used to assess collateralization, an important compensatory mechanism in patients with PAD[91]. Patients with extensive collateralization (assessed by angiography) have a shorter time to peak compared with those that collateralize poorly[91]. In contrast, no difference in ABPI was detectable between patients with good and poor collateralization.

CEUS shows promise for measuring tissue perfusion because it is cheap, easily available and does not use ionising radiation, but it remains to be validated against other "gold standard" modalities such as $^{15}$Oxygen PET. To date, CEUS has only been used to measure perfusion in the gastrocnemius and soleus muscle groups. Its use for other calf muscle compartments is limited by the presence of bone. As with all ultrasound techniques, CEUS is operator dependent and can be limited by artefacts created by patient movement. Although microbubble contrast agents are safe to use[92] and only needed in small doses, they are rapidly lost in the circulation.

**Computed Tomography Perfusion Imaging (CT)**

Computed tomography (CT) can accurately assess perfusion in the brain[93], heart[94] and solid organs[95], but has traditionally been less useful for evaluating

perfusion in the limbs. CT perfusion imaging of peripheral muscle is difficult because of the low baseline blood flow to these tissues compared with other structures. The signal to noise ratio during perfusion mapping is also affected by beam artefact from bone also, which limits the use of CT perfusion measurement in the lower limb. A recently described CT based method has, however, overcome this problem by averaging signal intensity changes over a number of voxels to improve the signal to noise ratio[96]. This technique has not been validated against other perfusion modalities and has only been carried out in a small cohort of normal subjects and not in patients with PAD.

CT imaging of the calf has recently been used to quantify changes in perfusion after revascularisation of the ischaemic limb by measuring blood flow, blood volume and mean transit time for contrast to reach the muscle[97]. This study found a significant increase in blood volume and blood flow to the calf post intervention, but not for mean contrast transit time. Individual muscle groups were not analysed but changes in perfusion were detected after successful revascularisation. CT based methods allow rapid acquisition of perfusion data and avoid the need for complex and expensive equipment. This method exposes the patient to ionising radiation and iodinated contrast agents and limits the possibility of measuring changes in perfusion by serial scanning.

**Magnetic Resonance Imaging (MRI)**

This is a promising modality for simultaneously assessing limb perfusion and the larger vasculature using conventional MRA. This non-invasive technique does not require ionising radiation, thereby allowing serial assessment of the

patient. Sequences that show the greatest promise include arterial spin labelling (ASL), blood oxygenation level dependent (BOLD) and first pass dynamic contrast enhanced (DCE) MRI.

### *(i) Arterial Spin Labelling (ASL) MRI*

This technique, developed to measure perfusion of the brain[98], has been used in the kidney[99], heart[100] and more recently, skeletal muscle[101–103]. ASL uses radiofrequency pulse sequences to place a magnetic "tag" onto the water component of blood proximal to the ROI. A T1-weighted image acquired in the ROI, after a delay to allow for inflow of tagged blood, is subtracted from a control image with no magnetic tagging. The difference in T1 signal between control and tag image is proportional to blood flow and can be used to construct perfusion maps over a designated time period[104]. ASL MRI can be considered analogous to PET perfusion imaging, but unlike PET, only uses blood as an endogenous tracer.

Different methods of ASL are available for perfusion imaging depending on the how the tagging is achieved. Continuous ASL (CASL) involves continuous saturation or tagging of arterial water proximal to the imaging slice[105]. This allows for a steady state in muscle magnetisation to be reached, which maximises signal contrast between the control and tagged images. CASL is hampered by magnetisation transfer effects that overestimate perfusion and make multi-slice imaging more complex[105]. Pulsed ASL (PASL) avoids this problem by tagging over a spatial region close to the imaging slice in pulses and acquiring the tag image between pulses following a post labelling delay.

The magnetisation transfer effect is less of a problem with PASL because less radiofrequency (RF) power is needed. There is, however, variable delay between tagging and blood reaching the imaging slice, which makes absolute quantification of perfusion more difficult[105]. Alternative sequences, including QUIPPS (I &II) and Q2TIPS, have been developed to tackle this problem. PASL is also limited by a lower signal to noise ratio compared with CASL. A method known as pseudo-continuous ASL (pCASL) aims to circumvent this problem by using short trains of RF pulses to mimic CASL, improving labelling efficiency and achieving a higher signal to noise ratio compared with PASL[106] (figure 1.12)

.

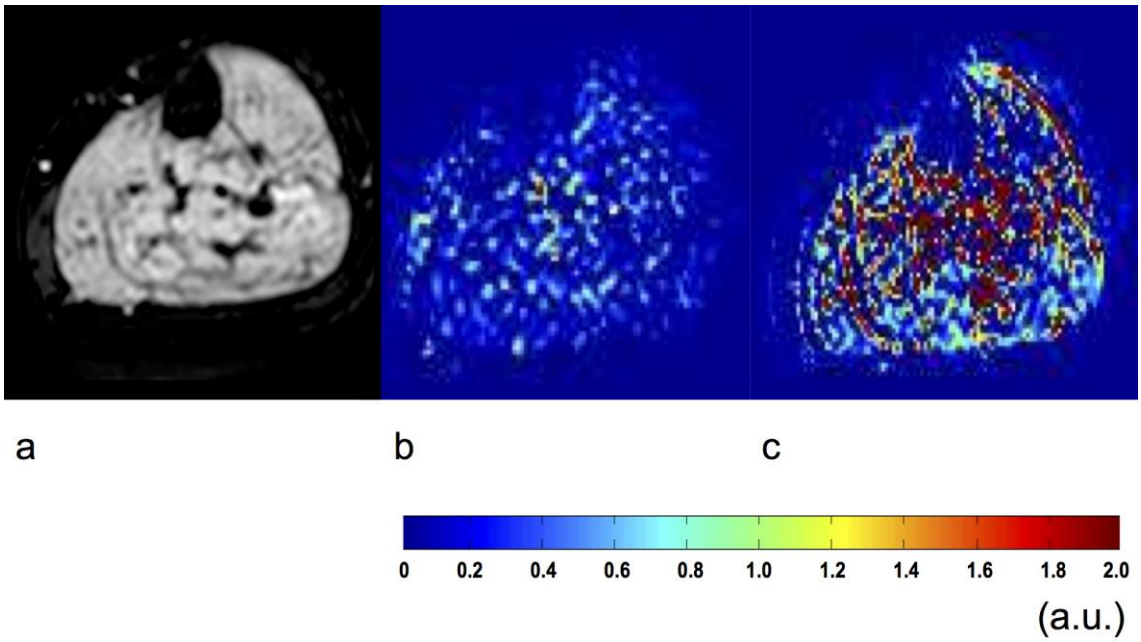


**Figure 1.12: Pseudo-continuous arterial spin labelling (pCASL) MRI sequence in the calf of a healthy volunteer showing echo planar image (a), perfusion map during cuff occlusion (b) and reactive hyperaemia (c). Minimal perfusion is seen during cuff occlusion but reactive hyperaemia demonstrates increased perfusion in all muscle groups in the calf (signal intensity in arbitrary units (a.u.) in perfusion maps).**

Like CEUS and PET, reactive hyperaemia or exercise is required to unmask perfusion deficits with ASL. This technique allows absolute quantification (ml/g/min) of perfusion in the tissues as well as measurement of parameters such as peak hyperaemic flow (PHF) and TTP[103] in a ROI over time. Although ASL has not been validated for the measurement of perfusion in the limb in man, comparison with radiolabelled microsphere measurements in the rat hindlimb ischaemia model and in the porcine cardiac model have shown good correlation for perfusion[100,107]. TTP increases with the severity of PAD, and PHF decreases[103]. Analysis of individual muscle groups in the calf reveals that PHF is preserved in the soleus with increasing severity of PAD compared to the other muscle groups. This may be explained by the dual blood supply of the soleus, which receives blood from both the peroneal and posterior tibial arteries. ASL shows that patients with PAD have lower muscle perfusion after exercise compared with age-matched controls[108].

ASL provides an objective, quantifiable measure of muscle perfusion without ionising radiation or gadolinium based contrast agents, but has limitations including: a low signal-to-noise ratio (because magnetically tagged blood represents only 0.5-1% of the full tissue signal[104]); relatively long scan times and patient movement causing image artefacts; calculations required to quantify perfusion are complex; vascular artefact from large blood vessels causes erroneous measurements; transit time (the time taken for blood to travel from the “tagging” region to the region of interest) is an important source of error that can be potentiated by disease in the peripheral arteries. Echo planar imaging

(EPI) provides faster acquisition, but is associated with magnetic field distortions, making quantification of the MRI signal complex.

***(ii) Blood Oxygenation Level Dependent (BOLD) MRI***

BOLD MRI uses the saturation state of haemoglobin as an endogenous contrast agent. It uses is discussed in more detail in chapter 1.4.

***(iii) First Pass Dynamic Contrast Enhanced (DCE) MRI***

This MRI technique measures cardiac perfusion and has been adapted for assessing perfusion in skeletal muscle[109]. T1 weighted MRI sequences capture the transit of intravenously administered paramagnetic contrast agents such as gadolinium through tissues, and measure changes in signal intensity in the muscle. Mathematical algorithms for tracer kinetics have been investigated to estimate myocardial blood flow, but this has yet to be used in the clinical setting[110].

A reduction in DCE MRI signal intensity, which correlated significantly with radiolabelled microsphere measurements of perfusion, has been demonstrated in the presence of ischaemia in the rat hind-limb model[111]. In man, DCE MRI measures detectable changes in muscle perfusion following thigh cuff-induced arterial occlusion of a healthy limb, compared with the uncuffed contralateral limb[112,113]. A small DCE MRI study, lacking age-matched controls, has suggested that patients with PAD may have a lower “perfusion index” than healthy individuals[114].

The most significant limitation associated with DCE MRI is the need for exogenous gadolinium based contrast agents with their inherent risk of nephrogenic systemic fibrosis (NSF) in patients with chronic kidney disease.

### 1.3.3 Kinetic models used in contrast-based techniques

Kinetic models are needed to quantify perfusion using contrast based imaging modalities to differentiate between the tracer in the arterial system and in the tissues. In PET imaging, $^{15}$Oxygen is freely diffusible into tissue from the intravascular space, which means a simple single compartment model can be applied to quantify muscle perfusion[115]. For DCE-MRI and ASL the modelling is more complex and quantifying perfusion is dependent on deconvolving the arterial input function (AIF), calculated from a major artery proximal to the ROI, from the tissue concentration. A non-linear relationship between AIF concentration and signal intensity can introduce errors. Partial volume, signal truncation and magnetisation transfer effects can also lead to inaccuracies. Finally, the bolus transit time, which is dependent on factors such as cardiac output and rate of injection, can also introduce variability[116].

## 1.4 Magnetic Resonance Imaging

### 1.4.1 Basic Principles

MRI has developed as an important clinical imaging modality ever since Paul Lauterbur and Sir Peter Mansfield independently developed this technique. Both men were awarded the Nobel Prize in 2003 and are considered the fathers of clinical MRI, however the origins can be traced further back for well over a century by seminal discoveries made by mathematicians, physicists and chemists[117].

MRI is based on the electromagnetic activity of atomic nuclei. A simple overview of MRI is shown in figure 1.13. Nuclei contain protons and neutrons, both of which spin around their axis. Protons possess a positive charge and the movement of an electrical charge results in an electrical current. The presence of an electrical current means there is also a magnetic field present. Hydrogen nuclei possess a single proton and clinical MRI scanners exploit the magnetic fields created by spinning hydrogen nuclei (protons) within the body. The hydrogen nucleus is the best for MRI as it is largely abundant in man in the form of water molecules, but also water content in tissues often changes in pathological conditions.

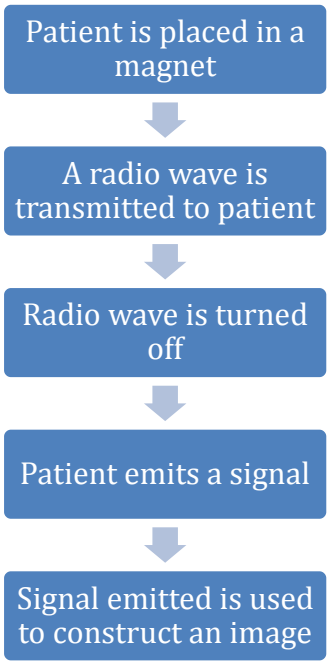


**Figure 1.13: Simple overview of principles involved in MRI**

Protons can therefore be thought of as tiny magnets and when placed in an external magnetic field ($B_0$), as happens in a MRI scanner, results in their alignment in either the parallel or anti-parallel direction to $B_0$, or z-axis of the magnetic field (figure 1.14). Alignment in the parallel and anti-parallel direction results in cancelling out of magnetisation, however as protons aligned in the anti-parallel direction requires a higher amount of energy, more protons align in the parallel direction resulting in a net magnetic field in the direction of $B_0$.

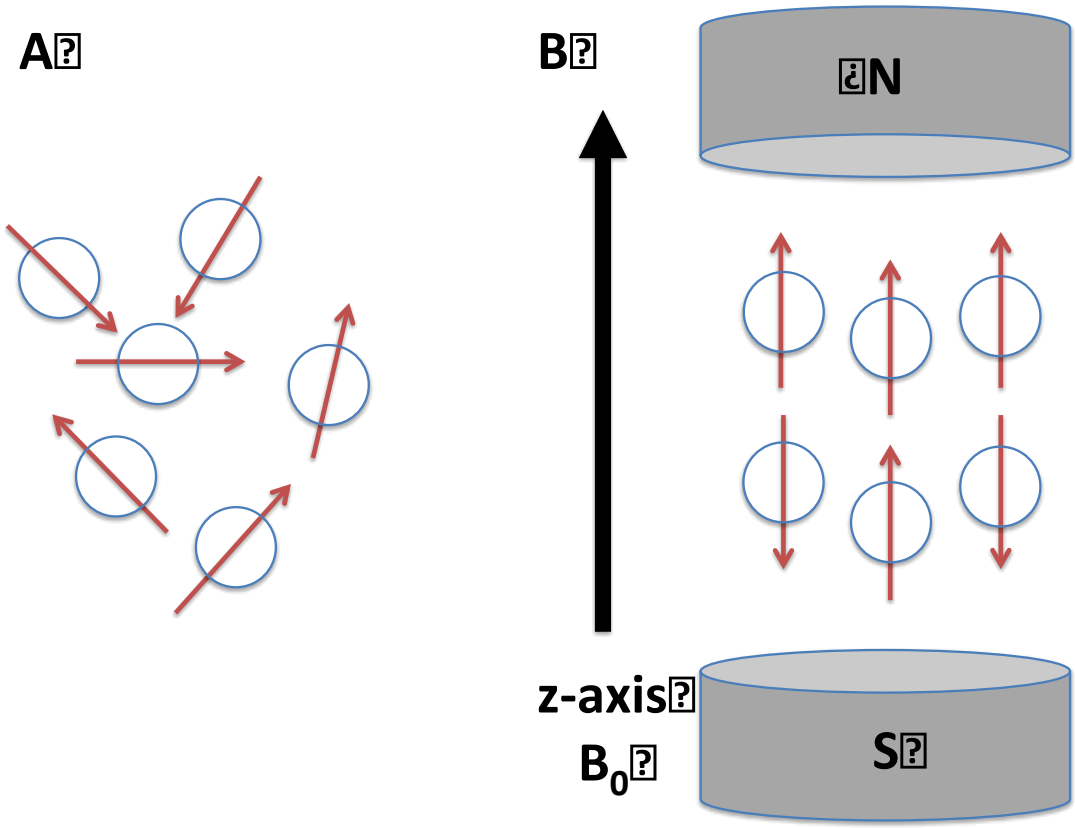


**Figure 1.14: Proton spin occurs in random directions (A), which align either in parallel or anti-parallel direction to the magnetic field in the presence of an external magnetic field ($B_0$).**

Interaction of spinning protons with an external magnetic field also results in the protons to wobble or precess. The frequency at which precession occurs is calculated by the Larmor equation, and is important because at this particular frequency, it is possible to alter the spin of the protons within the magnetic field. As a result of proton precession and alignment, magnetization when placed in an external magnetic field can be represented as a vector quantity in the longitudinal plane (z-axis) and the transverse plane (xy-axis)(figure 1.15).

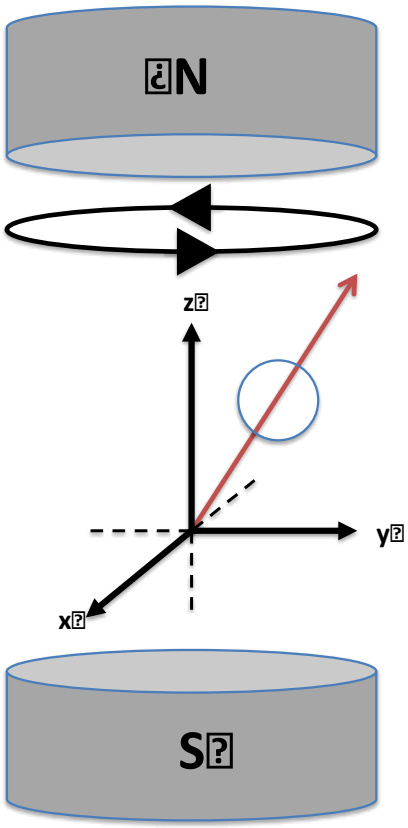


**Figure 1.15: Protons within a magnetic field not only align but also display a wobble motion known as precession. Magnetisation can therefore be seen as a vector quantity in the longitudinal (z-axis) and transverse (xy-axis).**

As precession is occurring in all protons, and occurs randomly there is no net magnetisation in the transverse plane. Therefore, when a patient is placed in the external magnetic field in an MRI scanner, the result is a net magnetisation in the z-axis. It should be noted that as this is in the plane of $B_0$ this signal cannot be measured directly and that only magnetisation in the transverse plane is detectable. To elicit a measurable MRI signal a radiofrequency (RF) pulse is transmitted to the patient. If the RF pulse has the same frequency as the precessing protons (which can be calculated using the Larmor equation) then transfer of energy occurs (resonance) resulting in; (1) protons moving from

a parallel to anti-parallel alignment, which results in a decrease in net longitudinal magnetisation in the z-axis, and (2) protons which were precessing randomly become synchronised and precess together in phase, resulting in the formation of net transverse magnetisation in the xy-axis. As the transverse magnetisation precesses around a receiver coil, it induces a current (in accordance with the Faraday's law of induction). This current ultimately becomes the MR signal. If the RF pulse results in abolishing longitudinal magnetisation completely, and the formation of maximal transverse magnetisation we can say that magnetisation has been flipped $90^0$, from the z-axis to the xy-axis. This is known as the flip angle (FA) in MRI.

When the RF pulse is turned off, the changes that occurred when the pulse was transmitted are reversed. Longitudinal magnetization recovers as protons that moved to a higher energy level anti-parallel alignment flip back to a lower energy parallel alignment. This results in energy release to the surroundings, known as spin-lattice relaxation. If we were to plot the recovery in longitudinal magnetisation after the RF pulse is switched off against time we see a curve as seen in Figure 1.16, also known as the T1 curve. This spin-lattice relaxation can be described as a time constant (usually measured in milliseconds), T1, based on this curve, which represents 63% recovery in the longitudinal magnetisation. Different tissues will have a different T1 dependent its composition and surrounding and therefore can be distinguished on MRI images, for example water has a long T1 compared to fat.

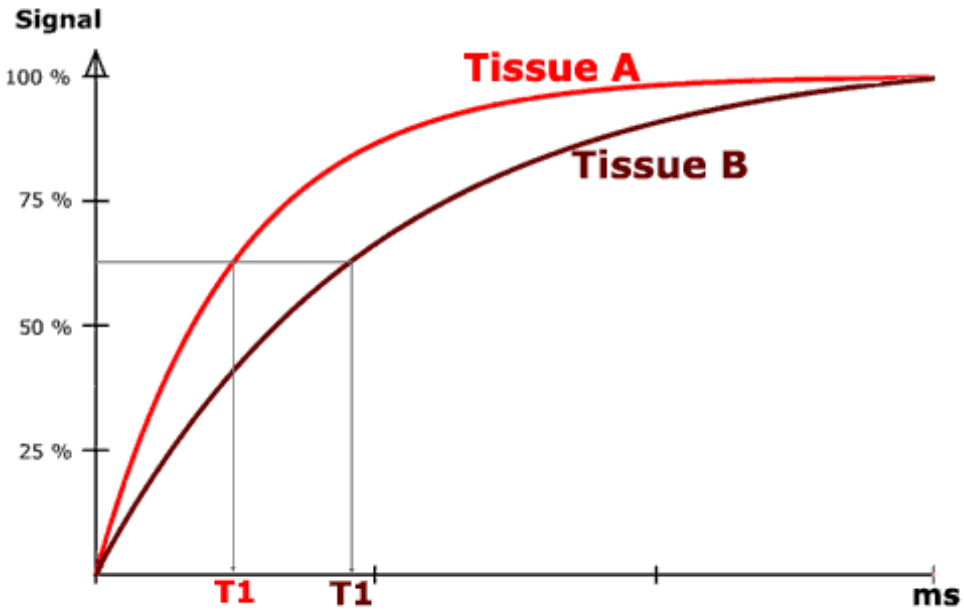


**Figure 1.16: T1 curve showing the return of longitudinal magnetisation after the RF pulse is switched off. The T1 time represents the time taken for the signal to reach 67% of longitudinal magnetisation prior to the RF pulse. Different composition of different tissues results in different T1 times.**

The second effect to occur after the RF pulse is switched off is the decay in net transverse magnetisation as the protons, which started to precess in phase, lose their synchronization. This is due to the interaction with neighbouring spinning protons resulting in inhomogeneities in the magnetic field. This is known as spin-spin relaxation and, as with T1 relaxation can be described as time constant, T2. If the transverse magnetisation decay is plotted against time (T2 curve), T2 represents the time taken for decay in transverse magnetisation to fall to 37% of its original value (Figure 1.17). Transverse magnetization can, however, be also dephased due to magnetic field inhomogeneities. The magnetic field is not exactly the same everywhere because of the limitations of magnetic construction or interaction with compounds that can distort the local

magnetic field, such as paramagnetic effects of de-oxygenated haemoglobin. The result of these magnetic field inhomogeneities results in a more rapid dephasing of precessing protons. The decay in transverse magnetization due to these factors is known as T2* decay and takes into account T2 relaxation in addition to the magnetic inhomogeneities. T2* decay is therefore always shorter than T2.

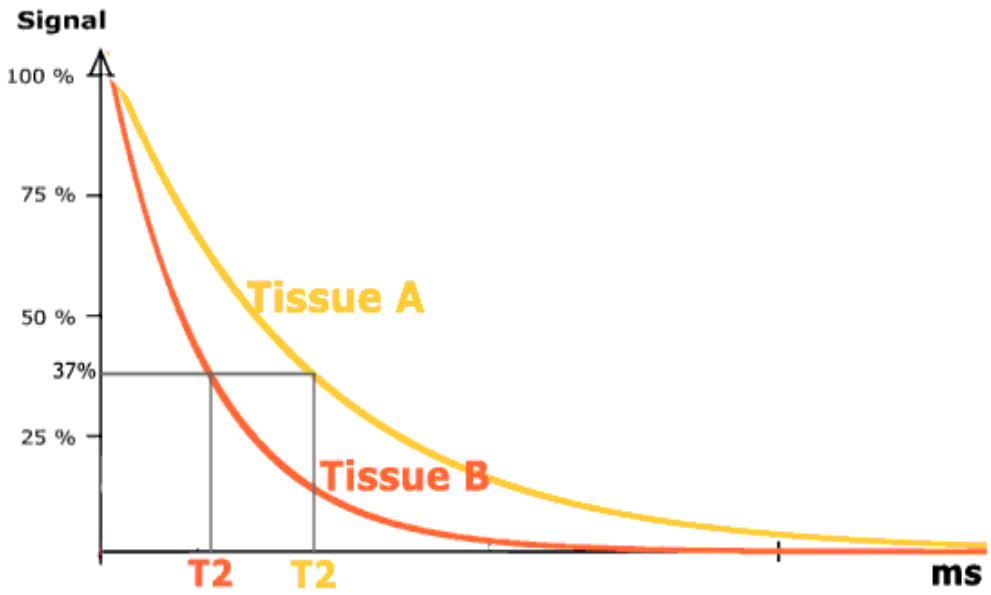


**Figure 1.17: T2 curve showing decay in transverse magnetisation after RF pulse is switched off. T2 time is defined as the time taken for the signal to reach 37% of its original. Different tissues will have different T2 due to their composition.**

### 1.4.2 Time to Repeat, Time to Echo

Manipulating the RF pulse forms the basis of the contrast generated with MRI, such as T1 weighted, T2 weighted images or contrast due to proton density. The two parameters that important in this process are time to repeat (TR) and

the echo time (TE). TR is the time between the applications of two RF pulses and is usually measured in milliseconds. TE (also measured in milliseconds) is the time between the application of the RF pulse and the peak of the echo detected following this application.

TR is directly related to T1 and affects T1 weighted images. When TR is short (typically less than 500milliseconds) it is possible to detect contrast between tissue due to its different composition, usually due to changes in water and fat content. As the T1 of water and fat are different, the amount of longitundinal relaxation that will have occurred will be different before the next RF is transmitted, which results in the contrast between the two. Therefore short TR will make the image T1 weighted. If TR is long (typically greater than 1500milliseconds), the tissues have time to recover their longitundinal magnetisation and as such there is little difference seen in T1 signal.

TE relates to the decay in transverse magnetisation and as such affects contrast on T2 weighted imaging. After a RF pulse is transmitted, transverse magnetisation is generated which will decay over time due to loss in synchronisation in precessing protons. However, if were to send in a RF pulse that flips magnetisation by $180^{o}$, this will result in refocusing of protons returning to be in phase, and therefore an increase in transverse magnetisation. The time taken for this refocusing is TE. The effect of this $180^{o}$ pulse is to neutralise the magnetic field inhomogeneities to produce a pure T2 effect. If we do not use a $180^{o}$ refocusing pulse however, the decay in transverse magnetisation is much faster, and this is due to these magnetic field inhomogeneities and as a result this is the T2* decay (Figure 1.18).

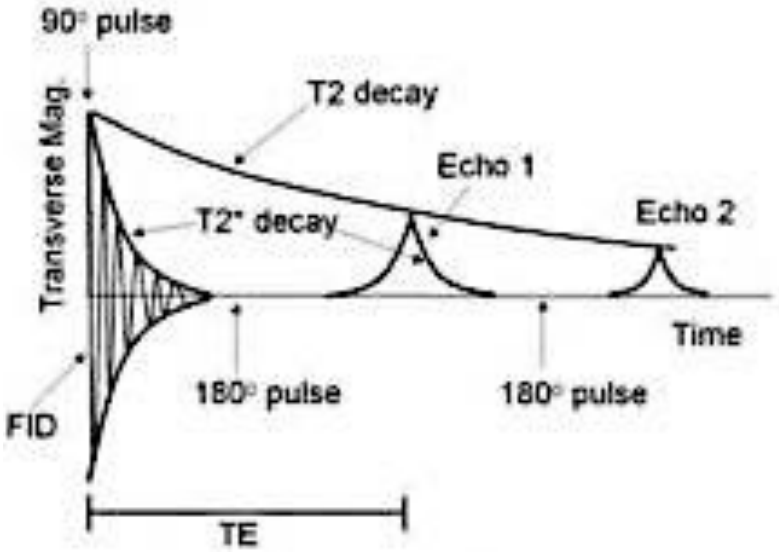


**Figure 1.18: T2* relaxation is faster than T2 relaxation due to both T2 effect and magnetic field inhomogeneities. An 180$^{o}$ refocusing pulse can eliminate the inhomogeneities to produce a true T2 effect.**

### 1.4.3 MR signal localisation

The area of the body to be examined can be selected by using a gradient field, which is superimposed on the external magnetic field. A gradient coils generate these gradient fields. Protons along this superimposed gradient have a different precession frequency compared to protons not exposed to the gradient field, and thus a RF pulse of can be generated which only excites protons in the area we wish to examine. Information detected is stored within the MR system in an area termed ‘k-space’. Their location is subsequently calculated with mathematical modeling using the inverse Fourier transform.

### 1.4.4 MR Sequences

Pulse sequences are waveforms created from the gradients and RF pulses used to generate a particular MR image. Pulse sequences are therefore the 'sheet music for the MR system orchestra'; a diagram of the timing instructions sent to the RF generator and gradient. There are two fundamental types of MR sequences are used. These are termed the spin-echo (SE) sequence and the second is a gradient-echo (GRE) sequence. Other MR sequences are essentially variations of these basic types. SE MRI sequences utilize a $90^{o}$ flip angle and a refocusing $180^{o}$ RF pulse to produce a T2 weighted image, eliminating any T2* effect. GRE sequences differ from SE in that the flip angle is usually less then $90^{o}$ and by the absence of $180^{o}$ refocusing RF pulse. This results in faster acquisition time compared to SE sequences as transverse relaxation recovers more quickly. As there is no refocusing $180^{o}$ pulse the MRI signal obtained is due to T2* effect and not T2 decay.

MR sequences can be either two-dimensional (2D), with one section acquired at a time, or three dimensional (3D) with a volume of multiple sections obtained using a single acquisition.

## 1.5 Blood Oxygenation Level Dependant (BOLD) MRI

Blood Oxygenation Level Dependent (BOLD) MRI was first developed in 1990 as a functional tool for mapping changes in oxygenation level in the blood supply to the brain[118]. The BOLD effect seen on MRI utilises the saturation state of haemoglobin as an endogenous contrast agent. Deoxyhaemoglobin is paramagnetic, whereas oxyhaemoglobin is diamagnetic, and it influences the water proton in its vicinity. The paramagnetic effect of deoxyhaemoglobin leads to increased inhomogeneity in the external magnetic field which results in a decrease in the T2* signal. A decrease in deoxyhaemoglobin, therefore, can be observed as increase in BOLD signal in T2* weighted MRI sequences.

Utilising the difference in magnetic properties of haemoglobin depending on its oxygenation status, and linking this with brain activation leading to an increase in blood flow[119], allowed BOLD MRI to be used to map areas of brain activation and subsequently be used as a functional tool to assess brain function and perfusion in a variety of neurological pathologies[120].

The development of BOLD MRI to measure brain perfusion preceded its use for the assessment of perfusion in other organs. It has now been used to determine perfusion in the heart[121–127] and kidney[128–135]. The angiogenic drive (and associated hyper-perfusion state) in tumours means that BOLD MRI can be utilised in the assessment of different cancers and more recently in the tumour response to medical therapies[136–138].

BOLD MRI has also been assessed as a tool for measuring perfusion in skeletal muscle, including quantification of perfusion in the ischaemic limbs of patients with PAD. The appeal of BOLD MRI is that it is an image modality that does not require the administration of exogenous gadolinium based contrast agents (as with DCE MRI), with its inherent risks of NSF in patients with chronic renal impairment, and does not expose patients to ionising radiation (as with PET or CT).

BOLD MRI was first used for measuring limb perfusion by Toussaint et al in 1996[139], who demonstrated a good correlation between perfusion measured by BOLD MRI and VOP in normal subjects. This stimulated more studies in utilising BOLD MRI to measure perfusion in skeletal muscle.

BOLD MRI measurements are usually taken through a section of the calf at rest. As mentioned before, hyperaemic response is required to evoke a measurable change in perfusion. Reactive hyperaemia after arterial occlusion offers the most reliable method of achieving this, and has been used in almost all BOLD MRI studies. T2* signal changes are measured prior to cuffing, during arterial occlusion inducing transient ischaemia (usually for a few minutes) and after cuff deflation provoking reactive hyperaemia. Signal intensity time course curves are generated from changes in T2*. Different parameters from this curve have been used to assess perfusion and, probably more importantly, changes in perfusion associated with the increased demand of reactive hyperaemia. Curve parameters most commonly used to assess muscle perfusion include minimum T2* during ischaemia (T2*Min), TTP, time to half

ischaemia (THIM) and maximum T2* (T2*Max) during reactive hyperaemia[140,141].

BOLD MRI has been used to detect changes in muscle perfusion in patients with PAD and healthy controls[101,142–144]. Patients with PAD have significantly reduced T2*Max and a prolonged TTP compared with age-matched healthy controls[142].

In patients with PAD undergoing revascularisation with angioplasty it has been shown the T2* signal intensity returns to baseline faster and there is a trend towards a higher T2*Max value and faster TTP, when compared with pre angioplasty of superficial femoral artery lesions in patients with intermittent claudication[143], indicating that arterial revascularisation has an impact on the BOLD MRI signal.

Changes in BOLD T2* signal intensity correlate with: LDF and TcO2 (measure skin perfusion) in the ischaemic-reactive hyperaemic model[144]; tissue oxygenation (measured by myoglobin proton MR spectroscopy)[145]; and perfusion measurements made using VOP adapted for MRI and ASL MRI[139].

Age related in muscle perfusion has also been investigated[146,147]. Studies have demonstrated that older subjects have a lower T2*Max, longer TTP and longer THIM compared to younger controls. Age related changes in muscle perfusion are due to a combination of reduced capillary density, increased vascular rigidity, increased sympathetic vasoconstriction and/or reduced vasodilatation[148–152]. If BOLD MRI is able to detect age related changes in

muscle perfusion without overt signs of PAD, then it can be reasoned that it can used to assess conditions where perfusion may be altered due to factors other than PAD, such as chronic compartment syndrome[153] and systemic sclerosis[154].

Although the source of the BOLD signal in peripheral skeletal muscle is not fully understood, it is generally accepted that the signal is mainly related to tissue oxygenation state[140,141]. BOLD MRI, unlike ASL, DCE MRI and PET, does not allow absolute quantification of perfusion, but instead relies on ratios in signal changes for semi-quantitative measurements. BOLD does, however, produce a better signal to noise ratio, which allows superior spatial and temporal resolution compared with ASL MRI. The lack of reproducibility has also been a weakness of BOLD MRI in the assessment of muscle perfusion[155].

## 1.5 Rationale for this study

CLI is major cause of morbidity and mortality[5]. Revascularisation is the mainstay of managing these patients to relieve their symptoms and prevent major limb loss in the future. Nevertheless up to a 30% of patients will eventually require a major amputation[1,3]. Traditionally revascularisation of the limb has concentrated on improving the major arteries leading to the limb, either with angioplasty or with open surgical techniques. This improves the “inflow” into the limb with the aim of increasing perfusion to the muscle. The pathophysiology of PAD is for one reason or another a lack or blood supply to the muscle in the limb, which may involve the major arteries supplying the limb,

but may also include a component of microvascular disease restricting perfusion at the more cellular level, as is the case in patients with diabetes mellitus.

At present we have no reliable method for the assessment of muscle perfusion in the leg[52]. Current methods to assess perfusion, such as VOP, LDI and TcPO2 either measure global changes in the limb or skin perfusion and can be unreliable. At present the success of revascularisation in patients with PAD is ultimately assessed by clinical improvement in symptoms. In the case of CLI and tissue loss, the clinical improvement is not immediate and therefore these patients have to wait to see if improvement occurs over a number of weeks. In a number of these patients a window of opportunity may be lost to intervene early to improve perfusion further if the revascularisation performed is ultimately found to be inadequate to rescue the limb. An imaging modality that assesses perfusion in the muscle directly and that can assess perfusion in individual muscle compartments may help in the management of patients with PAD, and reliably assess the success of revascularisation, with the ultimate aim to trying to improve limb salvage.

New developments on the horizon including stem cell and angiogenic cell therapies may help to improve the perfusion at the cellular level via angiogenesis and arteriogenesis[39,41,42]. Having a reliable, reproducible method to assess muscle perfusion may aid in the development of these techniques by identifying targets for cell therapy and to monitor changes in perfusion to identify if the treatment is successful.

More recently the concept of angiosomes[44] has been introduced in the planning of arterial revascularisation[45,46]. If the angiosome concept is to be believed then targeted revascularisation of arteries supplying the area to the lower limb mostly affected by PAD may improve the outcomes, particularly in CLI. Following this, an imaging modality they can assess segmental muscle perfusion would allow for identification of regions of the lower limb that are most ischaemic to target intervention and monitoring the success of revascularisation. Methods such as VOP and ABPI assess global change in the limb and as such would not identify particular angiosomes that require intervention.

An ideal imaging modality for the assessment of muscle/tissue perfusion in the lower limb would need to provide reliable and reproducible quantative or at least semi-quantative measures of perfusion with minimal risk to patients. MRI is attractive in that it does not subject the patient to exposure to ionising radiation, as with CT or PET. Also more recent developments in MRI sequences (ASL and BOLD) allow for the use of endogenous contrast agents without the need for intravenous administration of contrast (as with CEUS, CTA, DCE MRI, IGCA). MRI also provides anatomical information allowing for segmental assessment of muscle perfusion (unlike VOP and ABPI) and assesses deeper tissue perfusion, not just skin perfusion (unlike LDI, TcPO2).

Therefore both BOLD and ASL MRI represent very attractive methods for assessing muscle perfusion. ASL has the advantage of providing absolute quantitative measures of muscle perfusion but requires complex kinetic modelling, which has the ability to introduce errors in the measurement. Although BOLD MRI does not provide absolute quantitative measure of

perfusion it does have a much better signal to noise ratio compared to ASL, which helps in obtaining reliable and potentially reproducible measures of perfusion. As most perfusion imaging modalities require a model of evoking a hyperaemic response of some kind, and actually the changes in perfusion seem to provide more useful information rather than absolute measures of muscle perfusion, the disadvantage of not having absolute measures with BOLD MRI seems to be diminished. Also the advantage of using MRI perfusion imaging means that it can be easily combined with conventional MRA to provide both functional and anatomical imaging in patients with PAD, which can assist in planning and surveillance after intervention. The improved spatial resolution of BOLD MRI compared to ASL also makes this more attractive as imaging technique.

The introduction of advanced MRI perfusion techniques to assess tissue perfusion in other regions of the body along with the lack of a true measure of muscle perfusion in the lower limb warrants investigation to see if techniques can be translated into the lower limb musculature in a reliable and reproducible way.

## 1.6 Hypothesis

BOLD MRI can be used reliably and in a reproducible manner for the objective assessment of muscle perfusion in the lower limb.

## 1.7 Aims

1. Develop MRI sequences to accurately measure signal changes in BOLD contrast.
2. To assess the reproducibility of BOLD MRI for measuring muscle perfusion in the lower limb.
3. To quantify calf muscle perfusion, using BOLD MRI, in patients with CLI and compare this with normal healthy and age-matched controls.
4. To correlate changes in perfusion measured with BOLD MRI using histological measures of vascularity.
5. To evaluate the utility of BOLD MRI in the assessment of changes in perfusion after successful revascularisation

# CHAPTER 2

## General Methods for Imaging & Image Analysis

### 2.1 Introduction

Methods for imaging subjects with MRI and the analysis of images were consistent throughout the study and will be explained in this chapter.

### 2.2 Study Participants

This study complies with the Declaration of Helsinki and ethical approval for the recruitment of subjects to the study was obtained from the local ethics committee at Guy's & St Thomas' NHS Foundation Trust (10/H0804/67)(See Appendix 1). Subjects recruited for this study included young healthy controls without PAD, patients with critical limb ischaemia who were under the care of the Department of Vascular Surgery at Guy's & St Thomas' Hospital, and age-matched controls recruited from friends and family of patients, non-vascular patients admitted to hospital (e.g. hernia patients) and hospital volunteers. Age matched controls did not have evidence of PAD determined by ABPI and palpable pedal pulses. All subjects were provided with written information regarding the study and written consent was obtained.

All subjects recruited to the study were screened to assess eligibility to undergo scanning with MRI. To conform to local guidelines all subjects were required to complete a questionnaire, which was authorised by a trained MRI user, prior to

admission into the scanner. Exclusion criteria were: (i) presence of cardiac pacemaker/defibrillator or other magnetically active implants, such as cochlear implants, neurostimulators or insulin pumps; (ii) severe claustrophobia; (iii) fixed flexion deformities of the lower limb where the subject is unable to place the leg flat on the MRI table; and (iv) subjects unable to consent.

## 2.3 MRI

All subjects were scanned at 3 Tesla with a Philips Achieve scanner (Philips Healthcare, Best, The Netherlands). A 32-channel RF cardiac coil was placed over the lower calf of both limbs. The RF coil was fixed to the imaging table with the aid of Velcro straps to prevent coil movement. Both legs were fixed with the aid of sandbags to minimise movement artefact during scanning (Figure 2.1). All subjects were scanned on the same scanner. In all subjects a

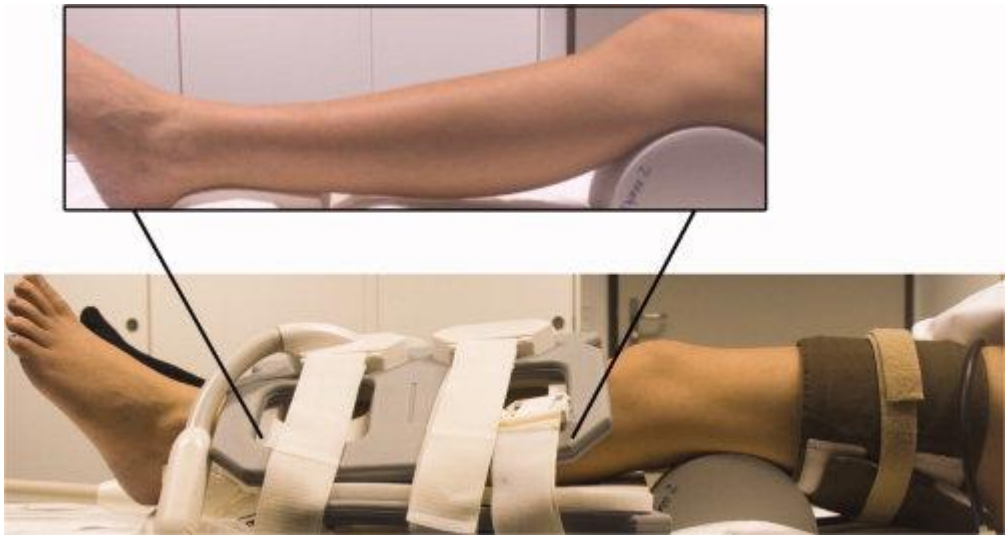

**Figure 2.1: Setup of subjects in the MRI scanner, with thigh cuff in place and 32-channel RF coil placed on the lower leg, centred on the largest part of the calf.**

T2 weighted image was also acquired at the same level of the calf as for perfusion imaging to accurately highlight the anatomy of the calf. MRI scanning time for all the perfusion-imaging sequences, along with anatomical scans was in the region of 20-25minutes.

All subjects were asked to refrain from nicotine, caffeine and strenuous exercise 4hours prior to imaging. The reason for this was that caffeine and nicotine are vasodilators, which may influence the ischaemia and reactive hyperaemia provoked with suprasystolic thigh cuffing. Similarly, strenuous exercise results in changes to perfusion in the lower limb with subsequent changes in T2* signal. All subjects were required to rest supine for a minimum of 5minutes prior to the start of the scan to reduce venous filling in the limb, which has been shown to influence T2* signal[101].

## 2.4 Cuffing Model for Eliciting Ischaemia & Reactive Hyperaemia

To elicit measurable changes in T2* a cuffing model was chosen to evoke first ischaemia and then subsequent reactive hyperaemia. This model was chosen over others for a number of reasons. The use of thigh cuff inflated to suprasystolic pressure and subsequently deflated allows for complete occlusion of inflow and outflow from the leg. This minimises the influence of venous filling on the T2* signal. This model also allows for standardisation for all participants in the study, as everyone is subjected to the same stress. Cuffing also eliminates the need for subject compliance during the study, therefore further reducing error. Finally the use of a cuff, as opposed to exercise models for

reactive hyperaemia, reduces motion artefact which would degrade image quality and affect image analysis of T2* signal.

Both legs were imaged with MRI and therefore both legs were cuffed, except for when assessing different MRI sequence. During development one leg was cuffed at a time to allow comparison of different MRI sequences sensitive to T2*. A 20cm MRI compatible cuff placed around the thigh was used. The dynamic imaging protocol was as follows: 2minutes baseline measurement, prior to cuff inflation to suprasystolic pressures. The cuff was then rapidly inflated, within 20seconds to 50mmHg above systolic pressure and maintained at this pressure for 5minutes (Ischaemic Phase). After 5minutes of the ischaemic phase the cuff was rapidly deflated via a one-way valve to evoke reactive hyperaemia. Scanning continued after cuff deflation for 5minutes. Therefore dynamic functional imaging took 12minutes (Figure 2.2). The same investigator was used to inflate the cuff each time.

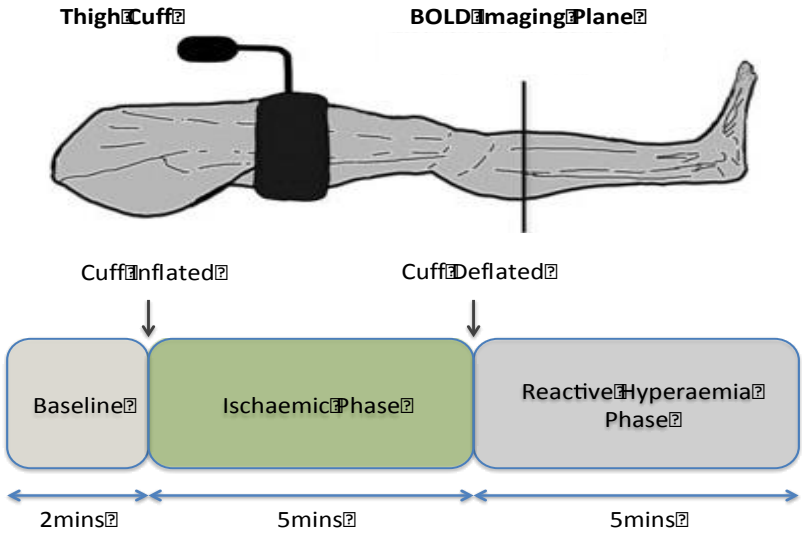


**Figure 2.2: Protocol for thigh cuff inflation and deflation to induce ischaemia and evoke reactive hyperaemia in subjects**

## 2.5 T2* response

Using the cuffing model to elicit ischaemia and reactive hyperaemia results in typical changes in T2* signal. During baseline imaging at the start of dynamic imaging the T2* signal is constant. Initiation of cuff inflation to suprasystolic pressures results in occlusion in flow to the muscle. This results in a decrease in oxygenated haemoglobin and with utilisation of oxygen an increase in deoxygenated haemoglobin. This results in a decrease in T2* signal during cuffing. When the cuff is deflated perfusion is increased. This results in an influx of oxygenated haemoglobin and washout of deoxygenated haemoglobin. The T2* signal rapidly increases to reflect this and results in an overshoot above the baseline as more oxygenated haemoglobin is delivered then is required. The overshoot settles back to baseline, as equilibrium between oxygenated and deoxygenated haemoglobin is re-established (See figure 2.3).

## 2.6 Image Analysis

To assess changes in perfusion using BOLD MRI signal intensity time course curves need to be generated throughout the dynamic imaging phases. Different regions of interest (ROI) can be drawn in individual muscle compartments or groups to identify segmental changes in T2* in the lower leg. These curves show the change in T2* signal as a result of cuffing and decuffing. Different parameters of the curve can then be analysed to assess perfusion in the muscle.

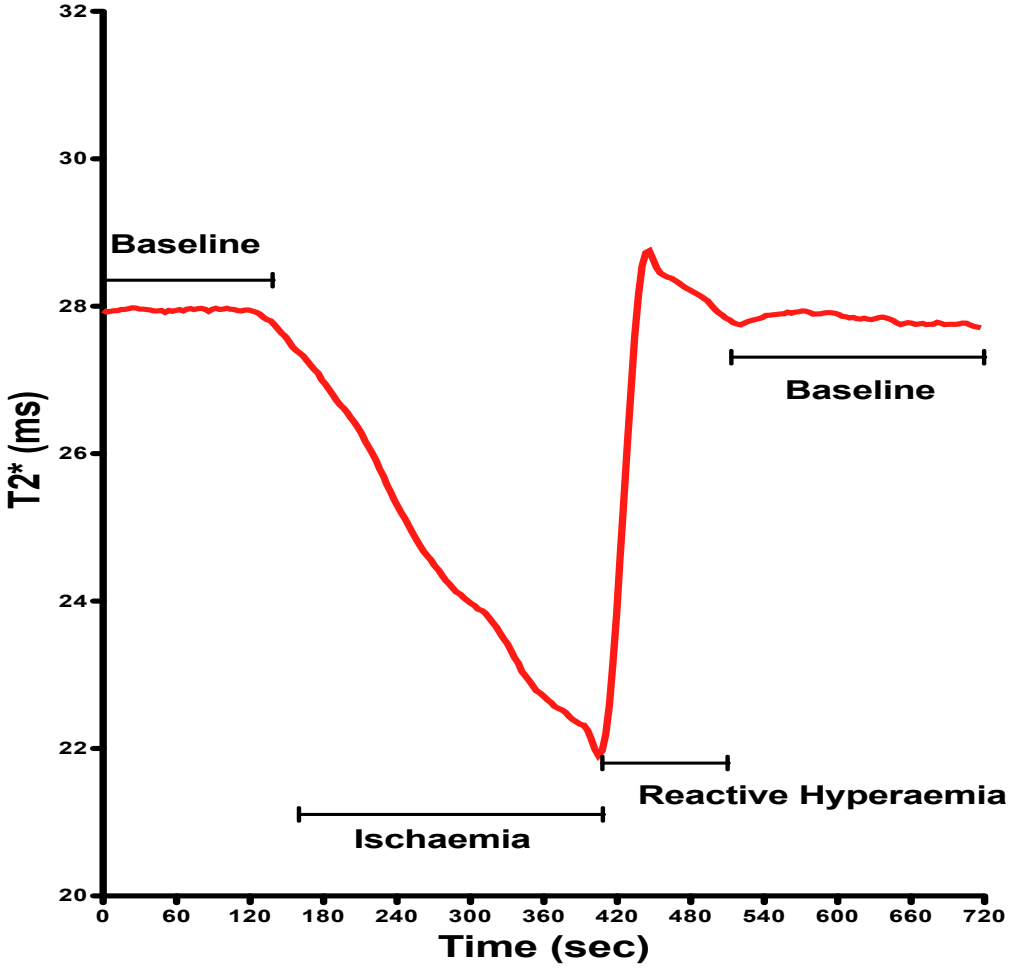


**Figure 2.3: Typical T2* signal response in a normal subject. Steady signal at baseline is followed by a decrease in T2* signal with cuff inflation and ischaemia. Cuff deflation results in reactive hyperaemia represented by an increase in T2* signal and overshoot before the signal falls back to a steady baseline.**

Dicom files of T2* images acquired, either T2* weighted EPI images or T2* maps from the GRE sequence, were imported into the software for analysis. For this study we used 5 muscle groups in the calf (anterior, lateral, soleus, gastrocnemius and deep posterior) to draw our ROI's in each leg. The T2 weighted anatomical image allowed for accurate delineation of each individual muscle compartment (Figure 2.4). This allowed comparisons of different muscle compartments, with their inherent blood supply. The use of the muscle

compartments also allows easier exclusion of major blood vessels, bone and soft tissue from the analysis allowing accurate delineation of T2* signal changes in the muscle only as a marker for perfusion.

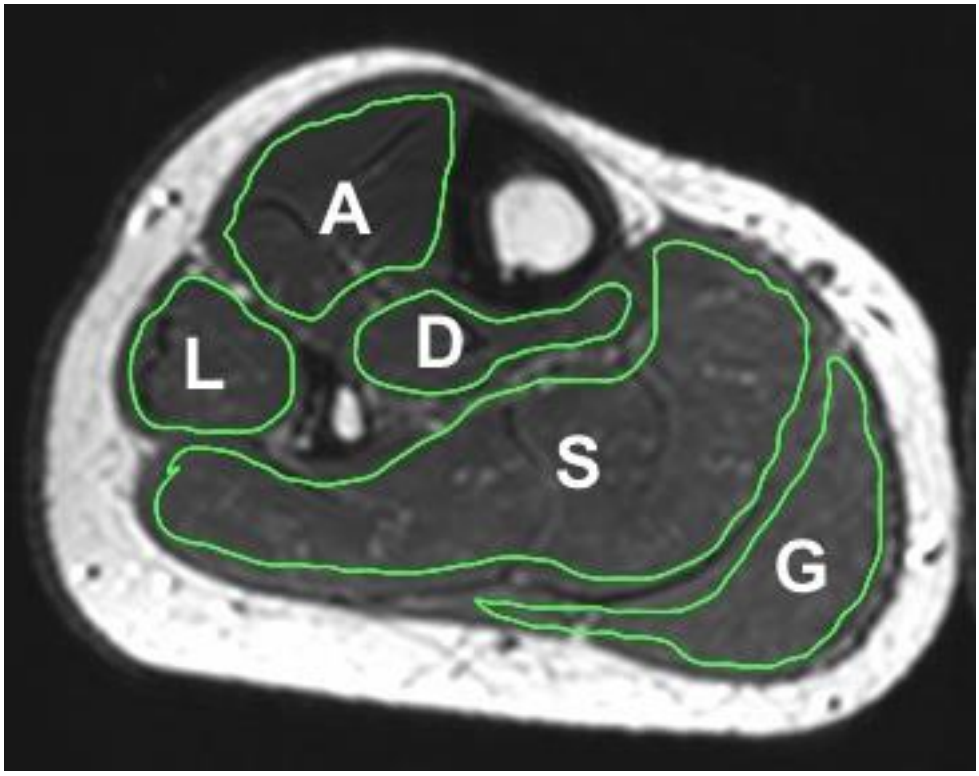


**Figure 2.4: T2 weighted anatomical image demonstrates the muscle compartment in the calf (A=Anterior, L=Lateral, D=Deep, S=Soleus, G=Gastrocneumius)**

To improve reliability and reproducibility of BOLD-MRI software was developed for automated analysis of images using MATLAB (Mathworks, Mass, USA) routines (Appendix 2). The software allowed the user to:

1. Import DICOM images from the dynamic imaging in a time ordered fashion for analysis of T2* signal changes.

2. The user to manually input ROI's in individual muscle groups on functional images, using the T2 weighted anatomical images.
3. The user to manually adjust the ROI's to account for any motion or volume changes in the limb related to cuffing and decuffing.
4. Automatic generation of signal intensity time course curves for each ROI inputted on a pixel by pixel basis for each region.
5. Automated analysis of different curve parameters.

Different aspects of the signal intensity curve can be analysed as a marker for perfusion. We analysed all parts of the curve using the automated software to try to identify the most informative parameter using the ischaemia-reactive hyperaemia cuffing model. Traditional measures from the curve have included TTP, T2*Max, T2*Min and THIM. However there are more aspects to the curve that can be assessed and some of the more traditional parameters can be assessed with a more accurate and objective method. The various parameters measured are shown in figure 2.5.

The software automatically generated signal intensity time course curves for each ROI inputted. From the curves the software calculated various parameters as follows. The gradient (Grad) was calculated by taking the first derivative of each point after cuff deflation until the maximum T2* value, and then taking the mean for the highest 10 values during this period. Signal reduction during the ischaemic phase (SRi) was calculated as a percentage drop in T2* signal from mean during initial baseline to the minimum T2* at the

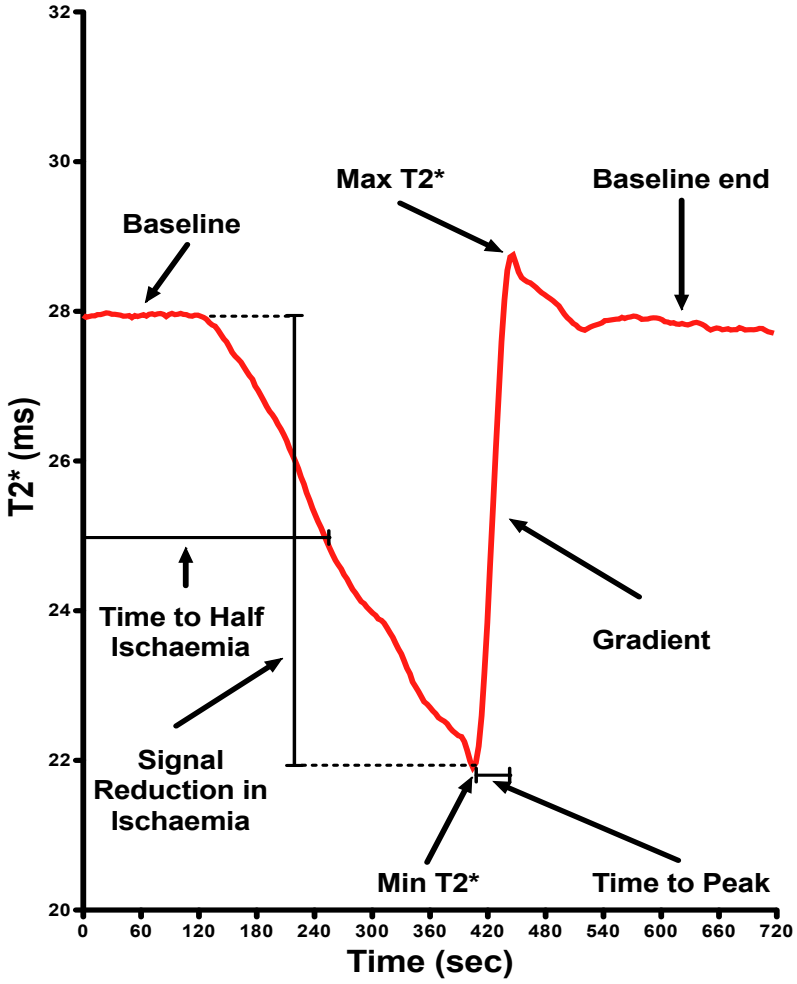


**Figure 2.5: Typical T2* signal intensity time course curve showing all the parameters assessed with the analysis software program**

end of the ischaemic phase. Baseline at the start was calculated as a mean of T2* signal over 90 seconds prior to cuffing, excluding 15seconds at the start of the scan and 15seconds before cuff was inflated. Baseline at the end was measured as a mean of the last 90seconds of dynamic imaging with BOLD-MRI. T2*Min value was calculated as the lowest T2* signal intensity prior to reactive hyperaemia and similarly T2*Max value was calculated as the highest signal after cuff deflation and initiation of reactive hyperaemia. TTP was

measured as time from cuff deflation till the maximum T2* in reactive hyperaemia. The time to half ischaemia (THIM) was calculated as the time from the start of the scan until 50% reduction in T2* signal after cuff inflation.

Image analysis was carried out by myself for all scans, with a second blinded user for reproducibility studies. The process of image analysis as described above took in the region of 20-30minutes with generation of signal intensity time course curves and curve parameters. Normalised signal intensity time course curves were created from the raw data to allow for comparisons between subjects.

## 2.7 Discussion

During this study, a standardised method for imaging subjects was used. This allowed for reliable and objective assessment between subjects. All subjects were imaged using the same 32-channel RF coil, with the same investigator used to inflate the cuff. The same MRI scanner was used. Also as both legs were imaged during BOLD-MRI development it was possible to use individual limbs, cuffed sequentially to compare different sequences. When comparison was made between patients and controls it was possible to use both legs in control patients to gather perfusion data, and also in PAD patients the symptomatic limb as well as the contralateral limb could be analysed.

The ischaemic-reactive hyperaemia cuffing model was utilised as this provides the most reliable and reproducible model for evoking changes in muscle

perfusion in the limb[140,141]. This model eliminates any motion artefact, which is particularly problematic in cross-sectional imaging, such as with BOLD-MRI. It also allows for a standardised method to provoke the stress.

Other methods to evoke reactive hyperaemia include the use of vasodilators, exercise and inhaling oxygen. The use of vasodilators, such as adenosine or prostaglandins, to evoke reactive hyperaemia requires invasive cannulation and extra monitoring of subjects is needed. Although vasodilators are generally thought to be safe, there are side effects associated such as chest pain, light headedness and difficulty breathing and are contra-indicated in certain cases. Further, they usually required to be administered via an intra-arterial route to provide maximal vasodilation, which carries a higher risk of complications, such as infection, bleeding and vessel injury, compared to intra-venous access.

Exercise testing has been extensively utilised as a method for producing reactive hyperaemia. The use of pedal ergometers allows for standardisation of the amount of work required by subjects. The problems arise with motion artefact, as perfusion assessment is required fairly rapidly after the cessation of exercise. It is not possible to perform MRI assessment during exercise as motion significantly degrades image quality and makes analysis of during a dynamic sequence almost impossible. Also for MRI, a compatible ergometer is required that can safely be used within the magnetic field of an MRI scanner. Exercise stressing also requires compliance on behalf of the subjects. This can more problematic in patients with PAD, where they are not able to achieve the amount of work required before the onset of symptoms of pain. PAD patients

also find it harder to keep their limbs still after exercise increasing issues with motion artefact.

Oxygen inhalation has also been used to increase the BOLD signal[156–158]. Problems with this method arise as most healthy individuals have an oxygen saturation of 98-99% and so inhalation of supplemental oxygen does not result in an increase in oxygenated haemoglobin but instead an increase in dissolved oxygen in the blood. This does not result in a major change in the ratio between oxygenated and deoxygenated haemoglobin, which forms the basis of the signal in BOLD-MRI. Also this method relies on adequate oxygen transfer in the lungs, which maybe impaired in patients with respiratory disease, making it difficult to distinguish between a ventilation deficit and oxygen delivery capacity.

The low perfusion of muscle at rest, coupled with the variability seen during exercise makes assessment of muscle perfusion difficult. This means the use of these models is important in measuring muscle perfusion because they ensure changes of perfusion throughout the duration of functional imaging and it is these changes that provide measurable outcomes when using many of the modalities. To be able to analyse these changes forms the basis by which BOLD-MRI is used as a tool for assessing muscle perfusion. The expected change in T2* signal provides a template by which we can determine perfusion changes in pathological conditions. Therefore it is important to have a robust method to analyse the functional images. The image analysis program developed here allows for a semi-automated method to determine changes in BOLD signal as a marker of perfusion, where the input of regions of interest is

required by the user, but the generation of signal intensity time course curves and the analysis of different curve parameters is done in an automated fashion. This allows for a standardisation of the analysis with a view of improving the reliability and reproducibility of BOLD-MRI. Previous studies have highlighted this as an issue when using this modality[155].

Previous studies with BOLD-MRI have identified certain curve parameters most useful in distinguishing between patients and controls[101,139,142–144,147,153–166101,139,142–144,147,154,155,157,159–166]. TTP, T2*Max, T2*Min and THIM have been shown to be most informative. However, analysis of these parameters can be difficult, particularly in patients with PAD. For example, when measuring TTP the overshoot in reactive hyperaemia can be difficult to identify. Also absolute measures of T2*Max and T2*Min can make comparison between subjects troublesome as the absolute values can differ from patient to patient. For circumvent some of these issues new parameters from the time course curves were identified. Grad measures the slope of the reactive hyperaemia portion of the curve and is analogous to TTP, but as it is not dependent on an identifiable peak value overcomes this shortcoming. SRi interrogates the ischaemic part of the curve and represents a percentage fall in signal during ischaemia. This overcomes the issues of using absolute values in measuring T2*Min, allowing for meaningful comparisons of values between subjects.

All imaging for this study was carried out using a 3T MRI scanner. Imaging at this higher magnetic field, compared to more conventional 1.5T scanners improves the signal to noise ratio when utilised in BOLD-MRI[127,160,167]. Imaging with a higher magnetic field scanner will also increase the sensitivity to

magnetic field inhomogeneities, with improved sensitivity to BOLD signal. The signal generated in BOLD-MRI is miniscule, approximately a few percent at 1.5T, making it difficult to distinguish above the intrinsic noise[167]. 3T scanners are now becoming more available in clinical use and there is now research being performed in humans on 4.7T, 7.0T and even 9.4T scanners. With the advances in both magnetic field strength and with computing power to develop more complicated sequences the accuracy of BOLD-MRI can only be improved.

# CHAPTER 3

## Development of BOLD MRI Sequence

### 3.1 Introduction

BOLD-MRI has traditionally been performed using echo-planar imaging (EPI) MRI sequences. EPI are fast acquisition MRI sequences that allow for speedy acquisition of k-space. However, the speed of acquisition comes at the cost of spatial resolution. Nevertheless, the speed of EPI makes it very attractive in BOLD-MRI, as temporal resolution is important in detecting changes in signal over time in response to stressors, such as in the ischaemia-reactive hyperaemia model. EPI sequence can come a variety of guises depending on the weighting of images needed. For BOLD-MRI the sequences need to be T2* weighted to capture BOLD signal in the tissue. This can be achieved with EPI using a gradient echo method (GE-EPI). As already discussed, to make sequences sensitive to T2* the $180^{o}$ refocusing pulse used in SE-MRI is absent and that is the case in GE-EPI. Signal acquisition is achieved by using gradient echo trains to acquire complete or partial k-space. This use of gradient trains with a single RF pulse allows for the rapid acquisition. Therefore it can be surmised that EPI gives excellent temporal resolution, at the expense of spatial resolution.

T2* weighted images can also be acquired using gradient echo (GRE) sequences. Similar to EPI, GRE does not have an $180^{o}$ refocusing pulse to

make it sensitive to T2*. It does not afford the same fast acquisition time as EPI due to the longer time needed to fill of k-space. The advantage of GRE over EPI is the spatial resolution is much improved as is the signal to noise ratio. With improvements in MRI processing power the temporal resolution has been improved, and also the signal to noise ratio can be further enhanced by the use of more echoes. These improvements, coupled with an increase in field strength of scanners results in closing the gap between EPI and GRE when utilised for BOLD-MRI. Almost all the studies using BOLD-MRI to assess perfusion in skeletal muscle have utilised GE-EPI sequences[101,139,142–144,147,153–166].

One of the criticisms levelled against BOLD-MRI is that it does not provide any values of absolute quantification of perfusion, unlike ASL-MRI. The differences between ASL and BOLD-MRI have been discussed before (See chapter 1.3.1 & 1.5). The main disadvantages of ASL are the lower signal to noise ratio and spatial resolution compared to BOLD-MRI. Also the kinetic modelling required to analyse the signal changes can introduce errors. The argument of absolute quantification of perfusion can be countered in the assessment of perfusion in the lower limb by the low perfusion of muscle at rest, and therefore the need for induction of hyperaemia to measure perfusion. Studies using ASL-MRI in the lower limb have relied on measuring parameters of the signal intensity time course curves during changes in perfusion rather then report absolute perfusion measures, much like BOLD-MRI does.

The sequences used in the assessment of perfusion in the lower limb were investigated in the present study, with the aim of trying to identify the most reliable method to use in future studies.

## 3.2 Aims

(i) To develop a gradient echo (GRE) MRI sequence that is sensitive to BOLD contrast, with improved spatial resolution over standard gradient echo, echo planar imaging (EPI) MRI and which can also accurately quantify T2* signal.

(ii) Compare GRE MRI with EPI MRI in the assessment of BOLD signal.

(iii) Compare the spatial resolution of GRE BOLD-MRI with ASL techniques for assessing muscle perfusion

## 3.3 Methods

### 3.3.1 Study Participants

Prior to testing the different MRI sequences on humans, water-based MRI phantoms were used to test scanning parameters and MRI performance throughout the dynamic sequence before testing on human subjects. These phantoms were used to ensure the scanner hardware was able to process the sequences throughout the dynamic imaging phase. The increase in the number of echoes used results in an increase demand on the processing ability of scanner hardware and scanning with the MRI phantoms allowed for assessment of this processing capability of the BOLD-MRI sequence.

Young healthy volunteers with no evidence of PAD were recruited to compare the different MRI sequences. All subjects provided written consent to participate in the study. All subjects were prepared for scanning as described in chapter 2.3. For comparing the EPI and GRE BOLD-MRI sequences each leg was cuffed separately and sequentially, with one limb used to test the EPI sequence and then the cuff placed on the contralateral limb to test the GRE sequence. The setup for cuff inflation and deflation is described in chapter 2.4. For ASL-MRI both limbs were cuffed at the same time.

### 3.3.2 MRI Sequences

All MRI scans were performed on a 3 Tesla Philips Achieva scanner, with a 32-channel cardiac RF coil. Two sequences were developed to study changes in T2* signal intensity.

**GRE MRI Sequence**

The first was a multi-echo single shot gradient echo (GRE) sequence. A 10mm slice at the widest part of the calf was acquired, with a field of view (FOV) including both legs of 288 x 288, and voxel size of 1.1 x 1.1 x 10mm$^3$. Parameters for imaging were as follows; time to repeat (TR) 66ms, 14 echo's with time to echo (TE) 4.6ms, 9.2ms, 13.8ms, 18.4ms, 23.0ms, 27.6ms, 32.2ms, 36.8ms, 41.4ms, 46.0ms, 50.6ms, 55.2ms, 59.8ms, 64.4ms, Flip angle 20°. Image acquisition for the 14 echoes was every 3seconds. This sequence allows accurate quantification of T2*. T2* maps were then reconstructed from the GRE BOLD-MRI sequence online by a Maximum Likelihood Estimate fit with

Rician noise correction, where noise is read in k-space, for precise and unbiased automated estimation of T2*. Dicom images of the T2* maps were exported to the image analysis software program.

**EPI MRI Sequence**

The second sequence was a multi shot gradient echo echo-planer imaging (EPI) sequence weighted to T2* signal changes. Image acquisition was every 3 seconds taking ten 5mm slices, 5mm apart around the widest part of the calf. Due to the faster image acquisition that is possible with EPI more slices were able to be imaged at the same time compared to the single slice acquired with GRE BOLD-MRI. Image parameters were TR 3000ms, TE 35ms with echo train length (ETL) of 39. This sequence allows imaging at different levels of the calf and measured changes in T2* signal but does not allow us to quantify T2*. Dicom images of the EPI T2* signal changes were exported to the image analysis software.

**ASL MRI Sequence**

ASL-MRI was performed on the same scanner with same 32-channel RF coil. A pCASL sequence, using a single shot, gradient echo EPI sequence was chosen as this gives good spatial resolution. Both limbs were cuffed simultaneously, with baseline imaging of 2minutes prior to cuffing, 5minutes image acquisition with the cuff inflated to suprasystolic pressures and 5minutes imaging after cuff deflation. 10mm slice thickness was acquired at the widest part of the calf. Image acquisition was every 4 seconds with a FOV involving

both legs of 288 x 288. Imaging parameters were; TR 3600ms, TE 17ms, flip angle $90^{o}$, with a tagging duration of 2seconds and post labelling delay of 1900ms.

### 3.3.3 Image Analysis

Signal intensity time course curves were generated for both the EPI and GRE BOLD-MRI sequences from different limbs in each subject and compared. The EPI sequence was sensitive to T2* but did not quantify the signal, therefore was represented in arbitrary units and measured changes in T2* signal. The GRE sequence was able to quantify T2* signal and as there was a discrepancy between units of the signal comparison of curve parameters was not conducted.

Changes in signal intensity were measured with pCASL to generate perfusion maps and also spatial resolution was looked at. Complex kinetic modelling was not carried out to absolutely quantify perfusion, as this was a comparison study only.

## 3.4 Results

### 3.4.1 MRI Sequence Testing on a MRI Phantom

MRI sequence testing was carried out using a water-based phantom for both the EPI and GRE BOLD-MRI. The purpose of the sequence testing was to ensure that imaging parameters were compatible with the scanner, and to test the performance of the individual sequences. Scanning was performed for 12minutes to simulate the dynamic portion of imaging, i.e. when cuff inflation

and deflation would occur. Similarly, the pCASL sequence was tested on the same phantom.

All 3 sequences were compatible with the processing capabilities of the scanner. No problems related to sequence parameters leading to the scanner being unable to acquire and process the images were encountered. These studies in the phantom were important to confirm that despite the high processing power needed to acquire and process the 14 echoes of GRE BOLD-MRI, this sequence was compatible with both the hardware and software of the scanner.

### 3.4.2 Comparison of EPI versus GRE BOLD-MRI

The 2 BOLD-MRI sequences were tested on 2 healthy volunteers, both male, median age 24years. The left leg was cuffed first and imaging acquired using the GRE BOLD-MRI sequences. The cuff was then placed on the right leg and imaging performed with the EPI BOLD-MRI sequence.

The higher spatial resolution of the GRE sequence over EPI BOLD-MRI is shown in figure 3.1, which is from the same subject.

Signal intensity time course curves were generated from ROI's drawn in the anterior, lateral, gastrocnemius and soleus muscle groups for each subject and for each BOLD-MRI sequence. The curves were then compared with each other to identify changes in T2* signal with cuff inflation and deflation, and to see the differences measured with each sequence.

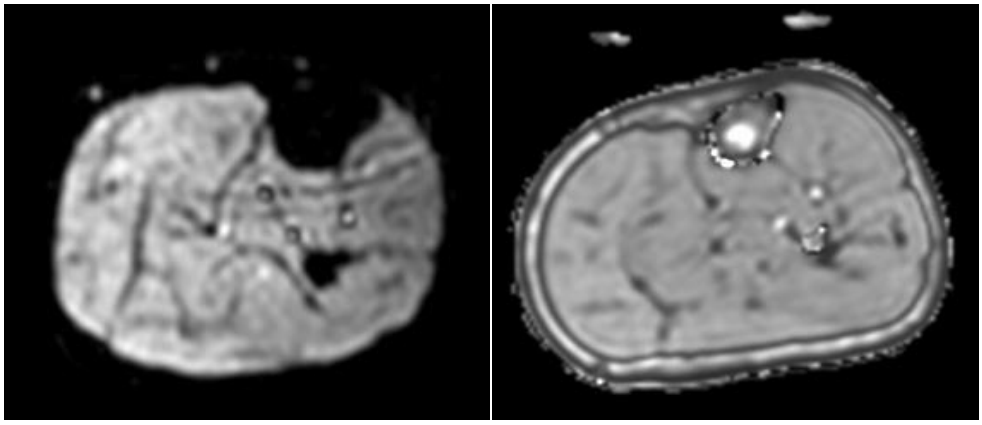

(a)  (b)

**Figure 3.1: EPI (a) versus GRE (b) BOLD-MRI showing the higher spatial resolution achieved with GRE sequence showing axial image from the calf.**

The signal intensity curves both subjects using the different BOLD-MRI sequences for the 4 muscle groups are shown in figure 3.2. The EPI sequence is sensitive to changes in T2* but does not accurately measure this. A greater variability in baseline measurement is seen with this sequence. The GRE MRI sequence allows for accurate measurement of T2* may represent a more sensitive measure of changes in T2* during cuffing and decuffing. This is highlighted with a more pronounced reactive hyperaemic response as seen in figure 3.2. This pattern is seen throughout the 4 muscle groups.

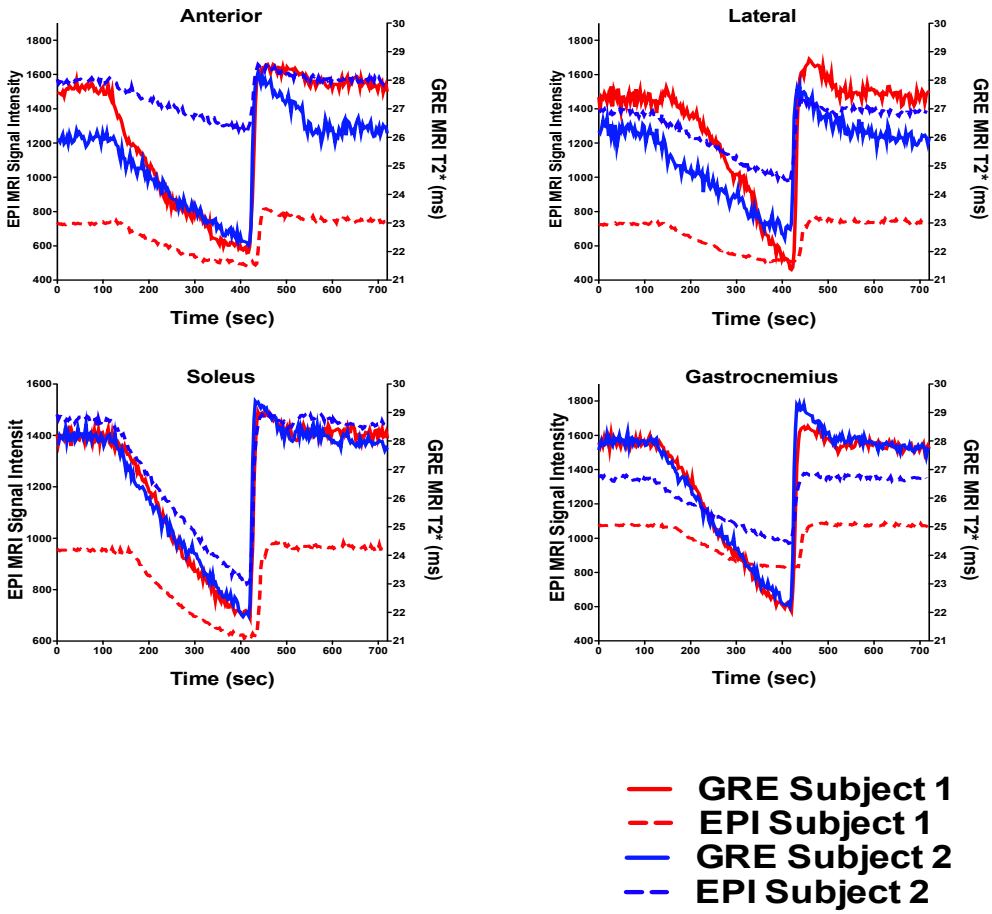


**Figure 3.2: Comparison of changes in T2* signal acquired using the EPI (dotted lines) and GRE (solid lines) BOLD-MRI sequences in 2 subjects (subject 1 in red and subject 2 in blue). ROI's were drawn in the anterior, lateral, soleus and gastrocnemius muscle groups**

### 3.4.3 Arterial Spin Labelling MRI

A pCASL technique was utilised to acquire perfusion images in one healthy volunteer (female, age 24years). This was a comparison study to look at the difference in spatial resolution. Perfusion maps were generated to show changes in perfusion. Figure 3.3 shows these perfusion maps and the spatial resolution attained with the pCASL technique. Compared to GRE BOLD-MRI the spatial resolution is much less. Perfusion maps show changes with

ischaemia after cuff inflation and the subsequent reactive hyperaemia. The maps demonstrate that the pCASL is detecting changes in signal intensity and therefore perfusion using ischaemia and reactive hyperaemia model. Complex kinetic modelling was not undertaken as this was a comparative study only, and therefore the units if signal intensity in the perfusion maps are in arbitrary units. Further modelling can be used to convert this into quantifiable measures of perfusion.

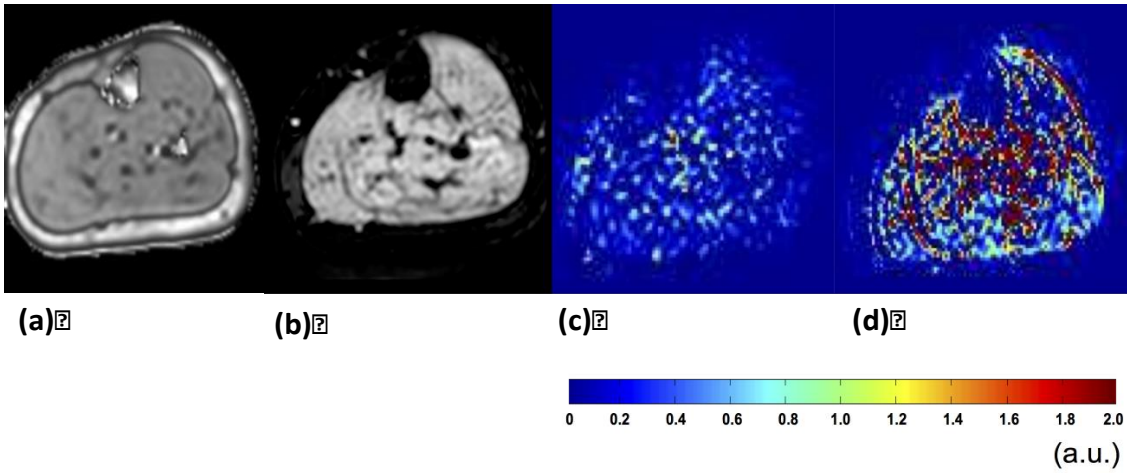


**Figure 3.3: Comparison of GRE BOLD-MRI and pCASL. A higher spatial resolution is achieved with GRE (a) compared with pCASL (b). Perfusion maps demonstrate change in perfusion as measured with pCASL during ischaemia (c) and reactive hyperaemia (d) (signal intensity for perfusion maps in arbitrary units)**

## 3.5 Discussion

BOLD-MRI has traditionally been performed using an EPI sequence weighted to be sensitive to T2* due to the rapid image acquisition speeds that can be achieved. The fast image acquisition speed is advantageous in functional imaging as it reduces the overall imaging time, and also rapid imaging is needed to measure changes in signal after a stimulus[120,140,141,168]. In functional

BOLD-MRI in the brain the rapid imaging is needed to detect task related brain activation.

The gold standard for acquiring images sensitive to BOLD contrast is GRE MRI, as this is the most sensitive to T2* signal changes[140,156]. As T2* decay is related to inhomogeneities in the local magnetic field this is most sensitive to the magnetic susceptibility changes in the magnetic field created by the ratio of deoxygenated and oxygenated haemoglobin that forms the basis of BOLD-MRI. GRE BOLD-MRI has been not been widely utilised compared to EPI due to the lower temporal resolution possible. Recent advances in hardware and processing power of the software, coupled with the higher magnetic field strength scanners have helped improve these weaknesses. This has allowed faster acquisition with GRE sequences and sensitivity to BOLD contrast is improved by increasing the number of echoes MRI scanners can process. To improve the sensitivity of BOLD-MRI these advances are crucial, as the signal changes that are being measured are small[167], and this will assist in making this image modality more objective and reproducible in the future[169].

Regardless, BOLD-MRI does not produce quantifiable measures of perfusion, rather it assesses how perfusion changes in response to a stimulus and this is then used as a marker of perfusion. ASL-MRI is an alternative to BOLD to measure perfusion. This uses water an endogenous contrast agent and magnetically labels this proximal to imaging slice. The change in magnetisation can then be used to measure perfusion. This does require kinetic modelling to produce quantifiable measures of tissue perfusion, which lends itself to the

introduction of errors. Also, the signal generated is very small[98,102], very much like BOLD-MRI.

In this chapter an optimised method of using BOLD-MRI using a more sensitive GRE technique is described. As already mentioned, GRE is much more of a gold standard for measuring BOLD signal due to its increased sensitivity to changes in T2* signal. This has its advantages of more commonly employed techniques of EPI-MRI. It has been demonstrated that the GRE technique provides much higher spatial resolution. This is important in muscle imaging as this can help delineate ROI's that are confined to muscle, accurately excluding areas containing blood vessels, bone and soft tissue. Accurate placement of ROI's in muscle, excluding these other areas, improves the sensitivity of the BOLD signal measured as T2* changes from other tissue will dilute the muscle signal. As mentioned the signal changes generated from BOLD-MRI are very small and therefore T2* signal from non-muscular tissue will very easily dilute the signal acquired.

The GRE BOLD-MRI technique described can also accurately quantify T2* signal. T2* signal is accurately by measuring the decay in signal after the RF pulse. The T2* signal is measured as time taken to reach 67% of the decay. The echoes are used to delineate the exponential decay in T2* after the RF pulse, with each echo providing a point on the curve. Therefore the higher the number of echoes employed, the more accurately the decay in signal can be mapped and subsequently T2* signal quantified (figure 3.4). Increasing the number of echoes come at a cost though, with more processing power required to calculate T2*, and also the MRI hardware has limited the amount of echoes

that can be utilised. If more echoes are used then usually this has been at the cost of temporal resolution. BOLD-MRI techniques to date have usually employed between 3-5 echoes to measure T2* decay[142–144,146,160], whereas the novel GRE sequence here has been able to use 14 echoes without loss in temporal resolution, with imaging occurring every 3seconds.

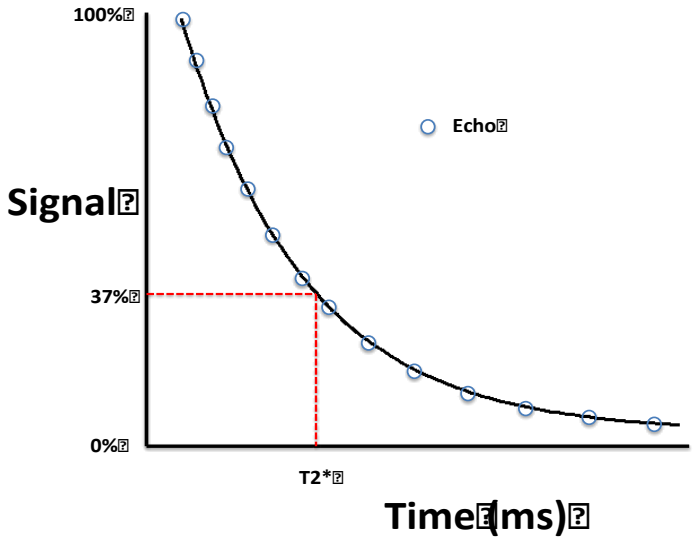


**Figure 3.4: Increasing the number of echoes (blue dots) improves the accuracy of extrapolating T2* decay and therefore more accurately determining T2* signal**

The improvements in software and hardware, such as using a 32-channel RF coil and imaging at higher magnetic fields, have allowed for better spatial resolution and accuracy in measuring T2*. This has helped negate some of the benefits concurred with EPI sequences. The much-improved spatial resolution is an important factor when differentiating the superiority of BOLD-MRI in comparison with ASL-MRI. The resolution of axial calf images obtained with ASL-MRI make it difficult to accurately delineate muscle groups using ROI's. It should also be noted that both ASL and BOLD-MRI analysis of skeletal muscle perfusion require the use of provocation of reactive hyperaemia to produce

measurable changes, and in fact even with ASL, it is the changes in perfusion, i.e. the changes in the signal intensity time course curves, that are most useful. This diminishes the importance of absolute quantification of perfusion in skeletal muscle that is possible with ASL but not with BOLD-MRI.

## 3.6 Summary

This part of the study shows that GRE and EPI BOLD-MRI sequences can be effectively used to measure perfusion in the lower limb. EPI has been favoured in the past mainly because it allows fast acquisition of images but speed of acquisition is becoming less of an issue with modern scanner hardware and processing power. This has allowed GRE, with its better signal to noise ratio, spatial resolution and more accurate measurement of T2*, to be increasingly favoured over EPI in BOLD-MRI studies. The improved spatial resolution and signal to noise ratio along with no need for complex kinetic modelling means that BOLD-MRI has a number of advantages over ASL. Furthermore, the absolute quantification of perfusion in skeletal muscle is much less important in the lower limb with the actual perfusion changes in response to provocation being much more useful indicator of perfusion.

For these reasons the GRE sequence was chosen for the subsequent studies outlined in this thesis.

# Chapter 4

## BOLD-MRI Assessment of Perfusion in Patients with Critical Limb Ischaemia

### 4.1 Introduction

Previous studies have attempted to use BOLD-MRI to assess perfusion in the lower limb[101,139,142–144,147,153–166]. These studies have shown that it is possible to measure changes in lower limb perfusion in healthy controls as well as in patients with PAD. Furthermore these studies have gone on to compare BOLD-MRI with other surrogate measures of muscle perfusion such as TcPO2[144], LDF[144,154], and VOP[139].

Previous studies using BOLD-MRI have mainly used EPI sequences for reasons described before. We optimised a GRE method for accurately quantifying T2* signal in attempt to improve sensitivity and reproducibility. This chapter outlines studies that used this novel GRE BOLD-MRI sequence to assess perfusion in young healthy and age-matched controls and compare this to patients with CLI.

### 4.2 Aims

(i) To identify which curve parameters are most discriminatory in assessing lower limb perfusion using BOLD-MRI.

(ii) To use GRE BOLD-MRI to measure changes in perfusion in healthy and age-matched controls and compare this to patients with CLI.

(iii) To assess inter-scan and inter-user reproducibility with GRE BOLD-MRI.

## 4.3 Methods

### 4.3.1 Study Participants

Young healthy controls, with an age less the 30years and age-matched controls without any evidence of PAD were recruited to the study. Patients admitted to St Thomas' Hospital with a diagnosis of CLI were recruited to the study. ABPI was measured in patients with CLI and age-matched controls. Further details are described in chapter 2.2.

### 4.3.2 Protocol for BOLD-MRI and Image Analysis

All subjects followed the protocol for cuffing described in chapter 2.3 and 2.4. Both legs were cuffed around the thigh and the same investigator was used for cuff inflation and deflation. The dynamic imaging protocol was the same for all subjects (2minutes baseline imaging, cuff then rapidly inflated to 50mmHg above systolic pressure and kept inflated for 5minutes during the ischaemic phase, cuff rapidly deflated to evoke reactive hyperaemia with imaging for 5minutes during this phase).

The MRI imaging protocol and method for reconstructing T2* maps are described in chapter 3.3.2. The GRE sequence was used to measure BOLD signal and T2* maps exported to the image analysis software for creation of

signal intensity time course curves and measuring curve parameters (see chapter 2.6). ROI's were drawn in the 5 muscle groups in the calf (anterior, lateral, soleus, gastrocnemius and deep posterior), with a reference T2 weighted anatomical image acquired in the same region of the calf as imaged with GRE BOLD-MRI, for comparison.

### 4.3.3 Comparison of controls and patients with CLI

Both limbs of young healthy and age-matched controls were compared with patients with CLI. For the CLI cohort both the symptomatic limb and the contralateral asymptomatic limb were analysed, as a patient control limb, giving a four-group comparison (young healthy, age-matched, patient asymptomatic and patient symptomatic limbs). Signal intensity time course curves were generated for the 4 groups and curve parameters were compared to determine perfusion differences.

To determine which curve parameters were most discriminatory in detecting perfusion with BOLD-MRI, we compared all curve parameters between the symptomatic and asymptomatic limbs in CLI patients. These 2 groups were chosen because the difference that would be expected between them would be the smallest and any parameter that can discriminate between these 2 groups would ultimately prove to be the most useful, especially when we use BOLD-MRI to assess change in perfusion after revascularisation.

### 4.3.4 Inter-user and Inter-scan Reproducibility of GRE BOLD-MRI

To assess inter-user reproducibility, 2 independent investigators blindly analysed the same BOLD-MRI images from both limbs in 7 healthy volunteers and signal intensity time course curves and curve parameters were compared.

Inter-scan reproducibility was investigated with the same blinded user analysing BOLD-MRI images from both limbs in repeat scans performed in 5 healthy volunteers performed 1-5 weeks apart. To ensure the same part of the calf was imaged, the tibial tuberosity was used as an anatomical landmark and the distance between this and the middle of the imaging slice was the same for repeat imaging. Signal intensity time course curves and curve parameters were analysed and compared to assess reproducibility between interval scans

### 4.3.5 Statistical Analysis

Statistical analysis was carried out using SPSS v20 (IBM Corp. Armonk, NY, USA) and Prism 5 (GraphPad Software Inc. California, USA). A one-way ANOVA (with Tukey Post Hoc test) was used for analysis of curve parameters between the healthy and age-matched controls and CLI patient's symptomatic and asymptomatic limbs, and for differences in ABPI between groups. Inter-user and inter-scan reproducibility was assessed using intraclass correlation coefficient (ICC), where an ICC >0.9 was deemed as excellent level of agreement and Bland Altman analysis. Analysis of different curve parameters to determine the most discriminatory parameters and also for inter-user and inter-scan reproducibility was assessed by paired t-test. Correlation analysis of

curve parameters against ABPI was performed using Spearman's correlation. All values are given as mean ± standard deviation (SD) and $P<0.05$ was deemed to be statistically significant

## 4.4 Results

### 4.4.1 Subject Demographics

37 patients with CLI (median age 66years range 37-86), 10 age-matched controls (median age 67years range 52-71) and 12 young healthy controls (median age 25years range 24-28) were recruited into the study (Table 4.1). 3 CLI patients were excluded, as they were unable to lie supine for a period long enough to undergo BOLD-MRI because of the severity of rest pain.

**Table 4.1: Demographics of the subjects recruited for this study**

| | Young Controls (n=12) | Age-matched Controls (n=10) | CLI Patients (n=37) |
|---|---|---|---|
| **Age (years, median and range)** | **25 (24-28)** | **67 (52-71)** | **66 (37-86)** |
| **Sex (m:f)** | **8:4** | **7:3** | **29:8** |
| **Smoker** | **1** | **1** | **26** |
| **Hypertension** | **0** | **2** | **29** |
| **Hypercholesterolaemia** | **0** | **1** | **20** |
| **Diabetes** | **0** | **0** | **13** |
| **Rutherford Classification** | | | |
| **IV** | | | **22** |
| **V** | | | **9** |
| **VI** | | | **6** |

The age ranges for the age-matched controls and CLI patients were similar. The table also shows the co-morbidities for the subjects recruited. The CLI patients had a higher proportion of smokers, and suffered with hypertension, diabetes mellitus and hypercholesterolaemia more than age-matched controls. Table 4.1 also highlights the Rutherford classification of CLI in the patient group, with 29 patients having Rutherford 4 (rest pain) compared to 9 with Rutherford 5 (minor tissue loss) and 6 having Rutherford 6 (major tissue loss). There were more males than females in each of the subject groups.

We compared the ABPI's for the age-matched controls and CLI patients groups, also comparing the ABPI between the symptomatic and contralateral asymptomatic control limbs in CLI patients. This is shown in figure 4.1. There was a significant difference in ABPI in age-matched controls (1.08 ± 0.04), CLI patient's asymptomatic limb (0.78 ± 0.18) and CLI patient's symptomatic limb (0.49 ± 0.14)($P<0.001$ for all groups, one way ANOVA, Tukey Post Hoc).

ABPI was only measurable in 19 of the 34 CLI patients in whom BOLD-CMR was performed. Either calcification in the below knee arteries or absence of a Doppler signal precluded reliable measurement in the remaining 15 patients.

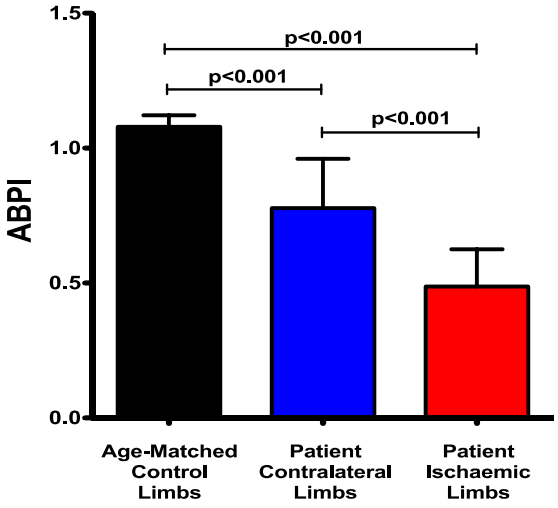


| | ABPI (mean ± SD) |
|---|---|
| Age-Matched Controls | 1.08 ± 0.04 |
| Patients Contralateral Limbs | 0.78 ± 0.18 |
| Patients Ischaemic Limbs | 0.49 ± 0.14 |

**Figure 4.1: Significant difference in ABPI measured in age-matched controls and the symptomatic and asymptomatic limbs in patients with CLI (One-way ANOVA, Tukey Post Hoc)**

### 4.4.2 Discriminatory Power of Curve Parameters

Automated curve analysis was performed for the CLI patient cohort and all the curve parameters were compared between the symptomatic and asymptomatic limbs. The curve parameters that were analysed are described in chapter 2.6 and figure 2.6, but in brief they are; Baseline T2* signal before cuffing, Time to half ischaemia (THIM), T2* at the end of cuffing (T2*Min), Signal reduction in ischaemia (SRi), Gradient of reactive hyperaemia (Grad), Time to peak (TTP), Maximum T2* in reactive hyperaemia (T2*Max) and Baseline T2* after reactive hyperaemia.

**Table 4.2: Comparison of curve parameters between the 2 limbs in patients with CLI (Paired t-test)**

| | Patient Contralateral Limbs | Ischaemic Limbs | p value |
|---|---|---|---|
| **Grad(ms/s)** | **0.28±0.14** | **0.17±0.11** | **p<0.0001** |
| **SRi(%)** | **11.03±5.62** | **8.68±5.11** | **p<0.0001** |
| Minimum T2*(ms) | 21.99±3.63 | 22.80±3.62 | p<0.01 |
| Baseline (Start)(ms) | 24.70±4.09 | 25.04±3.92 | p=0.16 |
| Baseline (End)(ms) | 24.64±4.07 | 24.85±3.93 | p=0.43 |
| Maximum T2*(ms) | 24.93±4.25 | 24.56±3.93 | p=0.20 |
| TTP(seconds) | 68.7±22.76 | 64.5±29.7 | p=0.14 |
| THIM(seconds) | 205.5±78.3 | 195.5±81.5 | p=0.24 |

Comparing the 2 limbs in CLI patients, 3 parameters were found to be most discriminatory in distinguishing between the two. Grad was found to be significantly higher in the asymptomatic patient control limb compared to the ischaemic limb (0.28 ± 0.14 ms/s vs. 0.17 ±0.11 ms/s, p<0.0001). Similarly, SRi was significantly higher in the asymptomatic control limb (11.03 ± 5.62% vs. 8.68 ± 5.11%, p<0.0001). T2*Min was also found to be significantly different between the 2 limbs (21.99 ± 3.63 ms vs. 22.80 ± 3.62 ms, p<0.01). None of the other parameters were significantly different between the 2 limbs in CLI patients (Table 4.2). For all subsequent perfusion comparisons between limbs/groups Grad and SRi were used to identify perfusion changes.

### 4.4.3 BOLD-MRI T2* Signature in the Ischaemic Limb Compared with Controls

Comparison of the BOLD-CMR T2* signal intensity curves from the limbs of young control subjects, age-matched controls, and CLI patients generated for each of the 5 muscle groups, demonstrated a clear difference between ischaemic limbs and control limbs, with the soleus musculature generating the most distinctive curve characteristics (Figure 4.2). In all groups there was a fall in T2* signal after cuff inflation during the ischaemic phase, but the signal for the ischaemic limbs plateaued sooner than the other groups and the total reduction in signal intensity was much less. During reactive hyperaemia the rise in T2* signal was faster in the young controls and most delayed in the ischaemic limbs of the CLI patients. A significantly lower Grad was measured in the ischaemic limb (0.17 ± 0.11ms/s) compared with the patient contralateral (0.28 ± 0.14ms/s, $p<0.001$), age matched (0.38 ± 0.17ms/s, $p<0.001$) and young control limbs (0.47 ± 0.16ms/s, $p<0.001$, Figure 4.3). Similarly, the SRi was lower in the ischaemic limb (8.68 ± 5.11%) compared with the patient contralateral (11.03 ± 5.62%, $p<0.001$), age-matched controls (13.77 ± 6.33%, $p<0.001$) and young controls (14.07 ± 5.09%, $p<0.001$, Figure 4.4). No relationship was seen with regards to BOLD derived parameters and duplex or angiographic extent of disease.

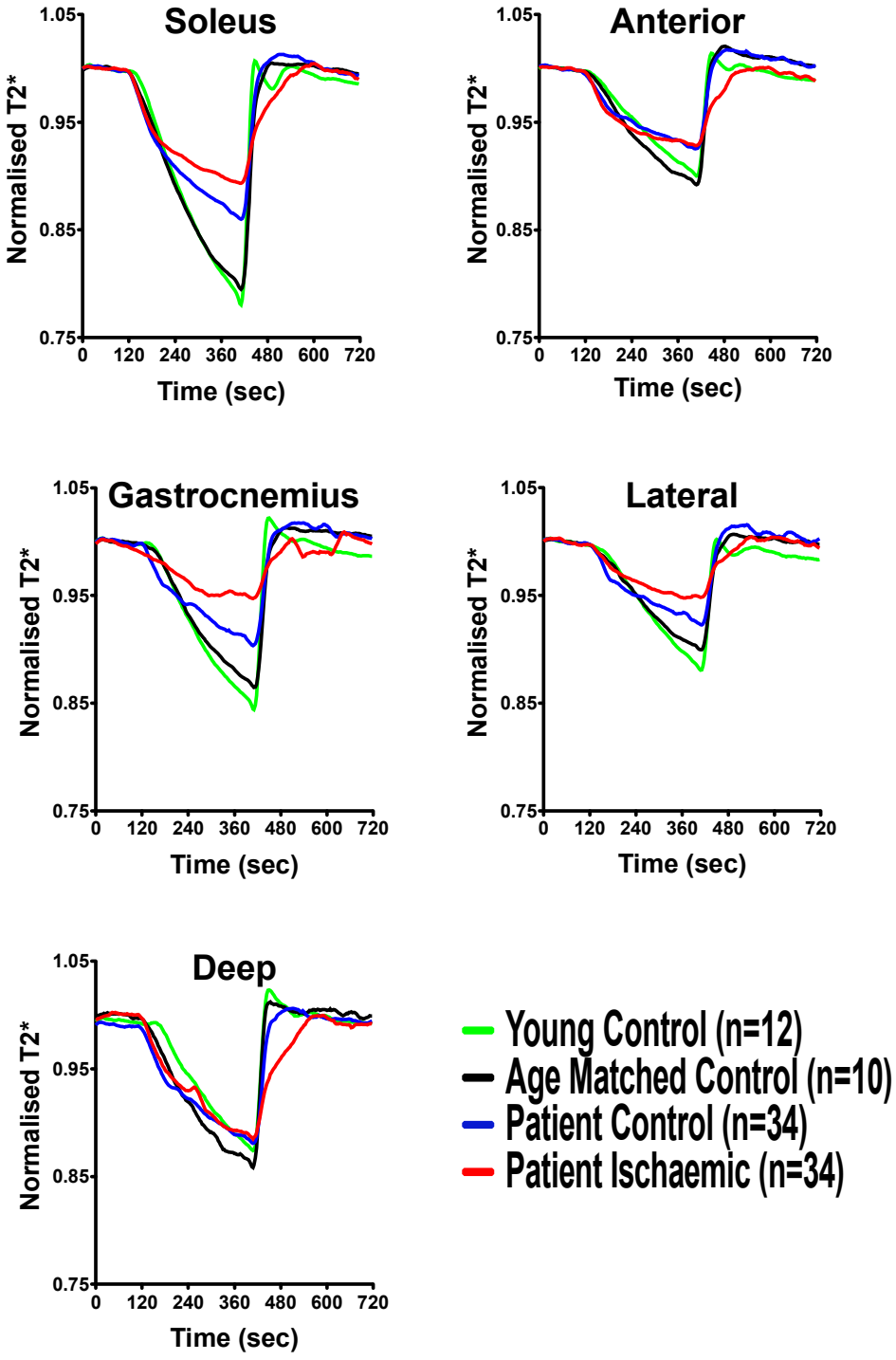


**Figure 4.2: T2* signal intensity time course curves for young healthy and age-matched controls compared to CLI patients control limb and ischaemic limb for the 5 muscle groups**

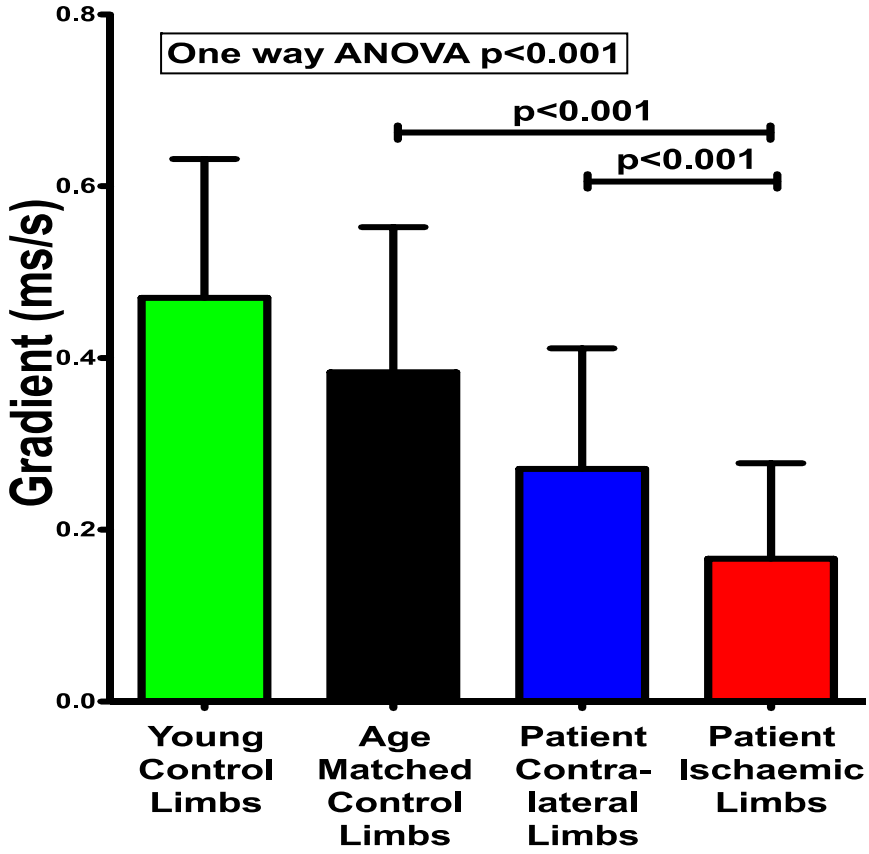


| | Gradient (ms/s) (Mean ± SD) |
|---|---|
| Young Control Limbs | 0.47 ± 0.16 |
| Age-Matched Control Limbs | 0.38 ± 0.17 |
| Patient Contralateral Limbs | 0.28 ± 0.14 |
| Patient Ischaemic Limbs | 0.17 ± 0.11 |

**Figure 4.3: Difference in gradient between the 4 groups (One-way ANOVA, Tukey Post Hoc)**

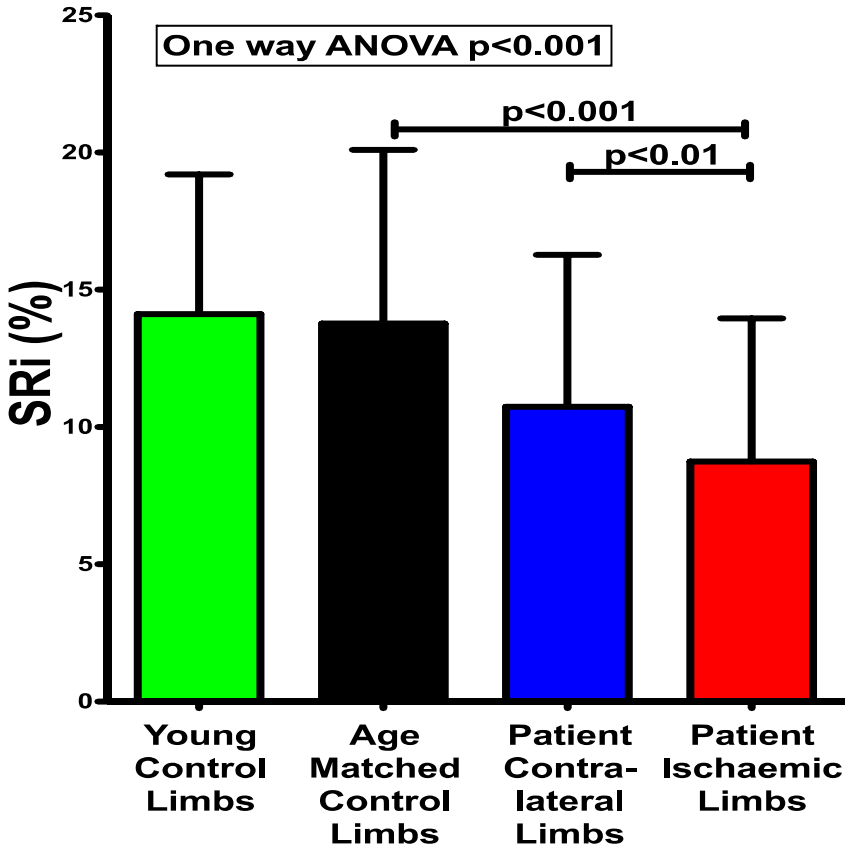


| | SRi (%) (Mean ± SD) |
|---|---|
| Young Control Limbs | 14.07 ± 5.09 |
| Age-Matched Control Limbs | 13.77 ± 6.33 |
| Patient Contralateral Limbs | 11.03 ± 5.62 |
| Patient Ischaemic Limbs | 8.68 ± 5.11 |

**Figure 4.4: Difference in signal reduction in ischaemia between the 4 groups (One-way ANOVA, Tukey Post Hoc)**

Curve parameters of Grad and SRi were compared with ABPI to see if any correlation existed between the BOLD-MRI derived perfusion parameters and the traditional method of grading ischaemia. No correlation (Spearman's Correlation) was seen between ABPI and Grad (r=0.34, p=0.20,) or with SRi (r-0.07, p=0.80)(Figure 4.5).

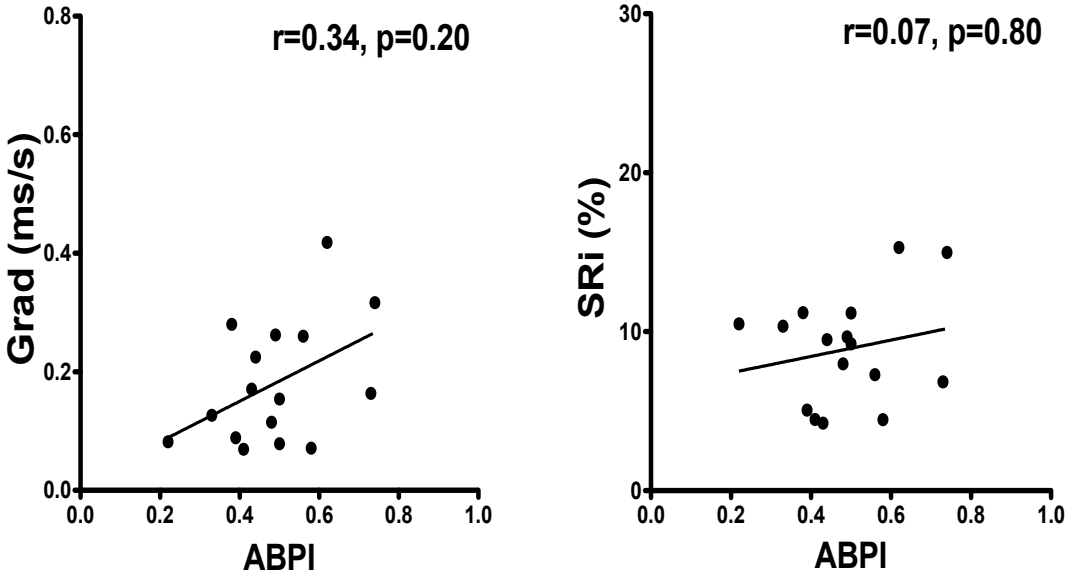


**Figure 4.5: Correlation of ABPI with BOLD-MRI parameters of Grad (A) and SRi (B) (Spearman's Correlation)**

Patients with CLI had multiple level disease, and it is difficult to draw correlation with extent of arterial disease and BOLD-MRI derived parameters as this sequence only allows imaging at a single level in the calf.

### 4.4.4 Subgroup Analysis in CLI Patients

In CLI patients, a subgroup analysis was performed to assess differences due to age, smoking and diabetes. Signal intensity time course curves were generated and compared for each groups, as well as automated analysis of the curve parameters Grad and SRi.

For analysis of difference in age, CLI patients under the age of 65years (n=13) were compared to over those 65years or above (n=21). Differences were seen in the signal intensity time course curves. Analysis of curve parameters showed a significant difference for Grad (<65years 0.21 ± 0.12ms/s vs. ≥65years 0.14 ± 0.1ms/s, p<0.005, unpaired t-test) and SRi (<65years 10.41 ± 5.04% vs. 7.69 ± 5.08, p<0.005, unpaired t-test)(Figure 4.6).

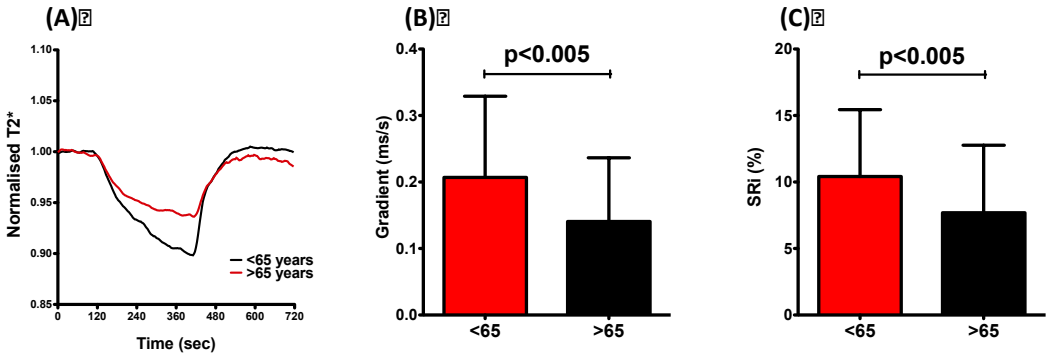


**Figure 4.6: Age related (<65 years vs. ≥65years) change in CLI Patients. Difference seen in signal intensity time course curves (A), Grad (B) and SRi (C) (unpaired t-test).**

Investigating differences between based in smoking history and diabetes did not any differences in CLI patients. For smoker (n=26) versus non-smoker

(n=8) Grad was 0.17 ± 0.11ms/s vs. 0.14 ± 0.11ms/s, and SRi was 8.80 ± 5.31% vs. 8.43 ± 4.31% (p>0.05, unpaired t-test for both). Similar signal intensity time course curve are generated between the 2 groups (Figure 4.7).

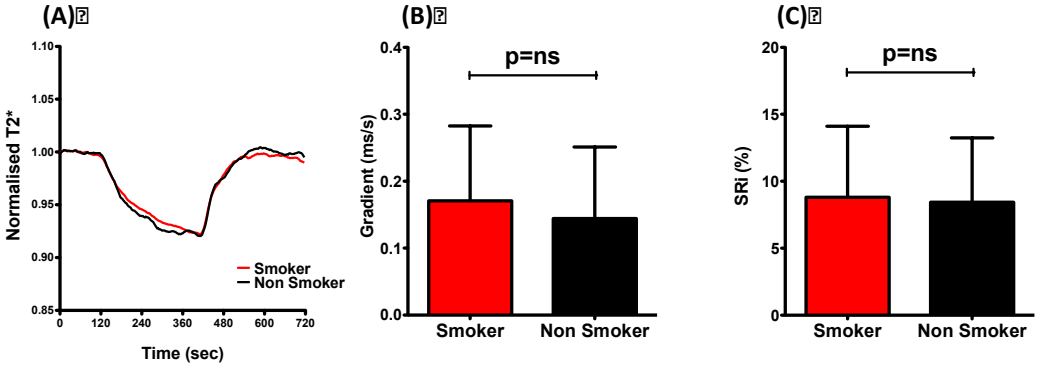


**Figure 4.7: Comparison of smoking history, with no difference in signal intensity time course curves (A), Grad (B) and SRi (C) (unpaired t-test).**

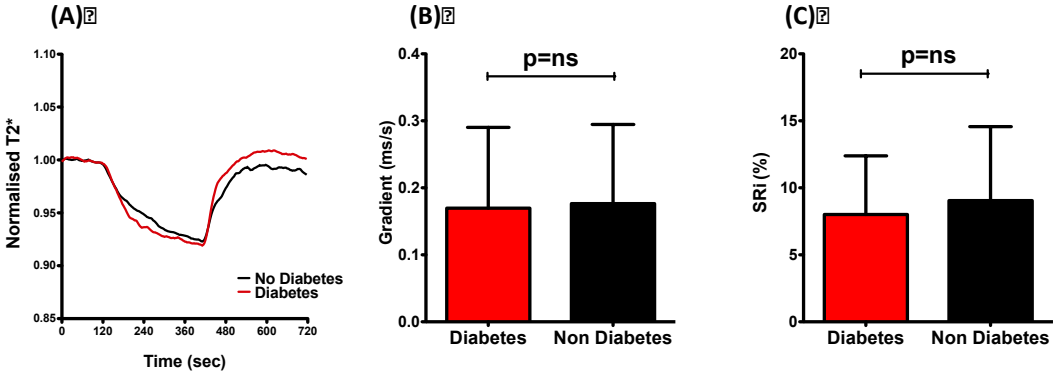


**Figure 4.8: Comparison of diabetic history, with no difference in signal intensity time course curves (A), Grad (B) and SRi (C) (unpaired t-test).**

Comparing diabetics (n=13) versus non-diabetics (n=21), signal intensity time course curves were similar, and Grad was 0.17 ± 0.12ms/s vs. 0.18 ± 0.12ms/s,

and SRi 8.01 ± 4.38% vs. 9.04 ± 5.52% ($p>0.05$, unpaired t-test for both)(Figure 4.8).

### 4.4.5 Inter-user and Inter-scan Reproducibility of BOLD-MRI

2 blinded, independent investigators analysing BOLD-MRI with the automated analysis software in 7 young healthy volunteers, assessed inter-user reproducibility. There was good reproducibility as evidenced by strong correlations for both Grad and SRi measurements (ICC = 0.99 (95% CI 0.98-0.99) and 0.99 (95% CI 0.98-0.99), respectively, $p<0.0001$ for both, Figure 4.9). Bland Altman analysis concurred with ICC (Grad: mean bias -0.002 (95% limits of agreement -0.05-0.05, SRi: mean bias -0.04 (95% limits of agreement -1.79-1.70), Figure 4.10). Similar T2* curves were generated by the two users. No significant difference was found between Grad and SRi measured by each of the 2 investigators (Figure 4.11).

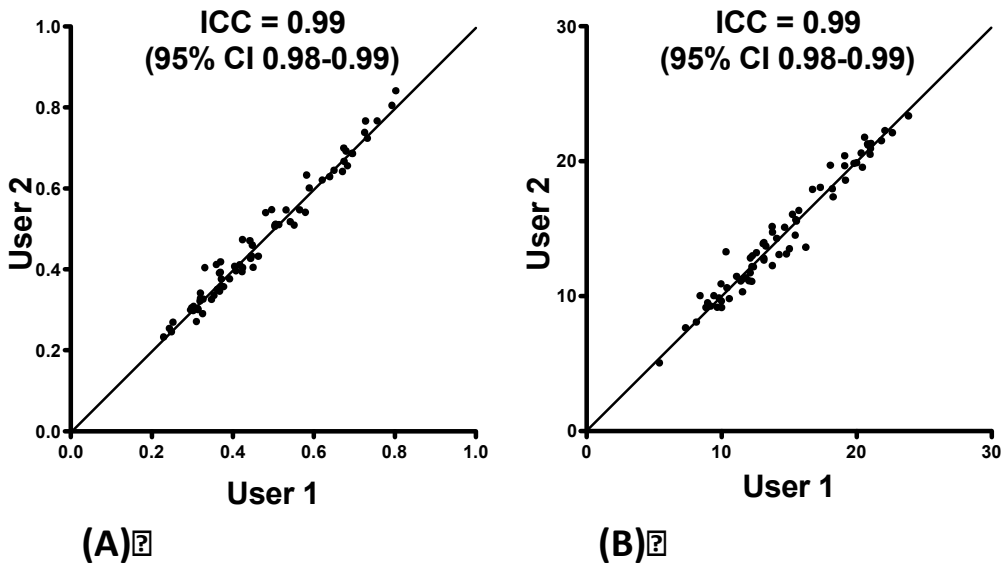


**Figure 4.9: Intraclass correlation coefficient for assessing intra-user reproducibility for Grad (A) and SRi (B)**

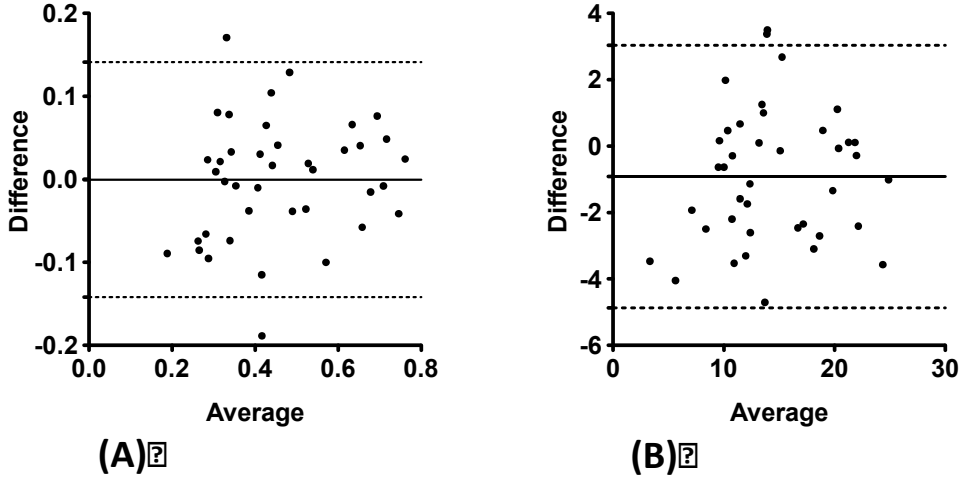


**Figure 4.10: Bland-Altman analysis of inter-user reproducibility for Grad (A) and SRi (B)**

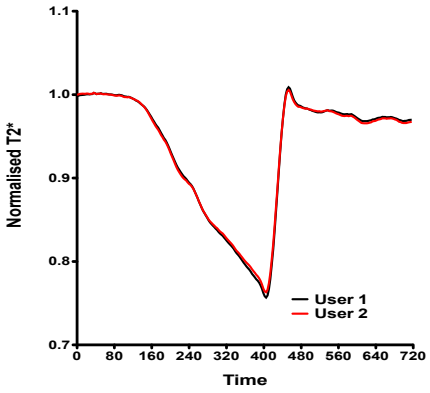


| | User 1 | User 2 | p values |
|---|---|---|---|
| Grad (ms/s) | 0.47±0.15 | 0.47±0.15 | p>0.05 |
| SRi (%) | 14.54±4.42 | 14.45±4.45 | p>0.05 |

**Figure 4.11: Example T2* signal intensity time course curves generated by the automated analysis software program showed good reproducibility between user. The table shows no significant difference in Grad and SRi as measured by the 2 users (paired t-test)**

5 young healthy volunteers underwent repeat BOLD-MRI imaging 1-5 weeks apart and serial scans were analysed by a single investigator to assess inter-scan reproducibility. There were excellent correlations for Grad and SRi between scans in the same subject (ICC = 0.95 (95% CI 0.90-0.98) and 0.96 (95% CI 0.90-0.98) respectively, $p<0.0001$ for both, Figure 4.12). Bland Altman analysis confirmed good reproducibility between scans for Grad (mean bias 0.0004 (95% limits of agreement -0.14-0.14)) and SRi (mean bias -0.92 (95% limits of agreement -4.88-3.04), Figure 4.13). No significant difference was found between Grad and SRi between interval scans for all muscle groups analysed (Figure 4.14).

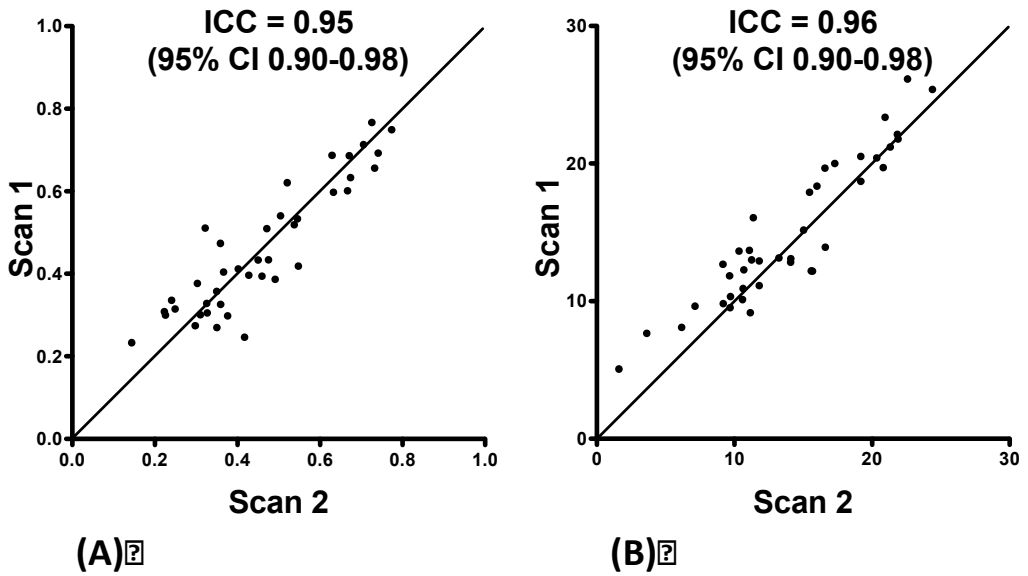


**Figure 4.12: Interclass correlation coefficient for assessing reproducibility between interval scans for Grad (A) and SRi (B)**

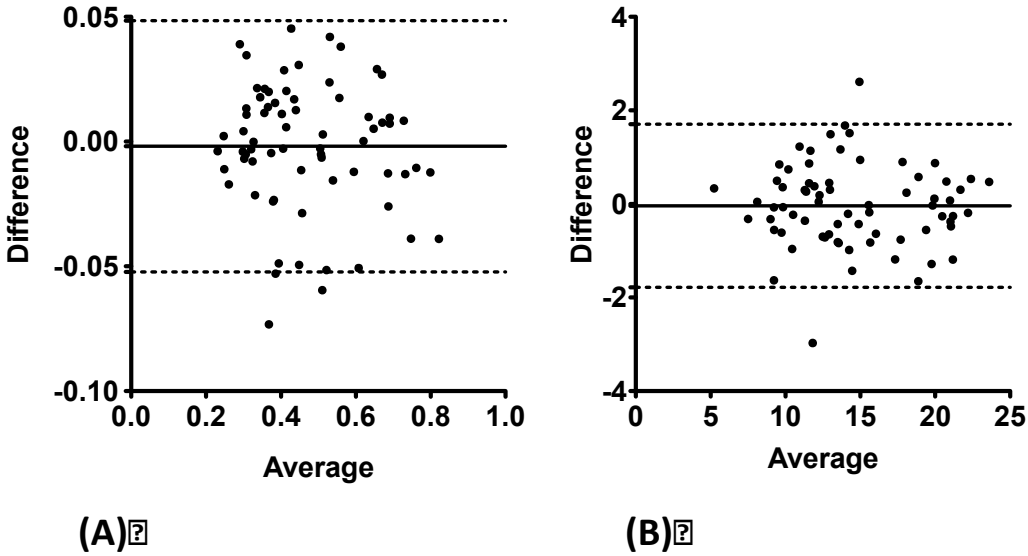


**Figure 4.13: Bland Altman analysis of inter-scan reproducibility for Grad (A) and SRi (B)**

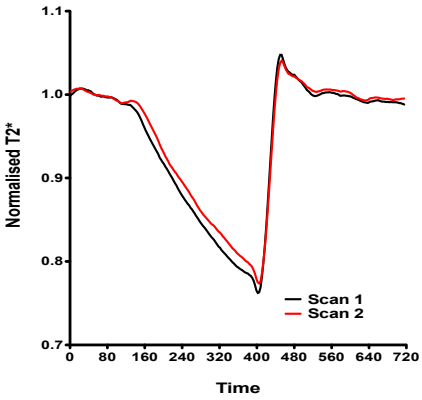


| | Scan 1 | Scan 2 | p values |
|---|---|---|---|
| Grad (ms/s) | 0.46±0.17 | 0.46±0.16 | p>0.05 |
| SRi (%) | 13.97±5.42 | 14.88±5.22 | p>0.05 |

**Figure 4.14: Example T2* signal intensity time course curves for the same subject scanned on 2 separate occasions. The table shows no significant difference for Grad and SRi between interval scans in the same subjects (paired t-test)**

## 4.5 Discussion

In this study, a novel BOLD-MRI method using a GRE sequence more sensitive to T2* signal was used to identify changes in muscle perfusion in the calf as a result of arterial occlusion and subsequent reactive hyperaemia. This method builds on previous studies investigating muscle perfusion using BOLD-MRI[101,139,142–144,147,153–166].

As already mentioned earlier, provocation testing is required to produce measurable changes in muscle perfusion. It is the changes as a result of these stimuli that produce measures that can be used to assess perfusion. What is not known is what measures are the best to assess muscle perfusion. The changes in perfusion represent a physiological response to changes in demand and ability to perfuse muscle. Similarly, provocation testing in the form of stress and treadmill testing is used in assessing cardiac perfusion, but this is different to the cuffing model used in this study. Cuffing induces ischaemia in muscle,

whereas in cardiac testing there is a functional change in the myocardium that requires increased perfusion. Nevertheless, the results are similar in that it results in a hyperaemic response.

This study has imaged the largest cohort of patients with limb ischaemia (n=37) with BOLD-MRI and compared them to young healthy, and age-matched controls. Compared to previous studies using BOLD-MRI in PAD patients[142,143,161], this is the first study to investigate patients with CLI, in whom the risk of limb loss is considerably higher[1,3]. Previous studies have looked at patients with IC, a more stable and mild form of PAD, which does not always require or warrant intervention.

### 4.5.1 Discriminatory Power of T2* Signal Changes

Two new parameters, Grad and SRi, were developed and tested for assessment of changes in perfusion, measured by T2* signal changes on BOLD-MRI. Both Grad and SRi allowed reliable, automated analysis of limb perfusion. Curve parameters used in previous BOLD-MRI studies include TTP, T2*Max, T2*Min and THIM[142,143,146,160,161,164] but we found Grad and SRi to be superior. Grad can be thought analogous to TTP and T2*Max. It calculates the maximum slope of the curve during reactive hyperaemia. As it is calculated from the mean of the 10 highest values measured from the first derivative of T2* signal from cuff deflation to T2*Max, it overcomes some of the weakness of using TTP and T2*Max as the inherent background signal noise can interfere with the BOLD signal. SRi is calculated as a percentage drop in signal form initial baseline T2* until the end of the ischaemic phase. Again the inherent

noise can influence the actual points that measured for these parameters. Also signal intensity time course curves are usually normalised to allow for the variation seen in T2* signal that occur between subjects, making direct comparison of T2* values difficult to interpret. The new parameters overcome this by using parameters that are dependent on the change in T2* signal rather than actual signal values.

Lack of reproducibility has been cited as a potential weakness of BOLD-MRI[155]. A number of reasons could account for this and are discussed in more detail later, but one reason could be related to how curve parameters are derived. As alluded to before, the actual BOLD signal generated is very low and difficult to distinguish and measure over the inherent signal noise from MRI scanners[167]. The noise makes the defining points along the curve difficult. Some of this is overcome by smoothing of curves to diminish the influence of background interference. Also, particularly in patients with PAD, the overshoot in reactive hyperaemia is dampened and in some cases completely absent. This is particularly the case as the severity of ischaemia increases, which makes identifying the exact point of the peak more difficult to define and therefore parameters such as T2*Max and TTP are prone to more errors.

The new parameters identified here overcome many of this weakness allowing for more reliable assessment of perfusion. The 2 parameters also interrogate different aspects of the curve. SRi assesses the ischaemic phase, measuring the drop in signal intensity. Grad, on the other hand looks at the response to reactive hyperaemia. Both would be expected to be impaired in the presence of PAD and therefore provide useful indication of both physiological reserve and

the ability to responds after the stress has been removed, i.e. reactive hyperaemia[170].

Both Grad and SRi were investigated in the CLI patients, comparing the ischaemic limb with the contralateral asymptomatic control limbs. The most sensitive marker of perfusion would ideally be able to reliably distinguish between ischaemic and non-ischaemic muscle in the same limb. Investigating the ischaemic limb and comparing this with the asymptomatic limb was chosen, as these 2 groups would be expected to show the smallest difference in perfusion to the muscle between limbs. The ischaemic limbs had a lower Grad and SRi compared the contralateral control limbs in CLI patients. T2*Min was also significantly different between the 2 limbs in CLI patients, but the difference was just significant and as it represents an absolute T2* value and is almost analogous with SRi, it was decided that the best parameters to go forward with were SRi along with Grad.

### 4.5.2 BOLD-MRI Assessment of Perfusion in CLI

This study has shown consistent changes in the curve profiles in patients with CLI compared to their own contralateral asymptomatic limb and with age-matched and young healthy controls. The signal intensity time course curves show a graduated response as the level of arterial disease increases. This is highlighted in the curve parameters that are measured. It would be safe to surmise that young healthy controls would be expected to have the best perfusion profiles and this is confirmed with BOLD-MRI derived parameters, with them having a higher Grad and SRi, compared to age-matched controls

and CLI patients. Similarly, age-matched controls have better signal intensity time course curves compared to CLI patients. Even in CLI patients, the asymptomatic contralateral control limbs have better perfusion profiles compared then the symptomatic ischaemic limbs. Patients with CLI almost always have evidence of disease in the contralateral limb[171] and therefore the fact that the profiles determined with BOLD-MRI show a graduated response in the different groups highlights that it may indeed be sensitive to the degree of severity of limb ischaemia.

The signal intensity time course curves demonstrated in this study are similar to previous studies[140,141], in that at baseline T2* signal is steady. The initiation of arterial occlusion by thigh cuff inflation to suprasystolic pressures results in a fall in T2* signal. This is most pronounced in healthy young volunteers, and the decrease is the least in the CLI patient's ischaemic limbs. The onset of reactive hyperaemia, after cuff deflation, results in a rise in T2* signal but again this is different between the groups. The ischaemic limbs show a more gradual increase, taking longer to reach a peak compared to the other groups, with much less of an overshoot. This is reflected in the curve parameters acquired from the different groups.

ABPI is currently used for confirming the diagnosis of PAD and for assessing improvements in blood flow to the foot after revascularisation. Unlike BOLD-MRI, ABPI cannot, however, be measured in all patients. This is reflected in the results of the present study, where we were unable to measure ABPI in just over 40% of the patients with CLI. There was no correlation between ABPI values and corresponding Grad or SRi, the former measuring global blood flow

into the limb rather than perfusion at tissue level. ABPI measure pressure in the leg and it would suggest that BOLD-MRI derived assessment of perfusion is to be believed then there are further processes that occur in determining perfusion. Pressure measurements reflect only the inflow of blood into the limb, but do not take into account the physiological processes that are occurring at cellular level in muscle perfusion. It could be that BOLD-MRI derived assessment of muscle perfusion takes this into account as it assessing the ratio of oxygenated and deoxygenated haemoglobin in muscle tissue. It should be noted, however, that the combination of clinical examination and ABPI remain a practical, simple and useful tool for the initial assessment of the critically ischaemic limb.

Ageing effects have been described previously when using BOLD-MRI[146,147,172]. This study has confirmed these findings, with younger CLI patients having a better perfusion profile compared to older patients. No difference is seen when investigating smoking history and diabetes. Age related change in perfusion are well established[173–175], and are postulated to be related to an increase in vascular disease burden along with loss in muscle mass and change in muscle fibre type. This leads to a reduced physiological reserve in muscle perfusion and this may explain the age related changes measured with BOLD-MRI, even in the face of PAD.

Patients with diabetes have been investigated with BOLD-MRI and differences in perfusion profiles have been detected[176]. However, this study compared diabetics with age-matched controls without evidence of PAD. Another study failed to show any difference between diabetics and non-diabetics[172]. In this

study the influence is PAD is certainly compounding any differences due to the presence of diabetes, and making any conclusion on the influence of diabetes is impossible. Smoking affects on BOLD-MRI have not been demonstrated previously, and this study does not show a difference.

### 4.5.3 Reproducibility of Novel GRE BOLD-MRI

Failure to show reliable reproducibility of BOLD-MRI has been cited as a major weakness of this imaging modality[155]. They're maybe a number of factors that result in this lack of reproducibility. The accuracy of T2* signal acquisition is major factor, and can be improved in a number of ways. Imaging with higher magnetic field scanners improves the BOLD signal[127,160], along with improvements in other MRI hardware, such as RF coils. The use of GRE sequences compared to EPI improves the spatial resolution, allowing for accurate exclusion of major blood vessels, bone and other soft tissue, which avoids erroneous T2* quantification caused by inadvertent inclusion of these structures. Increasing the number of echoes result in more accurate quantification T2*. These factors will improve the sensitivity of BOLD-MRI, which should aid reproducibility.

The study which highlighted the weakness in the reproducibility of BOLD-MRI was by Versluis et al[155]. The lack of reproducibility they have reported may well be due to a number of reasons. Firstly, they imaged at 1.5T reducing the amount of BOLD signal detected. Also they used a lower resolution EPI sequence with a small of number of echoes (number of echoes=6). This would have reduced the accuracy of T2* signal detected. Finally, their image analysis

was conducted with a single ROI incorporating the whole calf, including blood vessels and soft tissue (but excluding bone), which would have resulted in erroneous assessment of T2*. Furthermore, they analysed only 2 parameters for the assessment of reproducibility, namely T2*Max and TTP, but they do not mention how these parameters were calculated, whether this was done manually or in an automated fashion. These limitations in that study may have resulted in their findings of a lack or reproducibility.

Conversely, this study has demonstrated a number of developments, with the aim of improving reproducibility, such as imaging at higher field strengths (3T versus 1.5T), improved spatial resolution with GRE sequences, more accurate quantification of T2* achieved by using more echoes (14 in total), better delineation of ROI's to accurately exclude non-muscular tissue, and using automated analysis of curve parameters and parameters that are more reliably defined and measured. These improvements have been shown to improve the reproducibility using the novel GRE sequence in combination with better MRI scanners and hardware, and careful delineation of ROI's and automated analysis of curve parameters. The study has shown excellent reproducibility both between different users and also between scans in the same subject to the curve parameters we have established are the most important in the assessment of perfusion using BOLD-MRI.

Further improvement in the future will only aid in increasing the sensitivity and accuracy of BOLD-MRI, which should result in even more reliable assessment of perfusion with this modality. The introduction of higher magnetic field strength scanners is very near on the horizon, coupled with improvements in

scanner hardware, such as gradient coils and RF coils will accelerate these developments. Also, the processing power of software used in MRI is increasing allowing more complex sequences to be utilised, which would not have been possible in the past. The notion that BOLD-MRI is not reproducible, and therefore not suitable as clinical tool, can be considered no longer true as shown with the results of this study.

## 4.6 Summary

BOLD-MRI performed with the novel GRE sequence can detect perfusion differences between ischaemic limbs and control limbs. The modality is sensitive enough to detect incremental changes in perfusion, as represented by the different cohorts investigated. Automated analysis of curve parameters has the potential to reduce errors, which may impact on the reliability and objectivity of this technique. Furthermore, assessing the change in T2* signal may prove to be more useful then absolute values, with the introduction of 2 new parameters identified as most discriminatory in detecting differences in perfusion.

# Chapter 5

# Assessment of Perfusion After Lower Limb Revascularisation

## 5.1 Introduction

Patients with CLI are at significant risk of major limb loss[1,3], and therefore revascularisation is undertaken with the aim of salvaging the limb. Interventions include surgical and/or endovascular revascularisation. Patients with PAD, particularly those with CLI, usually have disease at multi-levels, with interventions performed in stepwise basis. The most proximal lesions are dealt with first, and more distal disease intervened on as required. Improvement in tissue perfusion is the most important determinant of limb salvage in critically ischaemic limbs that are revascularised using bypass surgery or angioplasty/stenting, but there is currently no reliable method for measuring the adequacy of perfusion in the lower limb[52].

Apart from assessment of clinical signs and symptoms, the only method widely employed in demonstrating the success of revascularisation is measuring the ABPI, but this may not be possible in all patients. ABPI is, in any case, a surrogate for lower limb perfusion and the absolute measures of sufficient revascularisation are clinical endpoints such as symptom improvement and tissue healing. These endpoints maybe easier to define in patients with IC or rest pain, as improvement in symptoms can readily be assessed, but tissue

healing usually only becomes apparent after a number of weeks and, for patients who may require more extensive revascularisation, a window of opportunity to improve tissue perfusion expediently would be lost resulting in amputation[177–179].

Having a method to rapidly and reliably assess the changes in perfusion after intervention would aid in the management of patients with CLI. It would allow for assessment of the adequacy of revascularisation, and help identify those patients where perhaps the further procedures are needed to fully optimise perfusion.

In the previous chapter, it was shown that the novel GRE BOLD-MRI sequence developed was able to accurately differentiate perfusion in patients with CLI against controls. Moreover, it was sensitive enough to distinguish between the symptomatic and asymptomatic limbs in CLI patients. If BOLD-MRI could also be used to provide information on changes in perfusion after revascularisation it may prove a useful adjunct in the management of patients with CLI.

## 5.2 Aims

(i) To use BOLD-MRI to assess changes in perfusion in patients with CLI before and after revascularisation.

(ii) To determine if BOLD-MRI can detect incremental changes in perfusion after segmental revascularisation.

## 5.3 Methods

### 5.3.1 Study Participants

Patients with CLI were imaged prior to and 1 to 14 days (median 3 days) after revascularisation with the GRE BOLD-MRI sequence. Intervention involved endovascular and/or open surgery of the aortic, iliac, common femoral or superficial femoral arteries (SFA). Patients undergoing distal bypass were excluded because of a possible risk of graft occlusion with cuffing and because haematoma secondary to open surgical intervention below the knee made interpretation of BOLD-CMR scans difficult. Successful revascularisation of the target vessels was confirmed by duplex and/or CT angiography, and related to ABPI measured before and after intervention.

Further details of study participants and consent process in described in chapter 2.2.

### 5.3.2 Protocol for BOLD-MRI and Image Analysis

All subjects underwent imaging using the MRI setup and cuffing protocol described in chapter 2.3 and 2.4. The GRE sequence described in chapter 3.3.2 was used and image analysis carried out as described in chapter 2.6 using the automated analysis software.

### 5.3.3 T2* Signal Changes With Revascularisation

Patients with CLI were imaged with the GRE BOLD-MRI sequence. T2* maps were analysed and the signal intensity time course curves were compared

before and after revascularisation. Comparison with CLI patients contralateral control limbs was also performed to assess the improvement in perfusion after intervention. The most discriminatory curve parameter's, i.e. Grad and SRi, determined before and after revascularisation were compared as was the change in ABPI.

### 5.3.4 Sensitivity of BOLD-MRI to Incremental Changes in Perfusion

To determine whether BOLD-MRI was sensitive to incremental changes in blood flow, the fold change in Grad and SRi after revascularisation was compared between patients in whom the SFA was patent after intervention and those in whom the SFA remained occluded. Not all CLI patients underwent interventions to recanalise the SFA, as dealing with more proximal disease was more severe and required intervention first. The fold change in ABPI was also measured and compared to the fold change in curve parameters.

Fold change in curve parameters and ABPI was calculated by dividing the post intervention value by the pre revascularisation value. Using fold change it was possible to determine if the patency of SFA had a measurable impact on the change in curve parameters compared to changes in ABPI. A fold change of >1 indicates that there was an improvement after revascularisation, whereas a fold change of <1 indicates the opposite.

### 5.3.5 Statistical Analysis

Statistical analysis was carried out using SPSS v20 (IBM Corp. Armonk, NY, USA) and Prism 5 (GraphPad Software Inc. California, USA). Analysis of pre

and post intervention changes in curve parameters (Grad and SRi) and ABPI was carried using a paired t-test. Correlation of fold change in ABPI compared to Grad and SRi was performed with Spearman Correlation. The fold change in the same curve parameters and ABPI was compared in patients who had a patent SFA and those in whom it was occluded using a Mann Whitney Test. All values are given as mean ± SD and $p<0.05$ was deemed to be statistically significant.

## 5.4 Results

### 5.4.1 Subject Demographics

13 patients with CLI were imaged before and after successful revascularisation. One patient was excluded due to the presence of significant oedema in the calf on pre and post intervention imaging interfering with accurate measurement of T2* signal. The lateral compartment was excluded in one patient due to loss of signal from coil artefact.

Table 5.1 shows the patients imaged for this study along with their respective interventions. It highlights that ABPI was only measurable in 5 patients pre intervention and 8 patients after revascularisation. 9 patients had Rutherford class 4 disease (rest pain), whilst the remaining 4 had Rutherford 5 disease (tissue loss). Mean follow up was 11 months (range 1-19months). Rest pain was resolved in all patients, and successful tissue healing was evident in all but 1 patient, who required bypass surgery after occlusion of their SFA stent 3 months post intervention.

**Table 5.1: Demographics, extent of disease and ABPI measurements of CLI patients imaged before and after revascularisation, along with their outcomes and follow-up.**

| | Sex | Age | Rutherford | Disease | ABPI Pre | ABPI Post | Procedure | Outcome | Follow up |
|---|---|---|---|---|---|---|---|---|---|
| 1 | M | 65 | 5 | SFA occlusion | +++ | +++ | SFA angioplasty and stenting | Tissue loss healed | 17 months |
| 2 | M | 52 | 4 | CIA/EIA/POP occlusion | Low | 0.62 | Femoral endarterectomy & Iliac stenting | Rest pain resolved | 13 months |
| 3 | M | 65 | 4 | CIA/EIA occlusion | Low | 1.06 | Femoral-Femoral crossover | Rest pain resolved | 13 months |
| 4 | M | 69 | 4 | Aorto-Iliac/SFA occlusion | Low | 0.46 | Axillo-Femoral bypass | Rest pain resolved | 12 months |
| 5 | M | 79 | 5 | CIA/EIA occlusion | +++ | ++<br>+ | Iliac angioplasty and Stent | Rest pain resolved | 2 months |
| 6 | M | 72 | 4 | CIA/EIA occlusion | 0.51 | 0.93 | Femoral-Femoral crossover | Rest pain resolved | 4 months |
| 7 | M | 65 | 4 | EIA stenosis, CFA occlusion | 0.22 | 0.7 | Femoral endarterectomy & Iliac angioplasty & Stenting | Rest pain resolved | 6 months |
| 8 | M | 79 | 4 | EIA/CFA/SFA occlusion | +++ | +++ | Femoral endarterectomy & Iliac angioplasty & Stenting | Rest pain resolved | 6 months |
| 9 | M | 62 | 4 | CIA/EIA occlusion | +++ | +++ | Iliac angioplasty and Stenting | Rest pain resolved | 12 months |
| 10 | F | 64 | 4 | CIA/SFA occluded | 0.43 | 0.81 | Femoral-Femoral crossover | Rest pain resolved | 19 months |
| 11 | F | 69 | 4 | SFA occlusion | +++ | +++ | SFA angioplasty and stenting | Rest pain resolved | 1 month |
| 12 | M | 75 | 5 | EIA stenosis, SFA occlusion | 0.58 | 0.95 | Iliac stenting & SFA angioplasty | In stent stenosis angioplasty, Improved | 16 months |
| 13 | M | 59 | 5 | EIA/SFA occlusion | 0.38 | 0.53 | Femoral endarterectomy & Iliac/SFA angioplasty & stenting | Stent occlusion needing bypass | 17 months |

### 5.4.2 Changes in Perfusion Pre & Post Revascularisation

T2* signal intensity time course curves in the ischaemic limb prior to intervention were consistent with curves typical of limbs with impaired perfusion (Figure 5.1).

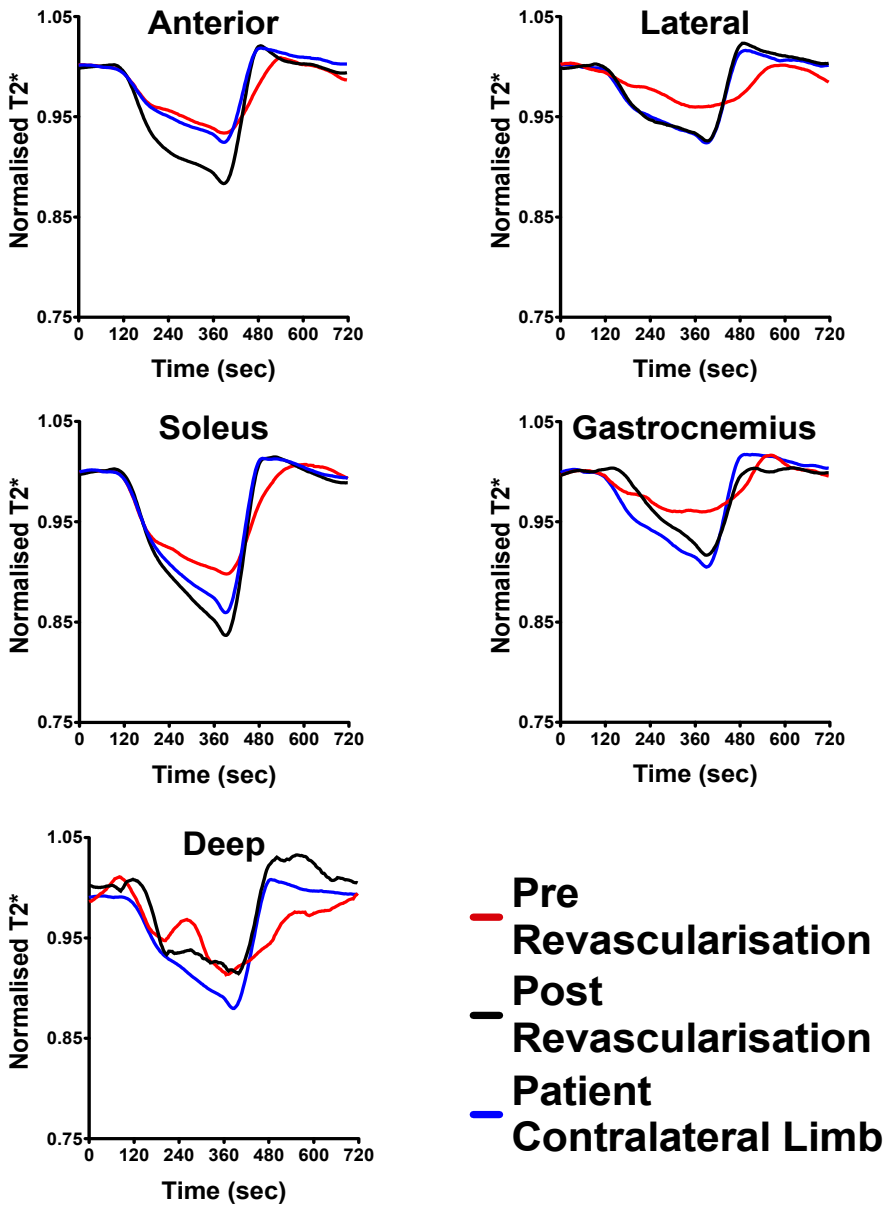


**Figure 5.1: T2* signal curve for ischaemic limbs pre and post revascularisation (n=12), compared to contralateral control limbs**

A significantly lower Grad and SRi confirmed this in the pre intervention ischaemic limbs compared to contralateral asymptomatic control limbs (Grad: 0.14 ± 0.10ms/s vs. 0.28 ± 0.14ms/s, p<0.0001 and SRi: 8.08 ± 5.04% vs. 11.03 ± 5.62%, p<0.005, unpaired t-test), and age-matched controls (Grad: 0.38 ± 0.17ms/s, p<0.0001 and SRi: 13.77 ± 6.33%, p<0.0001, unpaired t-test).

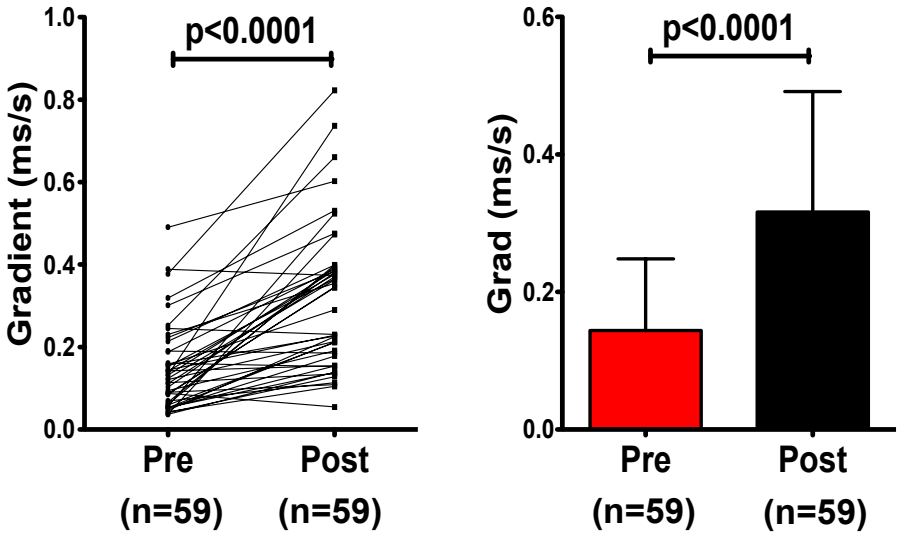


**Figure 5.2: Changes in Grad after revascularisation (paired t-test)**

Repeat BOLD-MRI after successful revascularisation, resulted in improvement in T2* signal intensity time course curves to resemble the perfusion profiles of CLI patients contralateral asymptomatic control limbs (Figure 5.1). Assessment of curve parameters showed a significant increase in Grad (Figure 5.2) and SRi (Figure 5.3) after revascularisation (Grad: 0.14 ± 0.10ms/s vs. 0.32 ± 0.18ms/s, p<0.0001; SRi 8.08 ± 5.04% vs. 11.57 ± 6.31%, p<0.005, paired t-test.

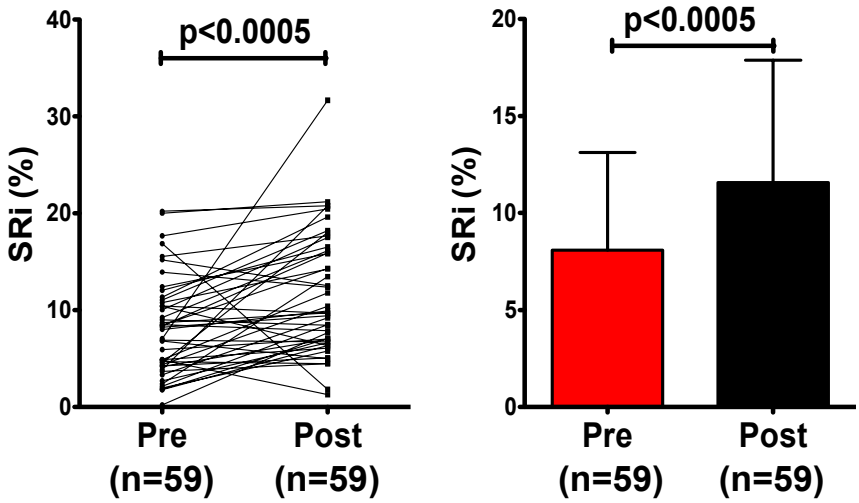


**Figure 5.3: Change in SRi after revascularisation (paired t-test)**

ABPI changes before and after revascularisation were also compared in those patients where it was measurable. A significant improvement was seen in ABPI after intervention (0.42 ± 0.14 vs. 0.76 ± 0.22, p<0.01, unpaired t test)(Figure 5.4).

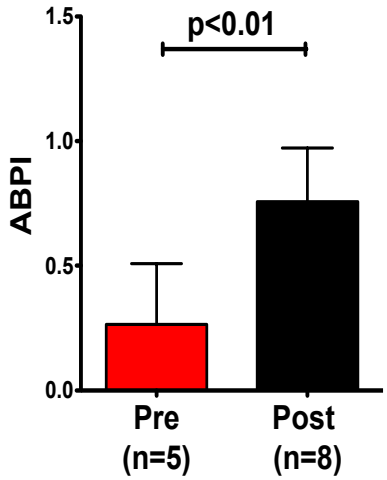


**Figure 5.4: Change in ABPI after revascularisation (unpaired t-test)**

Fold change in ABPI after successful revascularisation was correlated with fold change in Grad and SRi (Figure 5.5). No correlation was seen between ABPI and Grad (r=0.05, p>0.05, Spearman's Correlation) or with SRi (r=0.07, p>0.05, Spearman's Correlation).

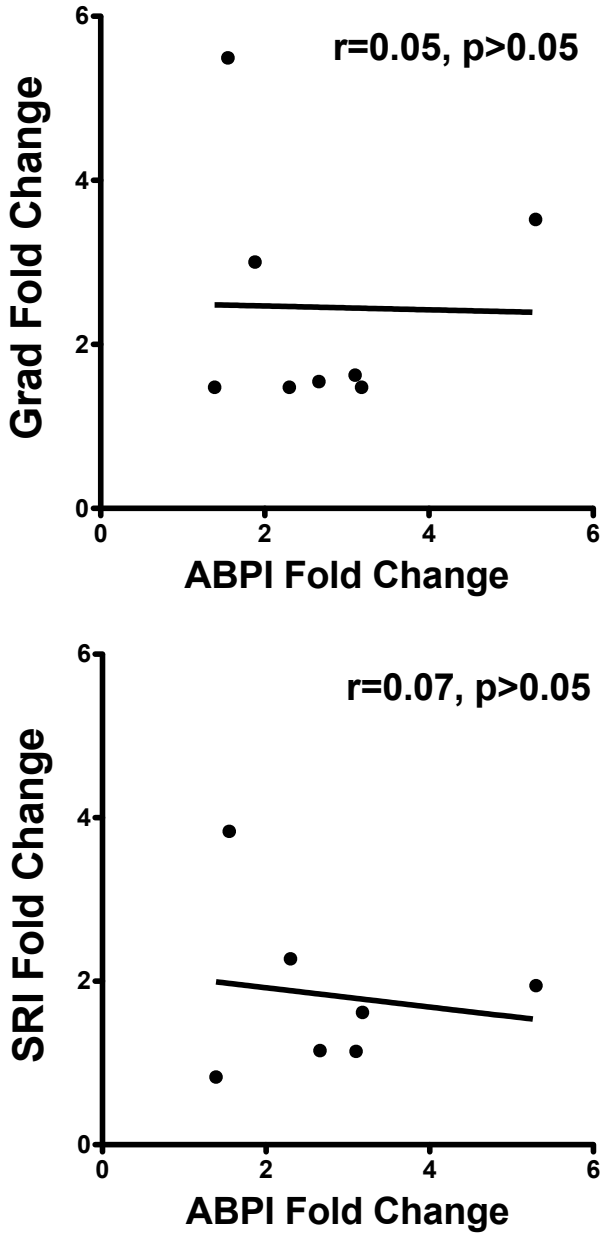


**Figure 5.5: Correlation of ABPI fold change with Grad and SRi (Spearman's Correlation)**

### 5.4.3 Sensitivity of BOLD-MRI to Incremental Changes in Perfusion

The extent of arterial disease was assessed in patients undergoing intervention. Not all patients had a patent SFA post revascularisation, as in some cases more proximal lesions were tackled to improve perfusion. Of the 12 patients undergoing intervention that could be assessed reliably with BOLD-MRI the patency of SFA after revascularisation was examined, and the changes in curve parameters dependent on this was analysed.

9 CLI patients had a patent SFA after revascularisation, whether the SFA was patent prior to intervention, or intervention included treating the SFA. In 3 patients the interventions were concentrated on tackling more proximal lesions, such aorto-iliac or common femoral artery disease, and after revascularisation the SFA remained occluded.

The fold change in Grad and SRi were compared depending in the patency of the SFA. Patients in whom the SFA was patent demonstrated a larger-fold increase in Grad compared with those in whom the SFA remained occluded after proximal revascularization ($3.49 \pm 2.56$ vs. $1.87 \pm 0.73$; $p < 0.05$). A similar trend was observed for SRi ($3.12 \pm 6.16$ with patent SFA vs. $1.81 \pm 1.27$ with occluded SFA; $p > 0.05$). Patency of the SFA had no significant effect on the fold change in ABPI after intervention ($2.56 \pm 1.61$ with patent SFA vs. $2.86 \pm 0.49$ with occluded SFA; $p > 0.05$)(Figure 5.5), in those CLI patients where it was measurable (n=5/9 patent SFA vs. n=3/3 occluded SFA).

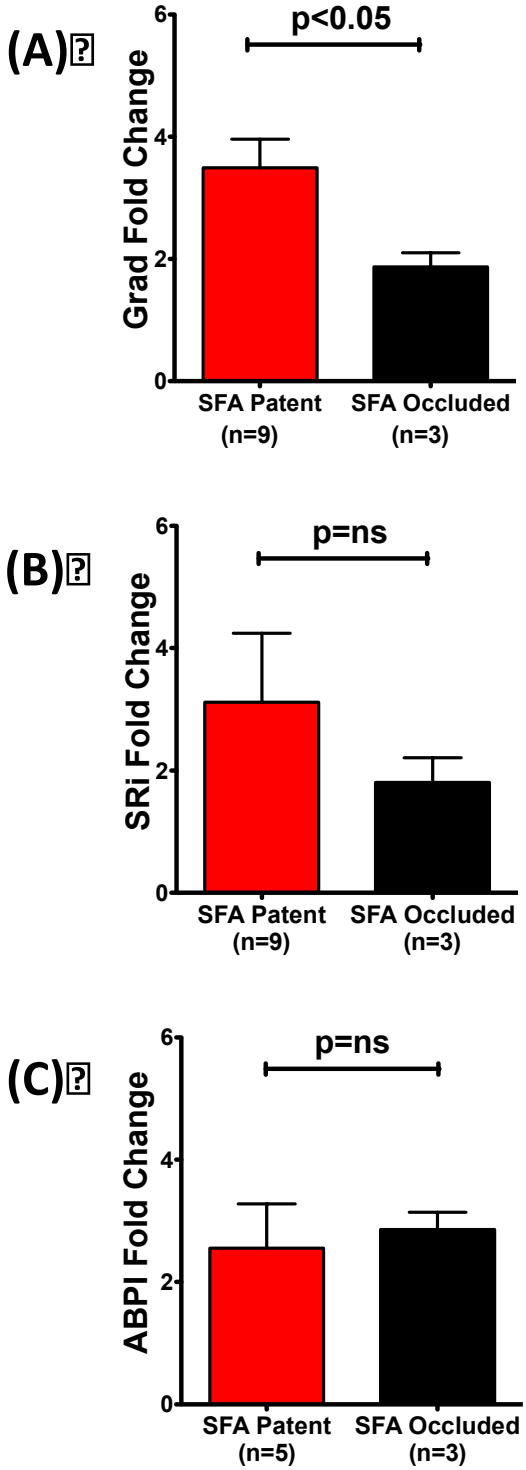


**Figure 5.5: Fold Change in Grad (A), SRi (B), and ABPI (C) after revascularisation depending on the patency of the SFA (Mann Whitney Test)**

## 5.5 Discussion

Having shown that the novel GRE BOLD-MRI sequence developed in this study can reliably differentiate between ischaemic limbs and control limbs in the previous chapter, the next step undertaken was to assess perfusion changes in CLI patients undergoing revascularisation.

### 5.5.1 Measuring Perfusion Changes after Revascularisation

In this study we have shown that BOLD-MRI can detect changes in perfusion after intervention. It can be seen that the T2* signal intensity time course curves from the ischaemic limbs in CLI patients prior to intervention are consistent with curves expected for limbs with poor perfusion. After successful revascularisation, the curve profiles change to resemble curves generated from asymptomatic limbs. This is confirmed by the change seen in curve parameters calculated and a significant improvement is seen in both Grad and SRi, with the values comparable to the contralateral, asymptomatic (control) limb in patients presenting with CLI

All patients underwent successful revascularisation, confirmed by improvements in clinical symptoms, and a rise in ABPI in those patients where ABPI was measurable. One patient did require further revascularisation, but this was 3months after their initial intervention and was due to stent occlusion. In this particular intervention the post-intervention BOLD-MRI carried out 1 week after intervention demonstrated that the perfusion had been improved by the revascularisation undertaken, and it was only 3months later did the stent

occlusion occur requiring further procedures. Up to that stage that patient had seen improvement in their symptoms. One further patient was found to have in-stent stenosis at follow-up imaging, but again at the time of post-intervention BOLD-MRI, their perfusion had been improved as evidenced by clinical symptoms and change in ABPI.

Only one study previously has attempted to investigate the role of BOLD-MRI before and after intervention in patients with PAD[143]. This study investigated 10 patients with IC undergoing SFA angioplasty and used BOLD-MRI with an ischaemia-reactive hyperaemia model to evoke changes in perfusion, however they only analysed the reactive hyperaemia portion of the curve. They showed a trend towards improved perfusion as indicated by change in parameters, but failed to show any significance with their technique or with the parameters they chose to evaluate perfusion. They did have a number of limitations in their study, as alluded to in previous chapters. This study was performed with 1.5T MRI scanner and using an GE EPI sequence with only 4 echoes making accurate quantification of T2* signal more difficult. They did show a significant improvement in patients ABPI's post intervention, suggesting that although BOLD-MRI was not sensitive enough to detect significant changes, the revascularisation performed was sufficient to improve perfusion.

This study is the first that has demonstrated that with the novel GRE BOLD-MRI sequence improvement in perfusion can reliably be detected. Utilising improved scanner technology and MRI sequences, along with improved image analysis, it has been shown that the impact of interventions can be immediately assessed

for adequacy with BOLD-MRI. This study has used the largest cohort to date to assess changes in perfusion after revascularisation with BOLD-MRI.

ABPI is widely utilised as a measure of adequacy of perfusion[1,3,52]. After revascularisation, an improvement in ABPI of >0.10 provides an indication if interventions have resulted in increasing blood flow to the limb[180]. ABPI is not measurable in every patient with PAD, such as with very calcified arteries. Also it can be difficult to accurately measure in patients with severe ischaemia, as encountered in CLI, where very low flow in the tibial vessels can be difficult to accurately detect. Variability in ABPI measurement and technique can also be problematic when using this technique[16,181].

This study confirms that successful revascularisation was performed not only by improvements in clinical symptoms, but also by post-procedure imaging and also by improvement in ABPI by >0.10. This improvement is also seen in perfusion measurement with the novel GRE BOLD-MRI technique. However, as seen in chapter 4, no correlation is seen with the improvement seen in ABPI after successful revascularisation and changes in BOLD-MRI derived perfusion measures. Therefore, it suggests that ABPI and BOLD-MRI derived measures are assessing different aspects of blood flow and perfusion in the limb. ABPI is a measure of pressure related changes in the limb, and such is dependent on the “inflow” of blood to the limb. It does not take into account the microvascular status of perfusion in the tissue.

Some of the changes in the curve characteristics can be attributed to the increased inflow of blood into the limb. The increase in SRi after

revascularisation seen could be related to the increase in inflow into the limb after intervention. This increased inflow would result in a greater reserve the muscles can accommodate during the ischaemic phase. The improved Grad can also be related to the improved inflow after the cuff is deflated to evoke reactive hyperaemia.

### 5.5.2 Incremental Changes in Perfusion After Revascularisation

An imaging modality that allows for sensitive assessment of perfusion would greatly assist in the management of patients with CLI. These patients usually have arterial disease at multiple levels and formulating a management plan can be challenging as it can be difficult to quantify the contribution each disease level has. For these patients, the most proximal disease is tackled first, but this may not be enough to adequately improve perfusion to salvage the limb[1,3]. An early objective assessment of the extent of improvement in limb perfusion after proximal revascularisation may help identify patients that need prompt revascularisation of the distal vasculature thereby improving limb salvage.

This study has shown that not only is the novel GRE BOLD-MRI sequence sensitive to changes in perfusion after successful intervention, but it is also able to detect perfusion changes depending on the status of the inflow. The main inflow vessel into the calf is the SFA. In some CLI patients, interventions were performed on more proximal vessels, i.e. aortic, iliac and/or common femoral artery, with the SFA occluded. In other patients, the SFA was either patent and more proximal lesions were intervened on, or that the SFA itself was revascularised in addition to treating the proximal disease. A greater fold

change in Grad was observed in cases where the SFA was patent after intervention. A similar trend was seen for SRi but the differences did not reach significance. The fold change in ABPI, however, was not associated with the patency of the SFA, suggesting the BOLD-MRI is more sensitive than ABPI for detecting incremental changes in lower limb perfusion. Having a patent SFA should results in a greater improvement in inflow into the calf and therefore one would expect the degree of improvement in perfusion to be greater, compared with cases where the SFA is occluded and calf perfusion is reliant on collateral flow distal to the revascularised proximal segment.

Particularly in patients with CLI who have tissue loss, the adequacy of the revascularisation procedure and its effect on downstream perfusion may not become apparent until there is failure to heal several weeks after intervention, by which time the opportunity to re-intervene may have been lost, resulting in limb loss. Rapid assessment of changes in perfusion may identify a group of patients where further revascularisation is warranted to enable a satisfactory outcome.

### 5.5.3 BOLD-MRI Assessment to Identify the Need for Further Intervention

The GRE BOLD-MRI sequence developed in this study has shown that it is sensitive to differences in perfusion in different groups, can identify changes in perfusion and can differentiate between incremental changes in perfusion. The patients undergoing pre and post intervention imaging had successful outcomes. What is needed to assess this technique further is investigating patients where the revascularisation has not been successful or adequate. It

can be hypothesised that in these patients the improvements detected with BOLD-MRI can identify these shortcomings and inform management plans to include further revascularisation.

With the advent of interventional MRI suites, it may even be possible to perform BOLD-MRI on table to identify those patients that require further procedures, which could then be performed immediately. These combined operating and imaging suites are beginning to inform management plans in interventional cardiology[182] and neuroradiology[183]. It is conceivable that the use of these facilities could be extended to patients with PAD, where baseline BOLD-MRI is undertaken, a procedure performed followed by repeat imaging. This may allow for immediate analysis of changes in perfusion to identify those cohorts of patients where further revascularisation is required, and this could be offered immediately.

## 5.6 Summary

This study has shown that the novel GRE BOLD-MRI sequence can reliably identify changes in perfusion after revascularisation. It is also sensitive to the incremental nature of the inflow of blood the lower limb. It can be envisaged that information gained from BOLD-MRI could help inform management decisions, and identify those patients where interventions are not sufficient to improve muscle perfusion. With interventional MRI suites, these further procedures could be performed immediately without the need for patients to return to operating room.

# CHAPTER 6

# Relating BOLD-MRI to Markers of Muscle Vascularity

## 6.1 Introduction

The basis of the signal generated in BOLD-MRI is dependent on the ratio of oxygenated and deoxygenated haemoglobin in tissue[118,140,141]. Factors that alter this ratio therefore influence the BOLD signal generated. Different physiological parameters have been postulated to influence skeletal muscle BOLD signal, such as blood flow, intravascular blood volume, cellular pH and fluid shifts, vessel diameter, and orientation[140]. However, it is generally accepted that the bulk of BOLD signal alterations in BOLD-MRI of skeletal muscle tissue is due to the delivery of oxygenated haemoglobin[142,144,145,156], and therefore muscle perfusion.

In cardiac perfusion imaging BOLD-MRI has been validated against PET[126] and fractional flow reserve[184] in man, and radiolabelled microspheres in animal models[125] and shows good correlation. In skeletal muscle, BOLD-MRI has been validated against TcPO2 and LDF showing a moderate to good correlation[144]. Correlation is also seen with plethysmography and BOLD-MRI[139]. However, these are methods of assessing skin perfusion and global changes in the limb.

In previous chapters we have described how novel GRE BOLD-MRI can differentiate between different groups and how intervention results in change in BOLD signal measured. However ABPI, which is the most common measure for assessing perfusion in the limb, does not correlate with curve parameters.

Histological endpoints can provide additional information regarding the status of perfusion in muscle. Capillary:fibre (C:F) is an established technique for assessing perfusion in skeletal muscle[185]. It has been shown that patients with PAD have a lower C:F ratio compared to age-matched controls[186]. No previous attempts have been made to relate BOLD-MRI in skeletal muscle with such histological endpoints, and such comparison would provide further evidence that this technique can provide a valuable adjunct in the management of patients with PAD.

## 6.2 Aims

(i) To compare novel GRE BOLD-MRI derived curve parameters in patients undergoing major amputation with C:F ratio.

## 6.3 Methods

### 6.3.1 Study Participants

Patients presenting with CLI with non-salvageable limbs requiring major amputation were recruited. These patients did not undergo any intervention on the admission for major amputation, as recent revascularisation may have

influenced histology and BOLD-MRI derived endpoints. Further details are described in chapter 2.2.

### 6.3.2 Protocol for BOLD-MRI and Image Analysis

All subjects underwent imaging using the MRI setup and cuffing protocol described in chapter 2.3 and 2.4. The GRE sequence described in chapter 3.3.2 was used and image analysis carried out as described in chapter 2.6 using the automated analysis software. The tibial tuberosity was used as an anatomical landmark and the distance from this to the middle of the imaging slice was measured.

### 6.3.3 Muscle Biopsies at the time of Major Amputation Surgery

At the time of major amputation, the level of the calf imaged with BOLD-MRI was marked using the tibial tuberosity as an anatomical landmark. Prior to amputation, $1cm^3$ muscle biopsies were obtained from ischaemic muscle at level of imaging with BOLD-MRI, from the five muscle groups (anterior, lateral, soleus, gastrocnemius and deep posterior). Biopsies ($1cm^3$) were also obtained from better-perfused muscle, proximal to the amputation level. From the proximal section, muscle biopsies were taken from the same five muscle groups in below knee amputations and biopsies taken from 3 muscle groups in above knee amputations (anterior, posterior, medial).

### 6.3.4 Immunohistochemical Staining for Capillary:Fibre Ratio

Muscle biopsies were fixed in 4% paraformaldehyde for 30minutes and dehydrated in PBS/15% sucrose for 12hours, PBS/30% sucrose for 48hours and PBS/40% sucrose for a further 24hours. Samples were dried, embedded in optimal cutting temperature compound (OCT, Sakura Finetek Inc., USA) and frozen in isopentane pre-cooled in liquid nitrogen. Immunohistochemical staining was carried out using 7µm-thick frozen sections with the fluorescently labelled antibodies: primary endothelial cell marker (CD31, Alexa Fluor 488-conjugated, 0.6mg/ml, Novus Biological, UK) and secondary basement membrane marker (laminin, Dylight 488-conjugated with Cy3 secondary, 0.85mg/ml, Novus Biological, UK).

Frozen slides were allowed to equilibrate at room temperature for 20 minutes. Tissue sections were then:

1. Rehydrated with PBS for 5minutes
2. Blocked in PBS containing 2.5mls FCS, 0.5g BSA, 50µl Triton x100 for 1hour.
3. Incubated with the primary antibody (1:100 in PBS containing 0.5mls FCS, 0.5g BSA) for 12hours.
4. Washed in PBS 500mls with T2O 250µl 3 times.
5. Incubated with the secondary antibody (1:200 in PBS containing 0.5mls FCS, 0.5g BSA) for 1hour.
6. Washed in PBS 500mls with T2O 250µl 3 times.

7. Mounted with Vectashield mounting medium containing DAPI and a coverslip sealed with nail polish to prevent drying.

Slides were visualised using a light microscope (Leitz, Leica, UK) and images captured using a mounted camera (EXi Blue, QImaging). The C:F ratio was determined by analysis of 4 fields of view in 2 sections of each biopsy obtained 5mm apart. The mean was calculated from this for each muscle groups and used as the C:F ratio for that muscle.

### 6.3.5 Statistical Analysis

Statistical analysis was carried out using SPSS v20 (IBM Corp. Armonk, NY, USA) and Prism 5 (GraphPad Software Inc. California, USA). Comparison of C:F ratio was made between biopsies from better perfused muscle proximal to the amputation site and those taken at the level of BOLD-MRI using an unpaired t-test. For each patient the C:F ratio from poorly perfused muscle at the level of BOLD-MRI imaging was normalised with the C:F ratio from proximal better perfused muscle and correlated with Grad and SRi parameters, generated from the automated analysis software, using Spearman's correlation. All values are given as mean ± SD and $p<0.05$ was deemed to be statistically significant.

## 6.4 Results

### 6.4.1 Study Demographics

3 CLI patients requiring primary major amputation were recruited (median age 61years, range 36-77, 2 females), with 2 undergoing below knee amputations (BKA) and the other having an above knee amputation (AKA). All 3 patients had undergone previous revascularisation attempts at limb salvage, but all had failed, with no intervention in the preceding 3months. The 2 patients having a BKA were diabetics and the patient undergoing AKA was a smoker. ABPI was not measurable in any of the amputation CLI patients.

All 3 patients were able to tolerate BOLD-MRI with the cuffing protocol and all muscle groups were analysed.

Muscle biopsies were harvested at the time of surgery, with tissue obtained from 5 muscle groups at the level of BOLD-MRI in the calf (n=15), and from proximal to the level of amputation (n=13, 5 muscle groups in BKA patients, and 3 muscle groups in AKA patient)

In all patients the amputation stumps healed primarily, with no secondary procedures required, meaning the perfusion to muscle in proximal to the amputation level was adequate.

### 6.4.2 Capillary:Fibre Ratio in Ischaemic Lower Limb Muscle

C:F ratio was measured as a histological marker of poor perfusion. The ratio was compared between ischaemic muscle, at the level of BOLD-MRI, and

better-perfused muscle, proximal to the amputation level. In the three patients who had amputations (one above knee and two below knee), both Grad (0.15 ± 0.10ms/s) and SRi (7.74 ± 1.05%) fell outside the range for age-matched control limbs (Grad 0.38 ± 0.17ms/s and SRi 13.77 ± 6.33%, p<0.0005 for both, unpaired test), confirming impaired perfusion in the ischaemic limb at the level of BOLD-MRI (Figure 6.1).

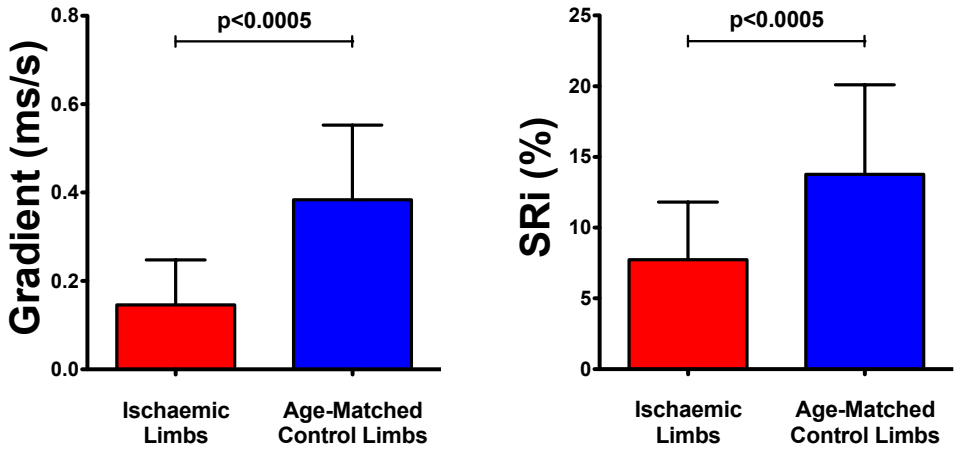


**Figure 6.1: Grad and SRi in CLI patients undergoing major limb amputation compared to age-matched controls (unpaired t-test).**

C:F ratio was compared in ischaemic muscle at the level of BOLD-MRI with ratios obtained from better-perfused muscle proximal to the level of amputation. A typical example of CD31 and laminin staining for C:F ratio is shown in Figure 6.2. Analysis of biopsies from well-perfused muscle proximal to the amputation level shows a significantly higher C:F ratio compared with biopsies from the

level of BOLD-MRI (4.15 ± 0.92 vs. 2.97 ± 0.79, p < 0.001 unpaired t-test)(Figure 6.3).

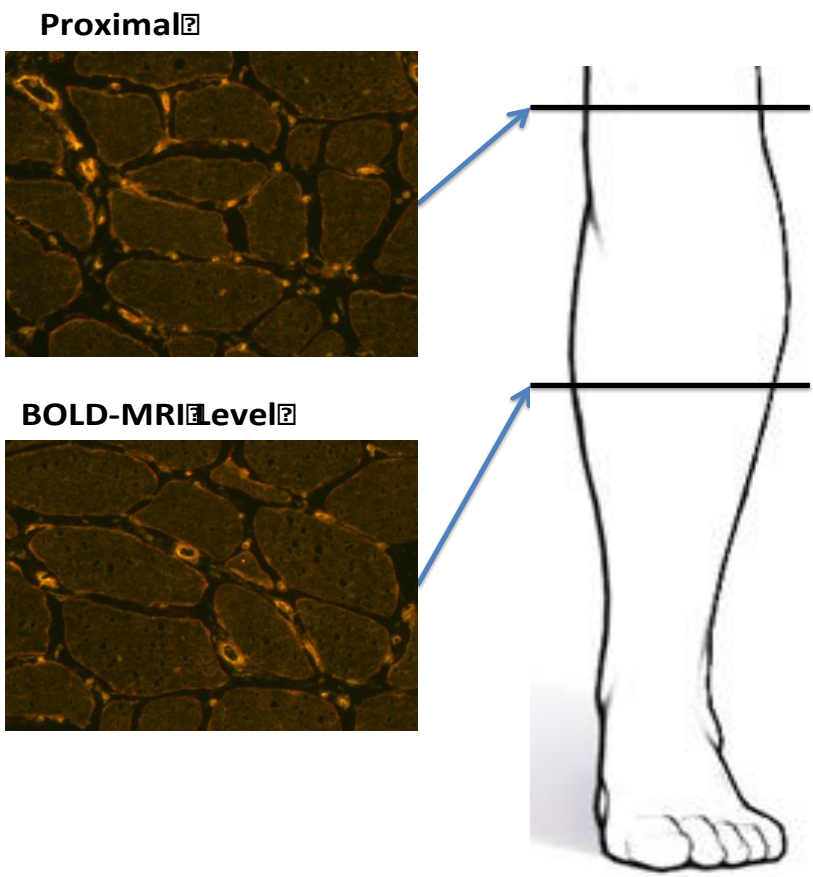


**Figure 6.2: Example of CD31 and Laminin co-staining to determine capillary:fibre ratio in muscle biopsies obtained from better-perfused muscle proximal to amputation level and ischaemic muscle at the level of BOLD-MRI. Capillaries' are seen in orange with co-staining.**

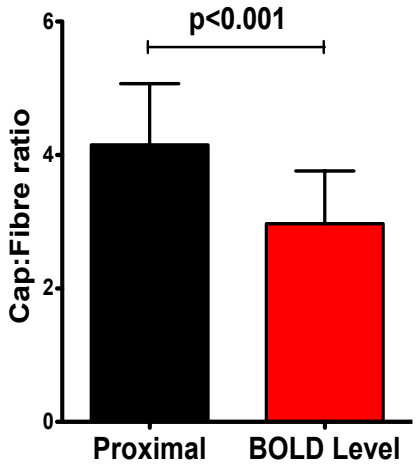


**Figure 6.3: Capillary:fibre ratio between better-perfused proximal to amputation and ischaemic muscle at level of BOLD-MRI (unpaired t-test).**

### 6.4.3 Correlation of BOLD-MRI with Capillary:Fibre Ratio

The C:F ratio in ischaemic muscle from each of the muscle groups in the calf was normalised to the C:F ratio in the proximal better-perfused muscle. This allowed comparison of the difference in the C:F ratio between better-perfused and ischaemic muscle in each patient undergoing amputation, and this was correlated with the BOLD-MRI derived parameters of Grad and SRi. There was a significant correlation between Grad and C:F ratio (r. 0.64, $p < 0.01$), but none was observed with SRi (r. 0.25, $p > 0.05$, Spearman's correlation)(Figure 6.4).

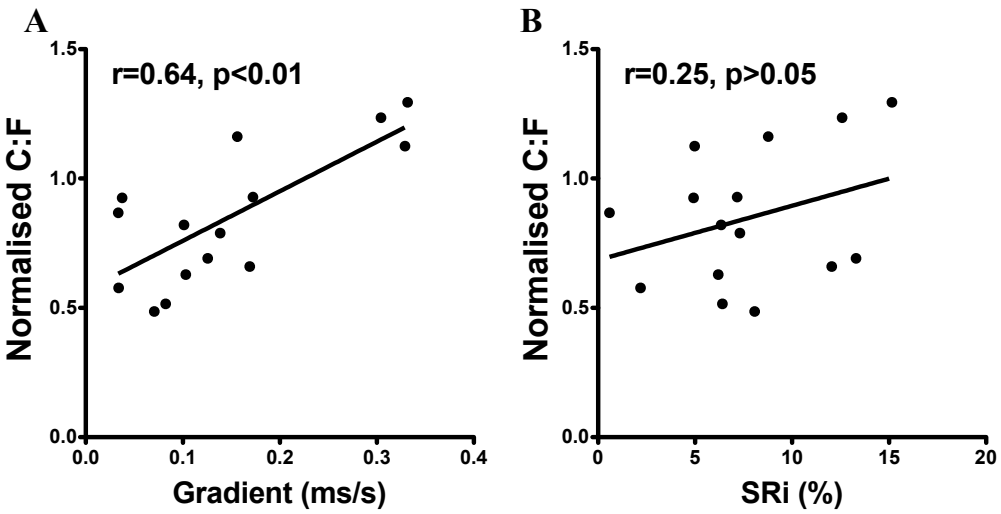


**Figure 6.4: Correlation of Grad (A) and SRi (B) in CLI patients undergoing major amputation with normalised capillary:fibre ratios (Spearman's correlation)**

## 6.5 Discussion

It is generally accepted that the signal generated in BOLD-MRI is mainly influenced by the ratio of oxygenated and deoxygenated haemoglobin in tissue[118,140,141], however other factors are believed to contribute in skeletal muscle BOLD. Validation of BOLD-MRI in skeletal muscle has concentrated on comparing it to methods such as TcPO2, LDF and VOP[139,144], but these modalities are surrogate markers of muscle perfusion. Furthermore, in previous chapters it has been demonstrated that although ABPI and BOLD-MRI do detect limb ischaemia, no correlation between the two has been found. There has been no study to date investigating it with histological endpoints or other methods of assessing muscle perfusion directly, e.g. PET.

This study is the first to attempt to validate BOLD-MRI in skeletal muscle with a histological marker of perfusion. Muscle imaged with the novel GRE BOLD-MRI sequence has been shown to be ischaemic compared to proximal muscle, as demonstrated by a significantly lower C:F ratio. The proximal muscle was adequately perfused as demonstrated by stump healing in all patients undergoing major amputation. The sequence we have used is only capable of imaging a single slice, as the processing power and hardware capability of coils do not permit imaging at multiple levels. It was therefore not possible to image both levels from which muscle biopsies were obtained. Imaging to include both levels would have required repeat imaging, with placement of the imaging slice at each level. The effects of consecutive scanning with repeat cuffing on perfusion imaging with BOLD-MRI is unknown, but an element of muscle perfusion adaptation may introduce errors in measurements. The CLI patients underwent surgery fairly rapidly after the decision was made to amputate and therefore repeat imaging at separate sittings was not possible.

C:F ratios measured in CLI patient were correlated with BOLD-MRI derived perfusion measures, Grad and SRi. A correlation has been shown for Grad but not SRi. This may suggest that Grad is a more sensitive marker of perfusion, and that reactive hyperaemia may be the more important aspect of using the cuffing arterial occlusion model to promote changes in perfusion. It maybe that this aspect of the curve represents that muscles ability to adapt to an increase demand for perfusion, whereas the ischaemic portion represents the ability to tolerate low perfusion. If you compare this to patients with IC, muscle pain occurs after exercise, representing the muscles ability to adapt, i.e. reactive

hyperaemia, whereas the ischaemic portion may represent the late changes that occur with CLI, i.e. rest pain representing low perfusion even at rest and therefore no ability to tolerate low perfusion. The fact this occurs later, may mean that the changes in SRi are not as profound as with Grad.

As a correlation between parameters obtained from BOLD-MRI and C:F, but no such association with ABPI has been demonstrated, it may also suggest that pressure derived measurements may represent an overall simplified view of perfusion in the limb. The macrovascular inflow may influence the ABPI more, whereas in BOLD-MRI as it is the muscle that is being assessed, this may represent what is occurring at the microvascular level, including the impact of inflow into the tissue. As the muscle represents the end organ that is poorly perfused in PAD, this measure may offer a more informative assessment of tissue dysfunction in patients with arterial disease.

As the BOLD-MRI sequence was unable to scan at multiple levels this does highlight a limitation to the correlation seen. Ideally we would correlate C:F ratios in the ischaemic muscle and better perfused proximal muscle with BOLD derived parameters at the respective levels. This does limit the inference we can draw about the correlation seen in this chapter.

## 6.6 Summary

This is the first study to attempt to validate BOLD-MRI derived parameters with histological markers of muscle perfusion, rather than surrogates (e.g. TcPO2, LDF, VOP). It has been shown that muscle imaged with BOLD-MRI is

ischaemic, with a lower C:F ratio compared to muscle better-perfused. Correlation of Grad with C:F ratios has also been demonstrated, suggesting that BOLD-MRI is in part assessing microvascular perfusion in the skeletal muscle.

# CHAPTER 7

# General Discussion and Future Work

## 7.1 Discussion

There is currently no reliable method for assessing muscle perfusion in the lower limb[52]. Techniques most commonly used include TcPO2, LDF and VOP, but these measure either skin perfusion or global changes in the limb. It is estimated that under resting conditions up to 70% of blood flow to the limb is directed to skeletal muscle with the remainder supplying the skin[58]. Skin perfusion has been shown to be maintained until the very late stages of PAD[78,187], and may represent terminal changes in patients with PAD. The most widely utilised technique for assessing the haemodynamic status of the limb in patients with PAD is ABPI. This measurement, albeit a simple clinical test to perform, provides only a surrogate of tissue perfusion and is more a global indicator of flow in the major lower limb vessels.

Patients with CLI exhibit the end stage of PAD, and as such are at high risk of morbidity and mortality[1,3]. Revascularisation is the mainstay of treatment for these patients, but this can be complex, given the fact that disease often affects multiple segments of the lower limb vessels and the patients' comorbidities. Prompt, objective assessment of the intervention undertaken is vital to ensure adequate perfusion has been restored to achieve limb salvage. Currently this is done with a combination of ABPI and assessment of clinical signs and

symptoms, but in patients with tissue loss, improvement in healing can take weeks and an opportunity to fully optimise perfusion maybe lost in that time[177–179].

Medical conditions such as diabetes, an important cause of limb loss and functional disability, affects the microcirculation as well as the larger vessels[188]. Conventional imaging does not allow reliable assessment of the microcirculation, and could, therefore, underestimate the degree of functional limb ischaemia if the main vessels are patent. Similarly, the impact of the collateral circulation (an important compensatory mechanism for maintaining limb perfusion when the main vessels are occluded) cannot be quantified[189]. An accurate method for assessing the functional effect of collaterals on tissue perfusion would be invaluable for determining the efficacy of novel treatments such as angiogenic cell therapy[42,190] that aim to promote collateralisation.

The gold standard for measuring perfusion in skeletal muscle is PET imaging. It allows for accurate mapping of perfusion with radiolabelled isotopes. The cost and infrastructure required for PET imaging, however, make its widespread use prohibitive, and also exposes patients to ionising radiation.

Imaging modalities such as MRI, that do not utilise ionising radiation and are capable of accurately measuring perfusion in muscle, hold promise in the assessment and management of patients with PAD. Three main MRI techniques have been used in perfusion imaging; BOLD, ASL and DCE. Unlike BOLD and ASL, DCE requires the administration of Gadolinium based contrast agents, with inherent risks of NSF in patients with chronic kidney disease.

The blood flow to muscle at rest is extremely low and therefore difficult to assess. Studies using methods such as PET have estimated this to be in the region of 1-2.2ml/min/100g muscle[54,55]. Therefore, techniques to measure skeletal muscle perfusion at rest need to be extremely sensitive to detect differences in patients with PAD. To detect measurable changes in perfusion, manoeuvres to increase muscle blood flow, i.e. hyperaemia, are commonly employed. The 3 most common methods used are, ischaemia to evoke reactive hyperaemia on restoration of blood flow, exercising to produce a functional hyperaemia, and vasodilators inducing a pharmacological hyperaemia. Similar methods are used in cardiac perfusion imaging, where exercise and stress testing is utilised to evoke a hyperaemic response to assess perfusion. This same analogy applies to skeletal muscle perfusion assessment.

In this study we used the ischaemia-reactive hyperaemia model for a number of reasons. This model provides the most reproducible and user independent method of increasing blood flow to muscle[140,141]. It is independent of the subject been imaged and the same conditions can be replicated every time. This is particularly useful if the same subject undergoes repeat imaging, allowing for accurate comparison of perfusion. In contrast, use of an exercise model would have required the use of MRI compatible ergometers. Moreover, it can be difficult for patients with PAD to exercise sufficiently and consistently to the same intensity each time perfusion is assessed. Exercising also increases motion in the limb, even after cessation, introducing artefacts on MRI. Pharmacological hyperaemia usually requires intra-arterial administration of

very short acting vasodilators, such as adenosine. Intra-arterial cannulation is not without risk and would add considerable time required to complete the imaging.

The cuffing protocol used in this study is a standard method using the ischaemia-reactive hyperaemia model, with baseline measurement followed by rapid cuff inflation to suprasystolic pressures. This occludes the inflow to the limb and induces ischaemia. The cuff inflation needs to be rapid in BOLD-MRI to minimise the influence of venous filling on T2* signal[101]. The cuff remained inflated for 5minutes to adequately stress the muscle, and to maximise the reactive hyperaemia. There is no consensus on how long the cuff needs to remain inflated. Reactive hyperaemia was evoked by rapid cuff deflation allowing inflow in to the limb.

By using reactive hyperaemia, with the same investigator inflating the cuff, the variability in hyperaemia was minimised, and therefore more reliable comparisons could be made.

### 7.1.2 Non-Contrast MRI Techniques for Assessing Muscle Perfusion

ASL and BOLD are the 2 non-contrast MRI techniques for assessing skeletal muscle perfusion. ASL-MRI magnetically tags the water molecules in blood proximal to the region of interest and then measure the signal in tissue based in this labelling. With kinetic modelling it possible to quantify perfusion based on the magnetic signal detected in muscle. BOLD-MRI uses the different magnetic properties of haemoglobin depending on it oxygenation status. Deoxygenated

haemoglobin is paramagnetic, which results in an increase in localised magnetic field distortions leading to a lower signal on MRI, particularly T2* relaxation. An increase in perfusion lowers the deoxygenated haemoglobin in tissue and therefore, and increase in T2* signal[52].

The present study compared the spatial resolution between ASL and BOLD MRI. ASL requires rapid image acquisition, usually with an EPI sequence, to capture the magnetically tagged blood, which comes at the expense of spatial resolution. An improved GRE sequence for BOLD-MRI has overcome this limitation of EPI sequences allowing for improved resolution. During sequence development an ASL technique using pCASL was compared with the novel BOLD-MRI and the improved spatial resolution was confirmed.

Spatial resolution is important in muscle perfusion studies to accurately excluded non-muscular tissue, such as bone, major blood vessels and soft tissue. Inclusion of these structures introduces errors in assessing muscle perfusion. The signal obtained is not a true reflection of what is occurring in muscle, but also includes artefact from these tissues.

Also, as BOLD-MRI acquires the majority of its signal directly from the ratio of oxygenated and deoxygenated haemoglobin in the tissue, complex kinetic modelling is not required to determine perfusion. This is also a potential source of error when assessing perfusion using ASL-MRI. The argument levelled against BOLD-MRI is that it does not provide absolute quantification of perfusion, but as already eluded to, due to the low perfusion state of muscle at rest and wide variations seen with increased demand, the absolute perfusion

may be less important than the actual changes in perfusion seen after provoking hyperaemia[52].

The signal generated in ASL-MRI from magnetically tagged water molecules in blood is very small. It is estimated the signal generated is only 0.5-1% over and above the background signal[104], making detection of a reliable signal difficult. The better signal to noise ratio of BOLD-MRI, along with the factors discussed above, means it maybe superior to ASL-MRI.

### 7.1.3 Novel GRE BOLD-MRI

In this study a novel GRE method has been described to acquire BOLD-MRI images. Traditionally an EPI sequence has been utilised to measure T2* signal due to the rapid acquisition this method allows[142–144,154,157,160,163,164,166,168]. This is important to assess changes in perfusion with the different models that are used to evoke changes in muscle blood flow. The limitation of EPI sequences is that an improvement in temporal resolution comes at the expense of spatial resolution, with the issues described with ASL-MRI above becoming a factor.

The novel sequence used in the present study relies on a gradient echo method to acquire changes in T2* signal. This results in improved spatial resolution. The improvement in scanner hardware and processing software allow for improved temporal resolution with images acquired every 3seconds. These improvements also allow for an increase in the number of echoes that can be used to measure T2* relaxation resulting in more accurate quantification is decay. This, coupled with imaging at higher magnetic field strengths (3T versus

1.5T) allows for more sensitive assessment of T2* signal changes with BOLD-MRI.

### 7.1.4 Reproducibility of BOLD-MRI

Although BOLD-MRI has been used to assess perfusion in the lower limb a lack of reproducibility has been a weakness[155]. The novel GRE sequence used in this study aims to overcome this by improving spatial and temporal resolution, increased sensitivity to T2* signal achieved with a higher number of echoes, and imaging at higher field strengths (3T).

The GRE sequence used in the present study shows excellent intraclass correlation for both inter-user and inter-scan reproducibility. The increased sensitivity of measuring T2* signal with this method has improved its reproducibility. An automated software program was used to allow for ROI's to be drawn accurately within muscle compartments, making full use of the improved spatial resolution and allowing automated generation and analysis of signal intensity time course curves and T2* curve parameters. The automated nature allows for objective assessment of T2* signal changes, reducing operator dependent error and improving reproducibility[159].

### 7.1.5 T2* signature in the Ischaemic Limb

Analysing the signal intensity time course curves obtained with BOLD-MRI reveals different perfusion profiles between different groups. At baseline there is steady T2* signal until cuff inflation and arterial occlusion. There is no difference between controls and patients with PAD/CLI. The absolute value of

T2* signal at baseline varies between subjects, and even within subjects between interval scans, and direct comparison is meaningless. For this reason T2* signal intensity time course curves were normalised to the baseline prior to cuff inflation to assess changes in T2* signal with cuff inflation and deflation and to allow meaningful comparison between subjects and between interval scans in the same subjects.

With the onset of ischaemia induced by arterial occlusion, a fall in T2* signal is seen in all group's, however the controls see a greater decrease in signal compared with CLI patients with an early plateau. Ischaemia results in a higher ratio of deoxygenated compared to oxygenated haemoglobin, and therefore a lower T2* signal. This is consistent with previous studies in patients with PAD[147]. This levelling off in T2* signal after cuffing in CLI patients may represent a reduced physiological reserve of muscle to ischaemic stress[191]. With the cuff deflation, reactive hyperaemia results and an increase in T2* signal is seen in all groups. The influx of oxygenated haemoglobin results in washout of deoxygenated haemoglobin and therefore a higher T2* signal. CLI patients have a slower rise in signal after cuff deflation compared to controls and again this consistent with previous reports in PAD subjects[142,143,155]. This slower rise in signal may be due to less efficient delivery of oxygenated haemoglobin to muscle and slower washout of deoxygenated haemoglobin.

Analysis of different parts of the T2* signal intensity time course curves results in curve parameters that can be used as a marker of perfusion. Previous studies have suggested that parameters such as TTP, T2*Max and THIM may represent the most discriminatory indicators of BOLD-MRI based perfusion

assessment[142,143,147,155,164]. These parameters interrogate both the ischaemic and reactive hyperaemic parts of the signal intensity curve, however reproducibility of these parameters has never been shown.

Using the automated analysis software program, two parameters (Grad and SRi) from the signal intensity time course curves were identified as being most informative in differentiating between CLI patients and controls. The Grad can be thought of as analogous to TTP, but the reason for choosing gradient is that it can be reliably and objectively measured. In some patients with CLI, the TTP is difficult to identify, as there is very little overshoot in reactive hyperaemia. With the automated analysis the gradient is calculated by taking the mean of the highest 10 readings of the first derivative during reactive hyperaemia. This allows for a more standardised approach to analyse curve parameters, reducing inter user variability. SRi is akin to THIM, assessing changes in T2* signal during the ischaemic phase. SRi can, however, be more readily measured, as the percentage drop in signal is automatically analysed, whereas THIM requires the user to identify specific points in the T2* curve. The analysis software developed does require manual selection of individual ROI's by the user. In future studies the reproducibility of our technique could be improved by using automated recognition of individual muscle compartments and exclusion of pixels from intra-muscular vessels which may introduce an element of error in T2* estimation in the muscle.

### 7.1.6 BOLD-MRI measurement of limb perfusion after successful revascularisation

Successful revascularisation results in changes in both the ischaemic and reactive hyperaemic parts of the curve, with curve resembling those obtained from control limbs. This is confirmed with improvement in curve parameters, with the values resembling those achieved from control limbs. This shows that BOLD-MRI can detect measurable improvement in muscle perfusion after successful revascularisation.

BOLD-MRI is also sensitive at detecting changes in perfusion related to the status of the inflow vessels. Patients with a patent SFA post intervention have a significantly improved T2* gradient compared with patients in whom the SFA remains occluded. A similar improvement is also seen in SRi, however this failed to reach significance. The status of the inflow is important, particularly in patients with CLI. These patients usually have multi level disease but in a significant proportion treating the disease in the more proximal vessels only is sufficient to resolve the symptoms. This is an advantage particularly when treating the full extent of multilevel disease can be a major undertaking in a patient population that is already has significant co-morbidities, which carries significant inherent risks of prolonged and complex procedure.

The patients recruited to the present study all had resolution of their CLI after intervention, and therefore future studies should investigate patients with a high risk of intervention failure to determine if BOLD-MRI can reliably identify at an early stage those that require further intervention. The advent of hybrid

magnetic resonance (MR)/X-ray (XMR) interventional facilities would facilitate the use of BOLD-MRI as a means of immediately assessing changes in perfusion 'on table'. This would inform the effects of incremental revascularisation on perfusion in the limb (considered as the end organ effect of restoring vessel patency) and determine the need for further intervention. For example, in the case of a patient with both iliac and SFA disease, on table BOLD-MRI could demonstrate a need for incremental recanalization of the SFA even after successful iliac intervention. Conversely, it may demonstrate that adequate improvement in perfusion had occurred with iliac revascularisation only. BOLD-MRI sequences could also readily be added to MR angiography studies to provide both functional and anatomical information simultaneously. This could be useful in planning interventions and assessing outcomes after revascularisation.

### 7.1.7 Correlation and Validation of BOLD-MRI with Established Methods for Assessing Perfusion

Limited studies have been performed in an attempt to validate BOLD-MRI in the lower limb. To date these studies have used methods such as TcPO2 and LDF to show a good correlation with BOLD-MRI derived parameters[144,154,192]. A reasonable correlation has also been shown with perfusion measured with ASL-MRI[101]. Histological correlation of muscle vascularity with perfusion determined by modalities such as PET have not been performed in the lower limb.

Perfusion assessment with BOLD-MRI in the heart has been validated against more robust endpoints[121]. BOLD-MRI has been compared with radiolabelled

microspheres in animal models, showing good correlation[124]. In human studies, BOLD-MRI has been correlated with established techniques of assessing coronary artery haemodynamics and cardiac muscle perfusion. When compared against coronary angiography, a significantly lower signal is detected with BOLD-MRI in myocardial segments perfused by coronary arteries with significant stenosis compared with myocardium supplied by non-stenosed vessels[123,127,193]. BOLD-MRI also compares favourably with gadolinium enhanced MRI[194] and SPECT imaging[123]. More recently, fractional flow reserve (FFR) has been correlated with BOLD-MRI[184]. FFR uses specialised wires with pressure sensors at the tip to measure the pressure changes across a stenosis in the coronary circulation. This provides a ratio, which has been shown to be predictive for detecting significant coronary artery lesion (FFR<0.75-0.8) requiring intervention[195]. BOLD-MRI signal has been shown to be significantly lower in myocardium supplied by coronary arteries with an FFR<0.8, compared to myocardium supplied by arteries with a FFR>0.8. Perhaps the gold standard imaging technique to measure myocardial perfusion remains PET, and it has shown that BOLD-MRI compares favourably with PET[122].

The present study included efforts to correlate BOLD-MRI in the lower limb with histological endpoints. In CLI patients undergoing major limb amputation, BOLD-MRI was performed prior to surgery and parameters were correlated to capillary:fibre ratio (a measure of tissue vascularity) obtained from muscle biopsy taking at the time of surgery from the imaging slice. Grad showed a good correlation with C:F ratio. This is the first attempt to validate BOLD-MRI in the lower limb with a marker of vascularity, and therefore of perfusion.

## 7.2 Limitations

A limitation of BOLD-MRI is its utility in patients undergoing distal bypass, where oedema and haematoma in the field of view may preclude accurate assessment of T2* signal in muscle. In addition the use of thigh cuff to induce ischaemia and evoke reactive hyperaemia would result in temporary occlusion of the bypass graft, with a theoretical risk of precipitating graft occlusion.

All subjects imaged before and after revascularisation had successful intervention with improvement in symptoms. This improvement was reflected in the BOLD-MRI derived parameters. To investigate the predictive potential of BOLD-MRI in assessing whether intervention is sufficient to allow for adequate muscle perfusion ideally imaging needs to be performed in a cohort of patients where revascularisation is not sufficient. Correlation with BOLD derived perfusion parameters with outcomes would allow for this to be investigated.

Not all CLI patients were able to remain still for the duration of the BOLD-MRI due to the presence of rest pain when supine. Although dynamic imaging was relatively rapid, taking only 12minutes, some patients did not tolerate the scan.

The effects of haemodilution and haematocrit are known to show a linear response to T2* signal in BOLD MRI[196–198], but the effects of conditions such as congestive cardiac failure and severe aortic stenosis where there is an impact on cardiac output is less known. This may have an influence on the T2* signal, but more work is required to fully evaluate the impact on BOLD-MRI.

Previous studies have shown a correlation of BOLD-MRI with other markers of perfusion such as LDI and TcPO2[144,154,192], this study only used ABPI as a marker of perfusion and failed to show any correlation. Validation of BOLD-MRI could have been strengthened if other markers of perfusion such as toe pressures or near-infrared spectroscopy had shown a correlation.

## 7.3 Future Work

This study has shown the utility of BOLD-MRI in assessing perfusion and its sensitivity to changes in perfusion. Correlation with histological endpoints in this study has assisted in confirming this. Further validation maybe warranted with comparison with radiolabelled microspheres in animal models, and with PET imaging in human studies.

A reliable method for assessing segmental muscle perfusion in the limb could aid the diagnosis and planning of interventions in patients with PAD. It would also facilitate rapid assessment of changes in perfusion to determine the adequacy of revascularisation procedures. This strategy could ultimately improve limb salvage in CLI patients and therefore, it maybe that BOLD-MRI merits further investigation in a clinical trial. This study has assessed the immediate changes in perfusion measured with BOLD-MRI in patients undergoing successful revascularisation. A study in a much larger cohort would allow measurement of BOLD derived parameters of perfusion in patients where intervention has not been successful. It may allow determination if BOLD-MRI

can predict whether revascularisation is sufficient or whether further intervention is warranted to improve clinical outcomes e.g. limb salvage. Furthermore, to assess adequacy of revascularisation a randomised controlled trial where patients undergo standard, currently accepted intervention could be compared to a group that undergo maximal revascularisation and BOLD measurements correlated with clinical outcome. Such trials would be needed before BOLD-MRI can be fully accepted as a reliable measure of muscle perfusion.

Development of medical angiogenic therapies requires a method for identifying areas of poor perfusion as a target, and also to be able monitor the progress of the therapy. BOLD-MRI maybe able to fulfil this role for future studies in novel angiogenic therapies. The highly reproducible and sensitive measures derived from BOLD-MRI suggest this method could meet the requirements for studies in this area. BOLD-MRI could also be combined with high-resolution contrast enhanced MRI sequences to accurately delineate and quantify collaterals formation. This could be correlated with improvements in perfusion and clinical outcomes.

This study was performed on a 3T MRI scanner that is readily available for clinical use. Newer scanners have been developed with higher magnetic field strengths (4.5T, 7T and 9.4T) are now becoming available in the research field which would be more sensitive to changes in BOLD signal. These scanners may improve the accuracy of BOLD-MRI further. This coupled with improved processing capabilities allowing for more complex MRI sequences would undoubtedly improve the sensitivity and accuracy of BOLD-MRI.

## 7.4 Summary

Tissue perfusion, rather than the anatomical extent of disease affecting the main vessels, determines the severity of ischaemia in the lower limb. BOLD-MRI can measure perfusion in the calf musculature with a high degree of accuracy and reproducibility and is sensitive to changes in perfusion after limb revascularisation. This technique could be combined with standard MRI angiography to provide functional as well as anatomical imaging.

The present study shows that BOLD-MRI consistently detects perfusion deficits in the ischaemic limb and quantifies improvements in perfusion after revascularisation. A reliable method for assessing segmental muscle perfusion in the limb would facilitate rapid detection of changes in perfusion to determine the adequacy of revascularisation procedures. BOLD based perfusion metrics may also allow assessment of pharmacologic and cell based angiogenic therapies being tested as part of clinical studies and merits further investigation in a clinical trial.

# APPENDIX 1

## Ethics Approval Documentation

NHS
National Research Ethics Service
South East London REC 1
(Formerly Guy's REC)
Governor's Hall Suite
St Thomas' Hospital
London
SE1 7EH

Telephone: 020 7188 2260
Facsimile: 020 7188 2258

05 January 2011

Mr Bijan Modarai
Academic Department of Surgery
1st Floor, North Wing
St Thomas' Hospital
Westminster Bridge Road
London SE1 7EH

Dear Mr Modarai

**Study Title:** **An investigation into the pathophysiology of lower limb ischaemia and how to promote therapeutic revascularisation in the critically ischaemic limb.**
**REC reference number:** **10/H0804/67**
**Protocol number:** **1.0**

Thank you for your letter of 25 September 2010, responding to the Committee's request for further information on the above research and submitting revised documentation.

The further information has been considered on behalf of the Committee by the Chair.

**Confirmation of ethical opinion**

On behalf of the Committee, I am pleased to confirm a favourable ethical opinion for the above research on the basis described in the application form, protocol and supporting documentation as revised, subject to the conditions specified below.

**Ethical review of research sites**

The favourable opinion applies to all NHS sites taking part in the study, subject to management permission being obtained from the NHS/HSC R&D office prior to the start of the study (see "Conditions of the favourable opinion" below).

The Committee has not yet been notified of the outcome of any site-specific assessment (SSA) for the non-NHS research site(s) taking part in this study. The favourable opinion does not therefore apply to any non-NHS site at present. I will write to you again as soon as one Research Ethics Committee has notified the outcome of a SSA. In the meantime no study procedures should be initiated at non-NHS sites.

**Conditions of the favourable opinion**

The favourable opinion is subject to the following conditions being met prior to the start of the study.

This Research Ethics Committee is an advisory committee to London Strategic Health Authority
*The National Research Ethics Service (NRES) represents the NRES Directorate within the National Patient Safety Agency and Research Ethics Committees in England*

Management permission or approval must be obtained from each host organisation prior to the start of the study at the site concerned.

For NHS research sites only, management permission for research ("R&D approval") should be obtained from the relevant care organisation(s) in accordance with NHS research governance arrangements. Guidance on applying for NHS permission for research is available in the Integrated Research Application System or at http://www.rdforum.nhs.uk.

*Where the only involvement of the NHS organisation is as a Participant Identification Centre (PIC), management permission for research is not required but the R&D office should be notified of the study and agree to the organisation's involvement. Guidance on procedures for PICs is available in IRAS. Further advice should be sought from the R&D office where necessary.*

*Sponsors are not required to notify the Committee of approvals from host organisations.*

**It is the responsibility of the sponsor to ensure that all the conditions are complied with before the start of the study or its initiation at a particular site (as applicable).**

**Approved documents**

The final list of documents reviewed and approved by the Committee is as follows:

| *Document* | *Version* | *Date* |
|---|---|---|
| Protocol | 1.0 | 01 June 2010 |
| Response to Request for Further Information | | 25 September 2010 |
| Participant Information Sheet: Healthy Volunteers | 1.1 | 25 September 2010 |
| Covering Letter | | 01 August 2010 |
| GP/Consultant Information Sheets | 1.0 | 01 June 2010 |
| REC application | Parts A - D | 15 July 2010 |
| Participant Information Sheet: Patients | 1.1 | 25 September 2010 |
| Questionnaire: MRI Safety | 1.1 | 25 September 2010 |
| Evidence of insurance or indemnity | KCL -September 2009 | |
| Investigator CV | Mr Bijan Modarai | 04 August 2010 |
| Investigator CV | Mr Ashish Patel | 04 August 2010 |
| Participant Consent Form: Patients | 1.1 | 25 September 2010 |
| Participant Consent Form: Healthy Volunteers | 1.1 | 25 September 2010 |

**Statement of compliance**

The Committee is constituted in accordance with the Governance Arrangements for Research Ethics Committees (July 2001) and complies fully with the Standard Operating Procedures for Research Ethics Committees in the UK.

**After ethical review**

Now that you have completed the application process please visit the National Research Ethics Service website > After Review

You are invited to give your view of the service that you have received from the National Research Ethics Service and the application procedure. If you wish to make your views known please use the feedback form available on the website.

The attached document *"After ethical review – guidance for researchers"* gives detailed guidance on reporting requirements for studies with a favourable opinion, including:

- Notifying substantial amendments
- Adding new sites and investigators
- Progress and safety reports
- Notifying the end of the study

The NRES website also provides guidance on these topics, which is updated in the light of changes in reporting requirements or procedures.

We would also like to inform you that we consult regularly with stakeholders to improve our service. If you would like to join our Reference Group please email referencegroup@nres.npsa.nhs.uk.

| **10/H0804/67** | **Please quote this number on all correspondence** |
|---|---|

With the Committee's best wishes for the success of this project

Yours sincerely

**Professor David Bartlett**
**Chair**

Email: stephanie.hill@gstt.nhs.uk

*Enclosures:* "After ethical review – guidance for researchers" *SL- AR2 for other studies*

*Copy to:* *Keith Brennan, Kings College London*

*R&D office, GSTFT*

# APPENDIX 2

## MATLAB Routine for Image Analysis

```
clear all
close all
%%*********************************************************************
***%%
%% READS IN A SERIES OF DICOM IMAGES
%%
%% CREATES AND SAVES OR LOADS IN SAVED MASK ROIS
%%
%% PLOTS TIME COURSES OF THE ROIS
%%
%% Written by Wesolek (Roman Wesolowski)
%%
%% contact me if you have problems modifying this script.
%%
%%*********************************************************************
***%%

%% Name and path of outcoming and incoming files
%path='/Volumes/DOCS/DATA/studies/';
%cd(path)
ROIcheck=input('Have you saved ROIs to use in this subject? [y/n]:
','s');
ROIcorr=input('Would you like to redo any of the ROIs? [y/n]: ','s');

[FileName,PathName] = uigetfile({'*','*'},'Input the first DICOM
functional image (exported from Osirix)');
im4D_info=dicominfo(strcat(PathName,FileName));
suffix=strfind(FileName
,'.');
FileName=FileName(1:suffix(1)-5);
dyns=im4D_info.NumberOfTemporalPositions;
name_dir=dir(strcat(PathName,FileName,'*'));
name_dir=name_dir(1:dyns);
datefile=num2str(char({name_dir.name}));
im4D=zeros(im4D_info.Rows,im4D_info.Columns,im4D_info.Private_2001_101
8,dyns);
h=waitbar(0,'Loading Files...');
for i=1:dyns
    im4D_info_=dicominfo(strcat(PathName,name_dir(i).name));
    im4D_info_.BitsAllocated=32;
    im4D(:,:,:,i)=im4D_info_.RescaleSlope*dicomread(im4D_info_);
    waitbar(i/dyns,h,strcat('Loading Files...
',num2str(round(i/dyns*100)),' %'));
%    fprintf(1,'File Name: %s \n',name_dir(i).name); %prints out all
the names of loaded files
end
close(h)
fprintf(1,'Total of %d functional files loaded \n',i);
colour_map='rkbmgrkbmgcy';
cd(PathName)
if ((ROIcheck=='n')||(ROIcorr=='y'))
    [FileNameA,PathNameA] = uigetfile({'*','*'},'Input the first DICOM
anatomical image (exported from Osirix)');
    imAnat_info=dicominfo(strcat(PathNameA,FileNameA));
    suffix=strfind(FileNameA,'.');
    FileNameA=FileNameA(1:suffix(1)-5);
    dyns=imAnat_info.NumberOfTemporalPositions;
```

```
    if (dyns==1)
        h=waitbar(0,'Loading Files...');
        slc=imAnat_info.Private_2001_1018;
        name_dir1=dir(strcat(PathNameA,FileNameA,'*'));
        name_dir1=name_dir1(1:slc);
        datefile=num2str(char({name_dir1.name}));
        for i=1:slc

imAnat(:,:,i)=dicomread(strcat(PathNameA,name_dir1(i).name));
%            fprintf(1,'File Name: %s \n',name_dir1(i).name);
            waitbar(i/slc,h,strcat('Loading Files...
',num2str(round(i/slc*100)),' %'));
        end
        close(h)
        fprintf(1,'Total of %d anatomical files loaded \n',i);
    else
        name_dir1=dir(strcat(PathName,FileName,'*'));
        name_dir1=name_dir1(1:dyns);
        datefile=num2str(char({name_dir1.name}));
        h=waitbar(0,'Loading Files...');
        for i=1:dyns

imAnat(:,:,:,i)=dicomread(strcat(PathNameA,name_dir1(i).name));
            waitbar(i/dyns,h,strcat('Loading Files...
',num2str(round(i/dyns*100)),' %'));
%            fprintf(1,'File Name: %s \n',name_dir1(i).name);
        end
        close(h)
        fprintf(1,'Total of %d anatomical files loaded \n',i);
    end
    figure(2)
    clims=[0 500];
    imagesc(imAnat(:,:,ceil(end/2),ceil(end/2)),clims);
    title('Anatomical Image')
    colormap(gray)
    k=0;
    check='y';
    cd ..; mkdir('ROIs'); cd('ROIs');
    info_out=im4D_info_;
    info_out.SeriesNumber=9901;
    info_out.AcquisitionNumber=99;
    info_out.SeriesDescription='ROIs';
    info_out.NumberOfTemporalPositions=1;
    info_out.Private_2001_1081=1;
    info_out.Private_2001_1082=1;
    info_out.EchoTrainLength=1;
    info_out.BitDepth=1;
    info_out.BitsAllocated=1;
    info_out.BitsStored=1;
    info_out.HighBit=1;
    info_out.RescaleSlope=1;
    info_out.Private_2005_140a=1;
%
mask_all=zeros([size(im4D,1),size(im4D,2),size(im4D,3),size(im4D,4)]);
    while (check~='n')
        mask=zeros([size(im4D,1),size(im4D,2),1]);
        if ROIcorr=='y'
            k=input('Which ROI (specific number) would you like to
correct? ');
        else
            k=k+1;
        end
        info_out.InstanceNumber=k;
        disp('double-click on the ROI when finished...');
        figure(1)
        image(im4D(:,:,ceil(end/2),1));
        title('Functional Image 1')
        ROI=impoly(gca);
```

```
        roi=wait(ROI);
%        roi=round(roi);
        mask(:,:,1) = roipoly(mask(:,:),roi(:,1),roi(:,2));
        figure(2)
        commandwindow
        ROI_size=size(mask(mask>0),1);
        fprintf(1,'Current ROI size is %i voxels \n',ROI_size);
%         figure(10)
%         imagesc(mask);
%         mask=round(imresize(mask,[size(im4D,1) size(im4D,2)]));
%         figure(11)
%         imagesc(mask);
        if (size(im4D,3)>1)
            propagate = input('Propagate across slices? [y/n]: ','s');
            if (propagate=='y')
                mask = repmat(mask,[1,1,size(im4D,3)]);
            end
        end
        prop_dyn=input('Propagate across all the dynamics? [y/n]:
','s');
        if (prop_dyn~='y')
            prop=input('Provide number of dynamics to propagate this
ROI to: ');
            mask_ = repmat(mask,[1,1,1,prop-1]);
            mask=cat(4,mask,mask_);
            prop_num=1;
            while
(prop_num<size(im4D,4))%(prop_int~='n')&&(prop_num<size(im4D,4)))
                prop=size(mask,4);
                figure(1)
                image(im4D(:,:,:,prop+1))
                ROI=impoly(gca,roi);
                image_title=strcat('Functional Image
',num2str(prop+1));
                title(image_title)
                fprintf(1,'Double click on the ROI to accept its new
position and shape \n');
                roi=wait(ROI);
%                 roi=round(roi);
                mask_=zeros([size(im4D,1),size(im4D,2),1,1]);
                figure(2)
                commandwindow
                mask_(:,:,1,1) =
roipoly(mask_(:,:),roi(:,1),roi(:,2));
                ROI_size=size(mask_(mask_>0),1);
                fprintf(1,'Current ROI size is %i voxels
\n',ROI_size);
                if ((size(im4D,3)>1)&propagate=='y')
                    mask_=repmat(mask_,[1,1,size(im4D,3),1]);
                end

                prop_num=input('Provide number of dynamics to
propagate this ROI to: ');
                if (prop_num>size(im4D,4))
                    prop_num=size(im4D,4);
                    fprintf(1,'Total number of functional scan has
been exceeded.\n The ROIs will only by saved to match %i dynamics
\n',prop_num);
                end
                prop=-prop+prop_num;
                mask_ = repmat(mask_,[1,1,1,prop]);
                mask=cat(4,mask,mask_);
            end
        else
            mask = repmat(mask,[1,1,1,size(im4D,4)]);
        end
        check=input('Do you want to create/correct another ROI? [y/n]:
','s');
```

```
        if k<10
            suffix=strcat('0',num2str(k));
        else
            suffix=num2str(k);
        end
        info_out.Filename=strcat(pwd,'/ROI_',suffix);
        h=waitbar(0,'Saving Files...');
        for t=1:size(mask,4)
            if (t<10)

dicomwrite(mask(:,:,:,t),strcat('ROI_',suffix,'_dyn_00',num2str(t),'.d
cm'),info_out,'ObjectType','MR Image Storage');
            elseif (t<100)

dicomwrite(mask(:,:,:,t),strcat('ROI_',suffix,'_dyn_0',num2str(t),'.dc
m'),info_out,'ObjectType','MR Image Storage');
            else

dicomwrite(mask(:,:,:,t),strcat('ROI_',suffix,'_dyn_',num2str(t),'.dcm
'),info_out,'ObjectType','MR Image Storage');
            end
            waitbar(t/size(mask,4),h,strcat('Saving Files...
',num2str(round(t/size(mask,4)*100)),' %'));
        end
        close(h)
        fprintf(1,'Total of %d ROI files saved \n',t);
%        mask_all=mask_all+mask;
%        mask=repmat(mask,[1 1 1 size(im4D,4)]);

masked_im(:,k)=squeeze(sum(sum((im4D.*mask),1),2))./squeeze(sum(sum((i
m4D.*mask)~=0,1),2));
        figure(3)
        if (k<6)
            plot(0:3:(3*size(im4D,4)-
3),masked_im(:,k),colour_map(k),'LineWidth',1.5);
        else
            plot(0:3:(3*size(im4D,4)-3),masked_im(:,k),strcat('--
',colour_map(k)),'LineWidth',1.5);
        end
        lgnd(k,:)=strcat('ROI',suffix);
        hold on
    end
else
    [PathName] = uigetdir('','Input the folder containing previosuly
saved ROI files');
    cd(PathName)
    dir_data=dir; dir_index=[dir_data.isdir];
    name_dir=dir_data(~dir_index);
    if (regexp('.DS_Store',name_dir(1).name)==1)
        name_dir=name_dir(2:end);
    end
    ROIin_info=dicominfo(strcat(PathName,'/',name_dir(1).name));
%    mask_all=zeros([size(im4D,1),size(im4D,2),1,1]);
    ROI_mask =
zeros([size(im4D,1),size(im4D,2),size(im4D,3),size(name_dir,1)/size(im
4D,4)]);
    h=waitbar(0,'Loading ROI Files...');
    for p=1:size(name_dir,1)
        ROI_in = strcat(PathName,'/',name_dir(p).name);
        ROI_mask(:,:,:,p) =
(dicomread(ROI_in)>0);%/ROIin_info.LargestImagePixelValue;
        waitbar(p/size(name_dir,1),h,strcat('Loading ROI Files...
',num2str(round(p/size(name_dir,1)*100)),' %'));
    end
    close(h)
    fprintf(1,'Total of %d ROI files loaded \n',p);

mask=reshape(ROI_mask,size(im4D,1),size(im4D,2),size(im4D,3),size(im4D
```

```
,4),size(ROI_mask,4)/size(im4D,4));

    for k=1:size(mask,5)
        if k<10
            suffix=strcat('0',num2str(k));
        else
            suffix=num2str(k);
        end

masked_im(:,k)=squeeze(sum(sum((im4D.*mask(:,:,:,:,k)),1),2))./squeeze
(sum(sum((im4D.*mask(:,:,:,:,k))~=0,1),2));
        figure(3)
        if (k<6)
            plot(0:3:(3*size(im4D,4)-
3),masked_im(:,k),colour_map(k),'LineWidth',1.5);
        else
            plot(0:3:(3*size(im4D,4)-3),masked_im(:,k),strcat('--
',colour_map(k)),'LineWidth',1.5);
        end
        lgnd(k,:)=strcat('ROI',suffix);
        hold on
    end
end
legend(lgnd);
xlabel('time [s]');
ylabel('T_2*');
title('Time course of T_2* changes for given ROIs');
hold off
cd ..
saveas(gcf,'allROIs.pdf','pdf');
saveas(gcf,'allROIs.fig');
%figure(2)
%imagesc(mask_all.*(im4D(:,:,1,ceil(end/2))));
masked_im_sm1=zeros(size(masked_im,1),size(masked_im,2));
masked_im_sm10=masked_im_sm1;
masked_im_sm20=masked_im_sm1;
for p=1:size(masked_im,2)
    masked_im_sm1(:,p)=smooth(masked_im(:,p),'moving');
    masked_im_sm10(:,p)=smooth(masked_im(:,p),10,'moving');
    masked_im_sm20(:,p)=smooth(masked_im(:,p),20,'moving');
end

for k=1:size(masked_im,2)
    figure(4)
    if (k<6)
        plot(0:3:(3*size(im4D,4)-
3),masked_im_sm1(:,k),colour_map(k),'LineWidth',1.5);
    else
        plot(0:3:(3*size(im4D,4)-3),masked_im_sm1(:,k),strcat('--
',colour_map(k)),'LineWidth',1.5);
    end
    hold on

    figure(5)
    if (k<6)
        plot(0:3:(3*size(im4D,4)-
3),masked_im_sm10(:,k),colour_map(k),'LineWidth',1.5);
    else
        plot(0:3:(3*size(im4D,4)-3),masked_im_sm10(:,k),strcat('--
',colour_map(k)),'LineWidth',1.5);
    end
    hold on

    figure(6)
    if (k<6)
        plot(0:3:(3*size(im4D,4)-
3),masked_im_sm20(:,k),colour_map(k),'LineWidth',1.5);
```

```
    else
        plot(0:3:(3*size(im4D,4)-3),masked_im_sm20(:,k),strcat('--
',colour_map(k)),'LineWidth',1.5);
    end
    hold on
end
figure(4)
    legend(lgnd);
    xlabel('time [s]');
    ylabel('T_2*');
    title('Time course of T_2* changes for given ROIs');
    saveas(gcf,'allROIs_sm1.pdf','pdf');
    saveas(gcf,'allROIs_sm1.fig');
figure(5)
    legend(lgnd);
    xlabel('time [s]');
    ylabel('T_2*');
    title('Time course of T_2* changes for given ROIs');
    hold off
    saveas(gcf,'allROIs_sm10.pdf','pdf');
    saveas(gcf,'allROIs_sm10.fig');
figure(6)
    legend(lgnd);
    xlabel('time [s]');
    ylabel('T_2*');
    title('Time course of T_2* changes for given ROIs');
    hold off
    saveas(gcf,'allROIs_sm20.pdf','pdf');
    saveas(gcf,'allROIs_sm20.fig');

clear c
baseline=mean(masked_im(5:34,:),1);
baseline_rtn=mean(masked_im(end-29:end,:),1);
[dip_val,dip_at]=min(masked_im_sm20,[],1);
for a=1:size(dip_at,2)
    dip_val(a)=masked_im_sm10(dip_at(a),a);
end
half_dip=baseline-(baseline-dip_val)/2;
for p=1:size(masked_im,2)
    [c(p) time_to_half_dip(p)]=min(abs(masked_im_sm20(1:dip_at,p)-
half_dip(p)));
end
drop=100-100*dip_val./baseline;
%[peak_val,peak_at]=max(masked_im_sm20,[],1);
for a=1:size(masked_im_sm10,2)
    [c,peak_at_]=findpeaks(masked_im_sm10(143:end,a));
    peak_at_=peak_at_+142;
    peak_val(a)=masked_im_sm10(peak_at_(1),a);
    peak_at(a)=peak_at_(1); clear peak_at_ c
end
grad=diff(masked_im_sm10);
max_grad=sort(grad(min(dip_at):max(peak_at),:));
max_grad=mean(max_grad(end-5:end,:),1);
dip_at=(dip_at-1).*3;
peak_at=(peak_at-1).*3;
time_to_half_dip=(time_to_half_dip-1).*3;
for p=1:size(masked_im,2)
    fprintf(1,'Curve analysis for ROI %i \n Baseline \t %.2f[ms] \n
Baseline-End \t %.2f[ms] \n Dip Value \t %.2f[ms] \n Dip Position \t
%i[s] \n Drop \t\t %.2f[%%] \n Peak Value \t %.2f[ms] \n Peak Position
\t %i[s] \n Mean Gradient \t %.2f[ms/s] \n Time to half-dip %i[s]
\n',p,baseline(p),baseline_rtn(p),dip_val(p),dip_at(p),drop(p),peak_va
l(p),peak_at(p),max_grad(p),time_to_half_dip(p));

table(p,:)=[p,baseline(p),baseline_rtn(p),dip_val(p),dip_at(p),drop(p)
,peak_val(p),peak_at(p),max_grad(p),time_to_half_dip(p)];
end
column_names=['ROI','Baseline','Baseline-End','Dip Value','Dip
```

```
Position','Drop [%]','Peak Value','Peak Position','Gradient','Time to
half-dip'];
xlswrite('ROI_analysis.xls',table,'ROIs','A2');
xlswrite('ROI_timecourses.xls',masked_im);
```

# APPENDIX 3

## Publications and Presentations

### Publications

**Bajwa A**, Wesolowski R, Patel A, Saha P, Ludwinski F, Ikram M, Albayati M, Smith A, Nagel E, Modarai B. Blood Oxygenation Level Dependent (BOLD)-CMR Derived Measures in Critical Limb Ischemia and Changes with Revascularization. *Journal of American College of Cardiology* 2016; 67(4):420-431.

**Bajwa A**, Wesolowski R, Patel A, Saha P, Ludwinski F, Smith A, Nagel E, Modarai B. Assessment of tissue perfusion in the lower limb: Current methods and techniques under development. *Circulation: Cardiovascular Imaging* 2014; 7(5):836-843

### Published Abstracts

**Bajwa A,** Wesolowski R, Patel AS, Saha P, Ludwinski F, Smith A, Nagel E, Modarai B.Blood oxygenation level dependent (BOLD) magnetic resonance imaging objectively measures perfusion deficits in the lower limb musculature. *British Journal of Surgery* 2015; 102(S5): 3

**Bajwa A,** Wesolowski R, Patel AS, Saha P, Ludwinski F, Smith A, Nagel E, Modarai B. Blood Oxygenation Level Dependent Magnetic Resonance Imaging: a Tool for Objective Assessment of Perfusion in the Lower Limb. *Circulation* 2014; 130: A17339

**Bajwa A**, Wesolowski R, Patel A, Saha P, Lyons O, Smith A, Nagel E, Modarai B. Blood oxygenation level dependent MRI: A novel perfusion imaging strategy for the ischaemic limb. *British Journal of Surgery* 2013; 101(S2): 2

## Oral Presentations

**Bajwa A,** Wesolowski R, Patel AS, Saha P, Ludwinski F, Smith A, Nagel E, Modarai B. Blood Oxygenation Level Dependent Magnetic Resonance Imaging (BOLD-MRI) Objectively Assesses Muscle Perfusion in Critical Limb Ischaemia. European Society of Vascular Surgery, Annual Meeting, Porto 2015

**Bajwa A.** Blood Oxygenation Level Dependent (BOLD) Magnetic Resonance Imaging Objectively Measures Perfusion Deficits in the Lower Limb Musculature British Heart Foundation Postgraduate Meeting, King's College London 2015

**Bajwa A,** Wesolowski R, Patel AS, Saha P, Ludwinski F, Smith A, Nagel E, Modarai B. Blood Oxygenation Level Dependant (BOLD) Magnetic Resonance Imaging Objectively Measures Perfusion Deficits in the Lower Limb Musculature. Society of Academic & Research Surgery Annual Meeting, Durham 2015. **Patey Prize Session**

**Bajwa A**, Wesolowski R, Patel A, Saha P, Lyons O, Ludwinski F, Smith A, Nagel E, Modarai B. A Novel Blood Oxygenation Level Dependent (BOLD) Magnetic Resonance Imaging Strategy for Assessing Muscle Perfusion in the Ischaemic Limb. Charing Cross International Vascular Symposium 2014 **(Prize Winner)**

**Bajwa A**, Wesolowski R, Patel A, Saha P, Smith A, Nagel E, Modarai B. Blood Oxygenation Level Dependent (BOLD) MRI: A Novel Perfusion Imaging Strategy for the Ischaemic Limb. The Cheselden Club 2013 **(Prize Winner)** & Stryker Training Day 2014 **(South West Thames Surgical SpR Trainee presentation Prize Winner)**

**Bajwa A**, Wesolowski R, Patel A, Saha P, Lyons O, Smith A, Nagel E, Modarai B. Blood Oxygenation Level Dependent (BOLD) MRI: A Novel Perfusion Imaging Strategy for the Ischaemic Limb. Vascular Society Annual Conference, Manchester 2013, **BJS Prize session**

## Poster Presentations

**Bajwa A,** Wesolowski R, Patel AS, Saha P, Ludwinski F, Smith A, Nagel E, Modarai B. Blood Oxygenation Level Dependent (BOLD)-CMR: A Clinically Relevant Diagnostic Tool That Is Sensitive to Changes In Lower Limb Perfusion. British Heart Foundation Fellow Meeting, Cambridge 2015

**Bajwa A,** Wesolowski R, Patel AS, Saha P, Ludwinski F, Smith A, Nagel E, Modarai B. Blood Oxygenation Level Dependent Magnetic Resonance Imaging: a Tool for Objective Assessment of Perfusion in the Lower Limb. American Heart Association Scientific Sessions, Chicago 2014

# References


1. Hirsch AT, Haskal ZJ, Hertzer NR, Bakal CW, Creager MA, Halperin JL, Hiratzka LF, Murphy WRC, Olin JW, Puschett JB, Rosenfield KA, Sacks D, Stanley JC, Taylor LM, White CJ, White J, White RA, Antman EM, Smith SC, Adams CD, Anderson JL, Faxon DP, Fuster V, Gibbons RJ, Hunt SA, Jacobs AK, Nishimura R, Ornato JP, Page RL, Riegel B. ACC/AHA 2005 Practice Guidelines for the management of patients with peripheral arterial disease (lower extremity, renal, mesenteric, and abdominal aortic): a collaborative report from the American Association for Vascular Surgery/Society for Vascular Sur. *Circulation*. 2006; 113:e463-654.
2. Diehm C, Allenberg JR, Pittrow D, Mahn M, Tepohl G, Haberl RL, Darius H, Burghaus I, Trampisch HJ. Mortality and vascular morbidity in older adults with asymptomatic versus symptomatic peripheral artery disease. *Circulation*. 2009; 120:2053–61.
3. Norgren L, Hiatt WR, Dormandy JA, Nehler MR, Harris KA, Fowkes FGR. Inter-Society Consensus for the Management of Peripheral Arterial Disease (TASC II). *J. Vasc. Surg.* 2007; 45 Suppl S:S5-67.
4. Criqui MH, Langer RD, Fronek A, Feigelson HS, Klauber MR, McCann TJ, Browner D. Mortality over a period of 10 years in patients with peripheral arterial disease. *N. Engl. J. Med.* 1992; 326:381–6.
5. Belch JJF, Topol EJ, Agnelli G, Bertrand M, Califf RM, Clement DL, Creager MA, Easton JD, Gavin JR, Greenland P, Hankey G, Hanrath P, Hirsch AT, Meyer J, Smith SC, Sullivan F, Weber MA. Critical issues in peripheral arterial disease detection and management: a call to action. *Arch. Intern. Med.* 2003; 163:884–92.
6. Peach G, Griffin M, Jones KG, Thompson MM, Hinchliffe RJ. Diagnosis and management of peripheral arterial disease. *BMJ*. 2012; 345:e5208.
7. Fowkes FGR, Housley E, Cawood EHH, Macintyre CCA, Ruckley C V, Prescott RJ. Edinburgh Artery Study: Prevalence of Asymptomatic and Symptomatic Peripheral Arterial Disease in the General Population. *Int. J. Epidemiol.* 1991; 20:384–392.
8. Weitz JI, Byrne J, Clagett GP, Farkouh ME, Porter JM, Sackett DL, Strandness DE, Taylor LM. Diagnosis and Treatment of Chronic Arterial Insufficiency of the Lower Extremities: A Critical Review. *Circulation*. 1996; 94:3026–3049.
9. Ness J, Aronow WS. Prevalence of coexistence of coronary artery disease, ischemic stroke, and peripheral arterial disease in older persons, mean age 80 years, in an academic hospital-based geriatrics practice. *J. Am. Geriatr. Soc.* 1999; 47:1255–6.
10. Newman AB, Siscovick DS, Manolio TA, Polak J, Fried LP, Borhani NO, Wolfson SK. Ankle-arm index as a marker of atherosclerosis in the Cardiovascular Health Study. Cardiovascular Heart Study (CHS) Collaborative Research Group. *Circulation*. 1993; 88:837–45.

11. Barrett-Connor E, Khaw K. Family history of heart attack as an independent predictor of death due to cardiovascular disease. *Circulation*. 1984; 69:1065–1069.

12. Cacoub PP, Abola MTB, Baumgartner I, Bhatt DL, Creager MA, Liau C-S, Goto S, Röther J, Steg PG, Hirsch AT. Cardiovascular risk factor control and outcomes in peripheral artery disease patients in the Reduction of Atherothrombosis for Continued Health (REACH) Registry. *Atherosclerosis*. 2009; 204:e86-92.

13. FONTAINE R, KIM M, KIENY R. [Surgical treatment of peripheral circulation disorders]. *Helv. Chir. Acta*. 1954; 21:499–533.

14. Rutherford RB, Flanigan DP, Gupta SK, Johnston KW, Karmody A, Whittemore AD, Baker JD, Ernst CB, Jamieson C, Mehta S, Wibur B, Olcott C, Cranley J, Jamieson C, Yao J, Raines J, Darling R, Buth J, Brewster D, Austen W, Siegel M, Stewart C, DeWeese J, Reid C, Peto R, Pike M, Armitage P, Breslow N, Cox D, Howard S, Mantel N, McPherson K, Peto J, Smith P, Peto R, Pike M, Armitage P, Breslow N, Cox D, Howard S, Mantel N, McPherson K, Peto J, Smith P, Underwood C, Charlesworth D, Colton T, Goldman L, Nussbaum S, Southwick F, Krogstad D, Murray B, Burke D, O'Malley T, Goroll A, Caplan C, Nolan J, Carabello B, Slater E. Suggested standards for reports dealing with lower extremity ischemia. *J. Vasc. Surg.* 1986; 4:80–94.

15. Rutherford RB, Baker JD, Ernst C, Johnston KW, Porter JM, Ahn S, Jones DN. Recommended standards for reports dealing with lower extremity ischemia: Revised version. *J. Vasc. Surg.* 1997; 26:517–538.

16. Al-Qaisi M, Nott DM, King DH, Kaddoura S. Vascular Health and Risk Management Ankle Brachial Pressure index (ABPi): An update for practitioners. *Vasc. Health Risk Manag.* 2009; 5:833–841.

17. Cao P, Eckstein HH, De Rango P, Setacci C, Ricco J-B, de Donato G, Becker F, Robert-Ebadi H, Diehm N, Schmidli J, Teraa M, Moll FL, Dick F, Davies AH, Lepäntalo M, Apelqvist J. Chapter II: Diagnostic methods. *Eur. J. Vasc. Endovasc. Surg.* 2011; 42 Suppl 2:S13-32.

18. Met R, Bipat S, Legemate DA, Reekers JA, Koelemay MJW. Diagnostic performance of computed tomography angiography in peripheral arterial disease: a systematic review and meta-analysis. *JAMA*. 2009; 301:415–24.

19. Solomon R. The role of osmolality in the incidence of contrast-induced nephropathy: a systematic review of angiographic contrast media in high risk patients. *Kidney Int.* 2005; 68:2256–63.

20. Levy EM, Viscoli CM, Horwitz RI. The effect of acute renal failure on mortality. A cohort analysis. *JAMA*. 1996; 275:1489–94.

21. Kock MCJM, Dijkshoorn ML, Pattynama PMT, Myriam Hunink MG. Multi-detector row computed tomography angiography of peripheral arterial disease. *Eur. Radiol.* 2007; 17:3208–22.

22. Collins R, Burch J, Cranny G, Aguiar-Ibáñez R, Craig D, Wright K, Berry E, Gough M, Kleijnen J, Westwood M. Duplex ultrasonography, magnetic

resonance angiography, and computed tomography angiography for diagnosis and assessment of symptomatic, lower limb peripheral arterial disease: systematic review. *BMJ*. 2007; 334:1257.

23. Thomsen HS, Morcos SK, Almén T, Bellin M-F, Bertolotto M, Bongartz G, Clement O, Leander P, Heinz-Peer G, Reimer P, Stacul F, van der Molen A, Webb JAW, ESUR Contrast Medium Safety Committee. Nephrogenic systemic fibrosis and gadolinium-based contrast media: updated ESUR Contrast Medium Safety Committee guidelines. *Eur. Radiol.* 2013; 23:307–18.
24. Todd DJ, Kagan A, Chibnik LB, Kay J. Cutaneous changes of nephrogenic systemic fibrosis: predictor of early mortality and association with gadolinium exposure. *Arthritis Rheum.* 2007; 56:3433–41.
25. Collaborative meta-analysis of randomised trials of antiplatelet therapy for prevention of death, myocardial infarction, and stroke in high risk patients. *BMJ*. 2002; 324:71–86.
26. Serebruany VL, Steinhubl SR, Berger PB, Malinin AI, Baggish JS, Bhatt DL, Topol EJ. Analysis of risk of bleeding complications after different doses of aspirin in 192,036 patients enrolled in 31 randomized controlled trials. *Am. J. Cardiol.* 2005; 95:1218–22.
27. A randomised, blinded, trial of clopidogrel versus aspirin in patients at risk of ischaemic events (CAPRIE). CAPRIE Steering Committee. *Lancet*. 1996; 348:1329–39.
28. Cacoub PP, Bhatt DL, Steg PG, Topol EJ, Creager MA. Patients with peripheral arterial disease in the CHARISMA trial. *Eur. Heart J.* 2009; 30:192–201.
29. Elmariah S, Mauri L, Doros G, Galper BZ, O'Neill KE, Steg PG, Kereiakes DJ, Yeh RW. Extended duration dual antiplatelet therapy and mortality: a systematic review and meta-analysis. *Lancet (London, England)*. 2015; 385:792–8.
30. Hirsch AT, Treat-Jacobson D, Lando HA, Hatsukami DK. The role of tobacco cessation, antiplatelet and lipid-lowering therapies in the treatment of peripheral arterial disease. *Vasc. Med.* 1997; 2:243–51.
31. Diehm N, Schmidli J, Setacci C, Ricco J-B, de Donato G, Becker F, Robert-Ebadi H, Cao P, Eckstein HH, De Rango P, Teraa M, Moll FL, Dick F, Davies AH, Lepäntalo M, Apelqvist J. Chapter III: Management of cardiovascular risk factors and medical therapy. *Eur. J. Vasc. Endovasc. Surg.* 2011; 42 Suppl 2:S33-42.
32. Willigendael EM, Teijink JAW, Bartelink M-L, Peters RJG, Büller HR, Prins MH. Smoking and the patency of lower extremity bypass grafts: a meta-analysis. *J. Vasc. Surg.* 2005; 42:67–74.
33. Stead LF, Perera R, Bullen C, Mant D, Hartmann-Boyce J, Cahill K, Lancaster T. Nicotine replacement therapy for smoking cessation. *Cochrane database Syst. Rev.* 2012; 11:CD000146.
34. MRC/BHF Heart Protection Study of cholesterol lowering with simvastatin in 20,536 high-risk individuals: a randomised placebo-controlled trial.

*Lancet*. 2002; 360:7–22.

35. Aung PP, Maxwell HG, Jepson RG, Price JF, Leng GC. Lipid-lowering for peripheral arterial disease of the lower limb. *Cochrane database Syst. Rev.* 2007;CD000123.

36. Regensteiner JG, Ware JE, McCarthy WJ, Zhang P, Forbes WP, Heckman J, Hiatt WR. Effect of cilostazol on treadmill walking, community-based walking ability, and health-related quality of life in patients with intermittent claudication due to peripheral arterial disease: meta-analysis of six randomized controlled trials. *J. Am. Geriatr. Soc.* 2002; 50:1939–46.

37. Lehert P, Comte S, Gamand S, Brown TM. Naftidrofuryl in intermittent claudication: a retrospective analysis. *J. Cardiovasc. Pharmacol.* 1994; 23 Suppl 3:S48-52.

38. Creutzig A, Lehmacher W, Elze M. Meta-analysis of randomised controlled prostaglandin E1 studies in peripheral arterial occlusive disease stages III and IV. *Vasa.* 2004; 33:137–44.

39. Rajagopalan S, Mohler ER, Lederman RJ, Mendelsohn FO, Saucedo JF, Goldman CK, Blebea J, Macko J, Kessler PD, Rasmussen HS, Annex BH. Regional angiogenesis with vascular endothelial growth factor in peripheral arterial disease: a phase II randomized, double-blind, controlled study of adenoviral delivery of vascular endothelial growth factor 121 in patients with disabling intermittent cl. *Circulation*. 2003; 108:1933–8.

40. Lederman RJ, Mendelsohn FO, Anderson RD, Saucedo JF, Tenaglia AN, Hermiller JB, Hillegass WB, Rocha-Singh K, Moon TE, Whitehouse MJ, Annex BH. Therapeutic angiogenesis with recombinant fibroblast growth factor-2 for intermittent claudication (the TRAFFIC study): a randomised trial. *Lancet (London, England)*. 2002; 359:2053–8.

41. Leeper NJ, Hunter AL, Cooke JP. Stem cell therapy for vascular regeneration: adult, embryonic, and induced pluripotent stem cells. *Circulation*. 2010; 122:517–26.

42. Patel AS, Smith A, Nucera S, Biziato D, Saha P, Attia RQ, Humphries J, Mattock K, Grover SP, Lyons OT, Guidotti LG, Siow R, Ivetic A, Egginton S, Waltham M, Naldini L, De Palma M, Modarai B. TIE2-expressing monocytes/macrophages regulate revascularization of the ischemic limb. *EMBO Mol. Med.* 2013; 5:858–69.

43. Dormandy JA, Rutherford RB. Management of peripheral arterial disease (PAD). TASC Working Group. TransAtlantic Inter-Society Consensus (TASC). *J. Vasc. Surg.* 2000; 31:S1–S296.

44. Taylor GI, Palmer JH. The vascular territories (angiosomes) of the body: experimental study and clinical applications. *Br. J. Plast. Surg.* 1987; 40:113–141.

45. Neville RF, Attinger CE, Bulan EJ, Ducic I, Thomassen M, Sidawy AN. Revascularization of a specific angiosome for limb salvage: does the target artery matter? *Ann. Vasc. Surg.* 2009; 23:367–73.

46. Iida O, Nanto S, Uematsu M, Ikeoka K, Okamoto S, Dohi T, Fujita M, Terashi H, Nagata S. Importance of the angiosome concept for endovascular therapy in patients with critical limb ischemia. *Catheter. Cardiovasc. Interv.* 2010; 75:830–6.

47. Rogers JH, Laird JR. Overview of New Technologies for Lower Extremity Revascularization. *Circulation*. 2007; 116.

48. Martens JM, Knippenberg B, Vos J-A, de Vries J-PP, Hansen BE, van Overhagen H, PADI Trial Group. Update on PADI trial: Percutaneous transluminal angioplasty and drug-eluting stents for infrapopliteal lesions in critical limb ischemia. *J. Vasc. Surg.* 2009; 50:687–689.

49. Hawkins BM, Hennebry TA. Local Paclitaxel Delivery for Treatment of Peripheral Arterial Disease. *Circ. Cardiovasc. Interv.* 2011; 4.

50. Tepe G, Zeller T, Albrecht T, Heller S, Schwarzwälder U, Beregi J-P, Claussen MDCD, Oldenburg A, Scheller B, Speck U. Local Delivery of Paclitaxel to Inhibit Restenosis during Angioplasty of the Leg. *N. Engl. J. Med.* 2008; 358:689–699.

51. Axel DI, Kunert W, Göggelmann C, Oberhoff M, Herdeg C, Küttner A, Wild DH, Brehm BR, Riessen R, Köveker G, Karsch KR. Paclitaxel Inhibits Arterial Smooth Muscle Cell Proliferation and Migration In Vitro and In Vivo Using Local Drug Delivery. *Circulation*. 1997; 96.

52. Bajwa A, Wesolowski R, Patel A, Saha P, Ludwinski F, Smith A, Nagel E, Modarai B. Assessment of tissue perfusion in the lower limb: current methods and techniques under development. *Circ. Cardiovasc. Imaging*. 2014; 7:836–43.

53. Exercise Physiology: Cardio/CNS contribution [Internet]. [cited 2017 Feb 1];Available from: http://www.medicine.mcgill.ca/physio/vlab/exercise/cardio_cns.htm

54. Ruotsalainen U, Raitakari M, Nuutila P, Oikonen V, Sipilä H, Teräs M, Knuuti MJ, Bloomfield PM, Iida H. Quantitative blood flow measurement of skeletal muscle using oxygen-15-water and PET. *J. Nucl. Med.* 1997; 38:314–9.

55. Burchert W, Schellong S, van den Hoff J, Meyer GJ, Alexander K, Hundeshagen H. Oxygen-15-water PET assessment of muscular blood flow in peripheral vascular disease. *J. Nucl. Med.* 1997; 38:93–8.

56. Elia M, Kurpad A. What is the blood flow to resting human muscle? *Clin. Sci. (Lond).* 1993; 84:559–63.

57. Korthuis RJ. Skeletal Muscle Circulation (Google eBook). Morgan & Claypool Publishers; 2011.

58. Wilkinson IB, Webb DJ. Venous occlusion plethysmography in cardiovascular research: methodology and clinical applications. *Br. J. Clin. Pharmacol.* 2001; 52:631–46.

59. Evans IL, Crawford ES, Debakey ME. Digital plethysmography in evaluation of surgery of degenerative arterial disease. *Surg. Forum*. 1957; 8:438–42.

60. Radke HM, Bell JW, Strandness DE, Jesseph JE. Monitor of digit volume changes in angioplastic surgery: use of strain gauge plethysmography. *Ann. Surg.* 1961; 154:818–25.

61. Whitney RJ. The measurement of volume changes in human limbs. *J. Physiol.* 1953; 121:1–27.

62. Breslau PJ, Slot HB, Greep JM. Comparative study of strain gauge plethysmography and Doppler ultrasound in patients with occlusive arterial disease of the lower extremities. *Angiology*. 1981; 32:840–5.

63. Steer HW, Fletcher EW, Morris PJ. A comparison between the ankle systolic pressure and mercury strain gauge plethysmography in the assessment of patients with arterial disease of the lower limbs. *Surgery*. 1980; 88:636–41.

64. Wårdell K, Jakobsson A, Nilsson GE. Laser Doppler perfusion imaging by dynamic light scattering. *IEEE Trans. Biomed. Eng.* 1993; 40:309–16.

65. Murray AK, Herrick AL, King TA. Laser Doppler imaging: a developing technique for application in the rheumatic diseases. *Rheumatology (Oxford).* 2004; 43:1210–8.

66. Klonizakis M, Manning G, Donnelly R. Assessment of lower limb microcirculation: exploring the reproducibility and clinical application of laser Doppler techniques. *Skin Pharmacol. Physiol.* 2011; 24:136–43.

67. Leonardo G, Arpaia MR, Del Guercio R. A new method for the quantitative assessment of arterial insufficiency of the limbs: cutaneous postischemic hyperemia test by laser Doppler. *Angiology*. 1987; 38:378–85.

68. Lantsberg L, Goldman M. Laser Doppler flowmetry, transcutaneous oxygen tension measurements and Doppler pressure compared in patients undergoing amputation. *Eur. J. Vasc. Surg.* 1991; 5:195–7.

69. Ray SA, Buckenham TM, Belli AM, Taylor RS, Dormandy JA. The predictive value of laser Doppler fluxmetry and transcutaneous oximetry for clinical outcome in patients undergoing revascularisation for severe leg ischaemia. *Eur. J. Vasc. Endovasc. Surg.* 1997; 13:54–9.

70. Arsenault KA, McDonald J, Devereaux PJ, Thorlund K, Tittley JG, Whitlock RP. The use of transcutaneous oximetry to predict complications of chronic wound healing: a systematic review and meta-analysis. *Wound Repair Regen.* 2011; 19:657–63.

71. Arsenault KA, Al-Otaibi A, Devereaux PJ, Thorlund K, Tittley JG, Whitlock RP. The use of transcutaneous oximetry to predict healing complications of lower limb amputations: a systematic review and meta-analysis. *Eur. J. Vasc. Endovasc. Surg.* 2012; 43:329–36.

72. Fife CE, Smart DR, Sheffield PJ, Hopf HW, Hawkins G, Clarke D. Transcutaneous oximetry in clinical practice: consensus statements from an expert panel based on evidence. *Undersea Hyperb. Med.* 2009; 36:43–53.

73. Flower RW. Injection technique for indocyanine green and sodium fluorescein dye angiography of the eye. *Invest. Ophthalmol.* 1973;

12:881–95.

74. Alander JT, Kaartinen I, Laakso A, Pätilä T, Spillmann T, Tuchin V V, Venermo M, Välisuo P. A review of indocyanine green fluorescent imaging in surgery. *Int. J. Biomed. Imaging*. 2012; 2012:940585.

75. Zimmermann A, Roenneberg C, Wendorff H, Holzbach T, Giunta RE, Eckstein H-H. Early postoperative detection of tissue necrosis in amputation stumps with indocyanine green fluorescence angiography. *Vasc. Endovascular Surg.* 2010; 44:269–73.

76. Zimmermann A, Roenneberg C, Reeps C, Wendorff H, Holzbach T, Eckstein H-H. The determination of tissue perfusion and collateralization in peripheral arterial disease with indocyanine green fluorescence angiography. *Clin. Hemorheol. Microcirc.* 2012; 50:157–66.

77. Wuestenfeld JC, Herold J, Niese U, Kappert U, Schmeisser A, Strasser RH, Braun-Dullaeus RC. Indocyanine green angiography: a new method to quantify collateral flow in mice. *J. Vasc. Surg.* 2008; 48:1315–21.

78. Rossi M, Carpi A. Skin microcirculation in peripheral arterial obliterative disease. *Biomed. Pharmacother.* 2004; 58:427–31.

79. Scremin OU, Figoni SF, Norman K, Scremin AME, Kunkel CF, Opava-Rutter D, Schmitter ED, Bert A, Mandelkern M. Preamputation evaluation of lower-limb skeletal muscle perfusion with H(2) (15)O positron emission tomography. *Am. J. Phys. Med. Rehabil.* 2010; 89:473–86.

80. Frackowiak RS, Lenzi GL, Jones T, Heather JD. Quantitative measurement of regional cerebral blood flow and oxygen metabolism in man using 15O and positron emission tomography: theory, procedure, and normal values. *J. Comput. Assist. Tomogr.* 1980; 4:727–36.

81. Iida H, Kanno I, Takahashi A, Miura S, Murakami M, Takahashi K, Ono Y, Shishido F, Inugami A, Tomura N. Measurement of absolute myocardial blood flow with H215O and dynamic positron-emission tomography. Strategy for quantification in relation to the partial-volume effect. *Circulation*. 1988; 78:104–15.

82. Bergmann SR, Fox KA, Rand AL, McElvany KD, Welch MJ, Markham J, Sobel BE. Quantification of regional myocardial blood flow in vivo with H215O. *Circulation*. 1984; 70:724–33.

83. Depairon M, Zicot M. The Quantitation of Blood Flow/Metabolism Coupling at Rest and After Exercise in Peripheral Arterial Insufficiency, Using PET and 15-0 Labeled Tracers. *Angiology*. 1996; 47:991–999.

84. Schmidt MA, Chakrabarti A, Shamim-Uzzaman Q, Kaciroti N, Koeppe RA, Rajagopalan S. Calf Flow Reserve with H215O PET as a Quantifiable Index of Lower Extremity Flow. *J. Nucl. Med.* 2003; 44:915–919.

85. Peñuelas I, Aranguren XL, Abizanda G, Martí-Climent JM, Uriz M, Ecay M, Collantes M, Quincoces G, Richter JA, Prósper F. (13)N-ammonia PET as a measurement of hindlimb perfusion in a mouse model of peripheral artery occlusive disease. *J. Nucl. Med.* 2007; 48:1216–23.

86. Fischman AJ, Hsu H, Carter EA, Yu YM, Tompkins RG, Guerrero JL, Young VR, Alpert NM. Regional measurement of canine skeletal muscle

blood flow by positron emission tomography with H2(15)O. *J. Appl. Physiol.* 2002; 92:1709–16.

87. Bellina CR, Parodi O, Camici P, Salvadori PA, Taddei L, Fusani L, Guzzardi R, Klassen GA, L'Abbate AL, Donato L. Simultaneous in vitro and in vivo validation of nitrogen-13-ammonia for the assessment of regional myocardial blood flow. *J. Nucl. Med.* 1990; 31:1335–43.
88. Maddahi J. Properties of an ideal PET perfusion tracer: new PET tracer cases and data. *J. Nucl. Cardiol.* 2012; 19 Suppl 1:S30-7.
89. Amarteifio E, Wormsbecher S, Krix M, Demirel S, Braun S, Delorme S, Böckler D, Kauczor H-U, Weber M-A. Dynamic contrast-enhanced ultrasound and transient arterial occlusion for quantification of arterial perfusion reserve in peripheral arterial disease. *Eur. J. Radiol.* 2012; 81:3332–8.
90. Lindner JR, Womack L, Barrett EJ, Weltman J, Price W, Harthun NL, Kaul S, Patrie JT. Limb stress-rest perfusion imaging with contrast ultrasound for the assessment of peripheral arterial disease severity. *JACC. Cardiovasc. Imaging*. 2008; 1:343–50.
91. Duerschmied D, Zhou Q, Rink E, Harder D, Freund G, Olschewski M, Bode C, Hehrlein C. Simplified contrast ultrasound accurately reveals muscle perfusion deficits and reflects collateralization in PAD. *Atherosclerosis*. 2009; 202:505–12.
92. Piscaglia F, Bolondi L. The safety of Sonovue in abdominal applications: retrospective analysis of 23188 investigations. *Ultrasound Med. Biol.* 2006; 32:1369–75.
93. Miles KA. Measurement of tissue perfusion by dynamic computed tomography. *Br. J. Radiol.* 1991; 64:409–12.
94. George RT, Jerosch-Herold M, Silva C, Kitagawa K, Bluemke DA, Lima JAC, Lardo AC. Quantification of myocardial perfusion using dynamic 64-detector computed tomography. *Invest. Radiol.* 2007; 42:815–22.
95. Tsushima Y, Unno Y, Koizumi J, Kusano S. Measurement of human hepatic and splenic perfusion using dynamic computed tomography: a preliminary report. *Comput. Methods Programs Biomed.* 1998; 57:143–6.
96. Barfett J, Velauthapillai N, Jaskolka JD. Perfusion in peripheral musculoskeletal structures from dynamic volumetric computed tomography using an en bloc approach. *J. Comput. Assist. Tomogr.* 2010; 34:626–32.
97. Huellner M, Banyai M, Strobel K, Veit-Haibach P. CT-perfusion in patients with symptomatic peripheral arterial disease (PAD): Change of perfusion parameters after interventional revascularisation and correlation with pre-interventional angiographic parameters. *J. Med. Imaging Radiat. Oncol.* 2012; 56:60.
98. Detre JA, Leigh JS, Williams DS, Koretsky AP. Perfusion imaging. *Magn. Reson. Med.* 1992; 23:37–45.
99. Roberts DA, Detre JA, Bolinger L, Insko EK, Lenkinski RE, Pentecost MJ, Leigh JS. Renal perfusion in humans: MR imaging with spin tagging of

arterial water. *Radiology*. 1995; 196:281–6.

100. Poncelet BP, Koelling TM, Schmidt CJ, Kwong KK, Reese TG, Ledden P, Kantor HL, Brady TJ, Weisskoff RM. Measurement of human myocardial perfusion by double-gated flow alternating inversion recovery EPI. *Magn. Reson. Med.* 1999; 41:510–9.
101. Duteil S, Wary C, Raynaud JS, Lebon V, Lesage D, Leroy-Willig A, Carlier PG. Influence of vascular filling and perfusion on BOLD contrast during reactive hyperemia in human skeletal muscle. *Magn. Reson. Med.* 2006; 55:450–4.
102. Raynaud JS, Duteil S, Vaughan JT, Hennel F, Wary C, Leroy-Willig A, Carlier PG. Determination of skeletal muscle perfusion using arterial spin labeling NMRI: validation by comparison with venous occlusion plethysmography. *Magn. Reson. Med.* 2001; 46:305–11.
103. Wu W-C, Mohler E, Ratcliffe SJ, Wehrli FW, Detre J a, Floyd TF. Skeletal muscle microvascular flow in progressive peripheral artery disease: assessment with continuous arterial spin-labeling perfusion magnetic resonance imaging. *J. Am. Coll. Cardiol.* 2009; 53:2372–7.
104. Liu TT, Brown GG. Measurement of cerebral perfusion with arterial spin labeling: Part 1. Methods. *J. Int. Neuropsychol. Soc.* 2007; 13:517–25.
105. Golay X, Hendrikse J, Lim TCC. Perfusion imaging using arterial spin labeling. *Top. Magn. Reson. Imaging*. 2004; 15:10–27.
106. Wu W-C, Jiang S-F, Yang S-C, Lien S-H. Pseudocontinuous arterial spin labeling perfusion magnetic resonance imaging--a normative study of reproducibility in the human brain. *Neuroimage*. 2011; 56:1244–50.
107. Pohmann R, Künnecke B, Fingerle J, von Kienlin M. Fast perfusion measurements in rat skeletal muscle at rest and during exercise with single-voxel FAIR (flow-sensitive alternating inversion recovery). *Magn. Reson. Med.* 2006; 55:108–15.
108. Pollak AW, Meyer CH, Epstein FH, Jiji RS, Hunter JR, Dimaria JM, Christopher JM, Kramer CM. Arterial spin labeling MR imaging reproducibly measures peak-exercise calf muscle perfusion: a study in patients with peripheral arterial disease and healthy volunteers. *JACC. Cardiovasc. Imaging*. 2012; 5:1224–30.
109. Nagel E, Klein C, Paetsch I, Hettwer S, Schnackenburg B, Wegscheider K, Fleck E. Magnetic resonance perfusion measurements for the noninvasive detection of coronary artery disease. *Circulation*. 2003; 108:432–7.
110. Hautvast G, Chiribiri A, Zarinabad N, Schuster A, Breeuwer M, Nagel E. Myocardial blood flow quantification from MRI by deconvolution using an exponential approximation basis. *IEEE Trans. Biomed. Eng.* 2012; 59:2060–7.
111. Luo Y, Mohning KM, Hradil VP, Wessale JL, Segreti JA, Nuss ME, Wegner CD, Burke SE, Cox BF. Evaluation of tissue perfusion in a rat model of hind-limb muscle ischemia using dynamic contrast-enhanced magnetic resonance imaging. *J. Magn. Reson. Imaging*. 2002; 16:277–

83.

112. Lutz AM, Weishaupt D, Amann-Vesti BR, Pfammatter T, Goepfert K, Marincek B, Nanz D. Assessment of skeletal muscle perfusion by contrast medium first-pass magnetic resonance imaging: technical feasibility and preliminary experience in healthy volunteers. *J. Magn. Reson. Imaging*. 2004; 20:111–21.

113. Thompson RB, Aviles RJ, Faranesh AZ, Venkatesh K, Wright V, Balaban RS, Mcveigh ER, Lederman RJ. Measurement of Skeletal Muscle Perfusion During Postischemic Reactive Hyperemia Using Contrast-Enhanced MRI With a Step- Input Function. *Magn. Reson. Med.* 2005; 54:289–298.

114. Isbell DC, Epstein FH, Zhong X, Dimaria JM, Berr SS, Meyer CH, Rogers WJ, Nancy L, Hagspiel KD, Weltman A, Kramer CM. Calf Muscle Perfusion at Peak Exercise in Peripheral Arterial Disease: Measurement by First-Pass Contrast-Enhanced Magnetic Resonance Imaging. *J. Magn. Reson. Imaging*. 2007; 25:1013–1020.

115. Watabe H, Ikoma Y, Kimura Y, Naganawa M, Shidahara M. PET kinetic analysis--compartmental model. *Ann. Nucl. Med.* 2006; 20:583–8.

116. Calamante F. Arterial input function in perfusion MRI: a comprehensive review. *Prog. Nucl. Magn. Reson. Spectrosc.* 2013; 74:1–32.

117. Geva T. Magnetic resonance imaging: historical perspective. *J. Cardiovasc. Magn. Reson.* 2006; 8:573–80.

118. Ogawa S, Lee TM, Kay a R, Tank DW. Brain magnetic resonance imaging with contrast dependent on blood oxygenation. *Proc. Natl. Acad. Sci. U. S. A.* 1990; 87:9868–72.

119. Roy CS, Sherrington CS. On the Regulation of the Blood-supply of the Brain. *J. Physiol.* 1890; 11:85–158.17.

120. Glover GH. Overview of functional magnetic resonance imaging. *Neurosurg. Clin. N. Am.* 2011; 22:133–9, vii.

121. Friedrich MG, Karamitsos TD. Oxygenation-sensitive cardiovascular magnetic resonance. *J. Cardiovasc. Magn. Reson.* 2013; 15:43.

122. Karamitsos TD, Leccisotti L, Arnold JR, Recio-Mayoral A, Bhamra-Ariza P, Howells RK, Searle N, Robson MD, Rimoldi OE, Camici PG, Neubauer S, Selvanayagam JB. Relationship between regional myocardial oxygenation and perfusion in patients with coronary artery disease: insights from cardiovascular magnetic resonance and positron emission tomography. *Circ. Cardiovasc. Imaging*. 2010; 3:32–40.

123. Friedrich MG, Niendorf T, Schulz-Menger J, Gross CM, Dietz R. Blood oxygen level-dependent magnetic resonance imaging in patients with stress-induced angina. *Circulation*. 2003; 108:2219–23.

124. Wright KB, Klocke FJ, Deshpande VS, Zheng J, Harris KR, Tang R, Finn JP, Li D. Assessment of regional differences in myocardial blood flow using T2-weighted 3D BOLD imaging. *Magn. Reson. Med.* 2001; 46:573–8.

125. Fieno DS, Shea SM, Li Y, Harris KR, Finn JP, Li D. Myocardial perfusion imaging based on the blood oxygen level-dependent effect using T2-prepared steady-state free-precession magnetic resonance imaging. *Circulation*. 2004; 110:1284–90.

126. Karamitsos TD, Recio-Mayoral A, Arnold JR, Leccisotti L, Bhamra-Ariza P, Howells RK, Searle N, Robson MD, Rimoldi OE, Camici PG, Neubauer S, Selvanayagam JB. Blood oxygen level-dependent MRI in patients with coronary artery disease and normal volunteers: a validation study against PET. *J. Cardiovasc. Magn. Reson.* 2009; 11:O37.

127. Manka R, Paetsch I, Schnackenburg B, Gebker R, Fleck E, Jahnke C. BOLD cardiovascular magnetic resonance at 3.0 tesla in myocardial ischemia. *J. Cardiovasc. Magn. Reson.* 2010; 12:1–9.

128. Neugarten J, Golestaneh L. Blood oxygenation level-dependent MRI for assessment of renal oxygenation. *Int. J. Nephrol. Renovasc. Dis.* 2014; 7:421–35.

129. Niendorf T, Pohlmann A, Arakelyan K, Flemming B, Cantow K, Hentschel J, Grosenick D, Ladwig M, Reimann H, Klix S, Waiczies S, Seeliger E. How bold is blood oxygenation level-dependent (BOLD) magnetic resonance imaging of the kidney? Opportunities, challenges and future directions. *Acta Physiol. (Oxf).* 2015; 213:19–38.

130. Schachinger H, Klarhöfer M, Linder L, Drewe J, Scheffler K. Angiotensin II decreases the renal MRI blood oxygenation level-dependent signal. *Hypertension*. 2006; 47:1062–6.

131. Prasad P V, Edelman RR, Epstein FH. Noninvasive evaluation of intrarenal oxygenation with BOLD MRI. *Circulation*. 1996; 94:3271–5.

132. Piskunowicz M, Hofmann L, Zuercher E, Bassi I, Milani B, Stuber M, Narkiewicz K, Vogt B, Burnier M, Pruijm M. A new technique with high reproducibility to estimate renal oxygenation using BOLD-MRI in chronic kidney disease. *Magn. Reson. Imaging*. 2015; 33:253–61.

133. Vink EE, Boer A, Verloop WL, Spiering W, Voskuil M, Vonken E, Hoogduin JM, Leiner T, Bots ML, Blankestijn PJ. The effect of renal denervation on kidney oxygenation as determined by BOLD MRI in patients with hypertension. *Eur. Radiol.* 2015; 25:1984–92.

134. Khatir DS, Pedersen M, Jespersen B, Buus NH. Evaluation of Renal Blood Flow and Oxygenation in CKD Using Magnetic Resonance Imaging. *Am. J. Kidney Dis.* 2015; 66:402–11.

135. van der Bel R, Coolen BF, Nederveen AJ, Potters W V, Verberne HJ, Vogt L, Stroes ESG, Krediet CTP. Magnetic Resonance Imaging-Derived Renal Oxygenation and Perfusion During Continuous, Steady-State Angiotensin-II Infusion in Healthy Humans. *J. Am. Heart Assoc.* 2016; 4:e003185.

136. Barrett T, Brechbiel M, Bernardo M, Choyke PL. MRI of tumor angiogenesis. *J. Magn. Reson. Imaging*. 2007; 26:235–49.

137. Jiang L, Weatherall PT, McColl RW, Tripathy D, Mason RP. Blood oxygenation level-dependent (BOLD) contrast magnetic resonance

imaging (MRI) for prediction of breast cancer chemotherapy response: A pilot study. *J. Magn. Reson. Imaging*. 2013; 37:1083–1092.

138. Kim CK, Park SY, Park BK, Park W, Huh SJ. Blood oxygenation level-dependent MR imaging as a predictor of therapeutic response to concurrent chemoradiotherapy in cervical cancer: a preliminary experience. *Eur. Radiol.* 2014; 24:1514–1520.
139. Toussaint J-F, Kwong KK, M′Kparu F, Weisskoff RM, Laraia PJ, Kantor HL. Perfusion changes in human skeletal muscle during reactive hyperemia measured by echo-planar imaging. *Magn. Reson. Med.* 1996; 35:62–69.
140. Jacobi B, Bongartz G, Partovi S, Schulte A-C, Aschwanden M, Lumsden AB, Davies MG, Loebe M, Noon GP, Karimi S, Lyo JK, Staub D, Huegli RW, Bilecen D. Skeletal muscle BOLD MRI: from underlying physiological concepts to its usefulness in clinical conditions. *J. Magn. Reson. Imaging*. 2012; 35:1253–65.
141. Partovi S, Karimi S, Jacobi B, Schulte A-C, Aschwanden M, Zipp L, Lyo JK, Karmonik C, Müller-Eschner M, Huegli RW, Bongartz G, Bilecen D. Clinical implications of skeletal muscle blood-oxygenation-level-dependent (BOLD) MRI. *MAGMA*. 2012; 25:251–61.
142. Ledermann H-P, Schulte A-C, Heidecker H-G, Aschwanden M, Jäger K a, Scheffler K, Steinbrich W, Bilecen D. Blood oxygenation level-dependent magnetic resonance imaging of the skeletal muscle in patients with peripheral arterial occlusive disease. *Circulation*. 2006; 113:2929–35.
143. Huegli RW, Schulte A-C, Aschwanden M, Thalhammer C, Kos S, Jacob AL, Bilecen D. Effects of percutaneous transluminal angioplasty on muscle BOLD-MRI in patients with peripheral arterial occlusive disease: preliminary results. *Eur. Radiol.* 2009; 19:509–15.
144. Ledermann HP, Schulte A, Thalhammer C, Aschwanden M, Jaeger KA. Calf muscles imaged at BOLD MR : Correlation with TcP O 2 and flowmetry measurements during ischaemia and reactive hyperaemia - Initial experience. *Radiology*. 2006; 241:477–84.
145. Lebon V, Brillault-Salvat C, Bloch G, Leroy-Willig A, Carlier PG. Evidence of muscle BOLD effect revealed by simultaneous interleaved gradient-echo NMRI and myoglobin NMRS during leg ischemia. *Magn. Reson. Med.* 1998; 40:551–8.
146. Schulte A, Aschwanden M, Bilecen D. Calf Muscles at Blood Oxygen Level – Dependent MR Imaging : Aging Effects at Postocclusive Purpose : Methods : Results : Conclusion : *Radiology*. 2008; 247:482–89.
147. Kos S, Klarhofer M, Ascwanden M, Scheffler K, Jacob A, Bilecen D. Simultaneous Dynamic Blood Oxygen Level-Dependent Magnetic Resonance Imaging of Foot and Calf Muscles. *foot*. 2009; 44:741–47.
148. Lin C-C, Ding H-J, Chen Y-W, Huang W-T, Kao A. Usefulness of thallium-201 muscle perfusion scan to investigate perfusion reserve in the lower limbs of Type 2 diabetic patients. *J. Diabetes Complications*. 2004; 18:233–236.

149. Bertoldi D, Parzy E, Fromes Y, Wary C, Leroy-Willig A, Carlier PG. New insight into abnormal muscle vasodilatory responses in aged hypertensive rats by in vivo nuclear magnetic resonance imaging of perfusion. *J. Vasc. Res.* 2006; 43:149–56.

150. Muller-Delp JM. Aging-induced adaptations of microvascular reactivity. *Microcirculation*. 2006; 13:301–14.

151. Payne GW, Bearden SE. The microcirculation of skeletal muscle in aging. *Microcirculation*. 2006; 13:275–7.

152. Proctor DN, Koch DW, Newcomer SC, Le KU, Leuenberger UA. Impaired leg vasodilation during dynamic exercise in healthy older women. *J. Appl. Physiol.* 2003; 95:1963–70.

153. Andreisek G, White LM, Sussman MS, Langer DL, Patel C, Su JW-S, Haider M a, Stainsby J a. T2*-weighted and arterial spin labeling MRI of calf muscles in healthy volunteers and patients with chronic exertional compartment syndrome: preliminary experience. *AJR. Am. J. Roentgenol.* 2009; 193:W327-33.

154. Partovi S, Schulte A-C, Staub D, Jacobi B, Aschwanden M, Walker UA, Imfeld S, Broz P, Benz D, Zipp L, Takes M, Jäger KA, Huegli RW, Bilecen D. Correlation of skeletal muscle blood oxygenation level-dependent MRI and skin laser Doppler flowmetry in patients with systemic sclerosis. *J. Magn. Reson. Imaging*. 2014; 40:1408–13.

155. Versluis B, Backes WH, Van Eupen MGA, Jaspers K, Nelemans PJ, Rouwet E V, Teijink JAW, Mali WPTM, Schurink G-W, Wildberger JE, Leiner T. Magnetic resonance imaging in peripheral arterial disease: reproducibility of the assessment of morphological and functional vascular status. *Invest. Radiol.* 2011; 46:11–24.

156. Noseworthy MD, Bulte DP, Alfonsi J. BOLD magnetic resonance imaging of skeletal muscle. *Semin. Musculoskelet. Radiol.* 2003; 7:307–15.

157. Bulte DP, Alfonsi J, Bells S, Noseworthy MD. Vasomodulation of skeletal muscle BOLD signal. *J. Magn. Reson. Imaging*. 2006; 24:886–90.

158. Noseworthy MD, Kim JK, Stainsby JA, Stanisz GJ, Wright GA. Tracking oxygen effects on MR signal in blood and skeletal muscle during hyperoxia exposure. *J. Magn. Reson. Imaging*. 1999; 9:814–20.

159. Schewzow K, Andreas M, Moser E, Wolzt M, Schmid AI. Automatic model-based analysis of skeletal muscle BOLD-MRI in reactive hyperemia. *J. Magn. Reson. Imaging*. 2013; 38:963–9.

160. Partovi S, Schulte A-C, Jacobi B, Klarhöfer M, Lumsden AB, Loebe M, Davies MG, Noon GP, Karmonik C, Zipp L, Bongartz G, Bilecen D. Blood oxygenation level-dependent (BOLD) MRI of human skeletal muscle at 1.5 and 3 T. *J. Magn. Reson. Imaging*. 2012; 35:1227–32.

161. Aschwanden M, Partovi S, Jacobi B, Fergus N, Schulte A-C, Robbin MR, Bilecen D, Staub D. Assessing the end-organ in peripheral arterial occlusive disease-from contrast-enhanced ultrasound to blood-oxygen-level-dependent MR imaging. *Cardiovasc. Diagn. Ther.* 2014; 4:165–72.

162. Towse TF, Slade JM, Meyer RA. Effect of physical activity on MRI-

measured blood oxygen level-dependent transients in skeletal muscle after brief contractions. *J. Appl. Physiol.* 2005; 99:715–22.

163. Meyer RA, Towse TF, Reid RW, Jayaraman RC, Wiseman RW, McCully KK. BOLD MRI mapping of transient hyperemia in skeletal muscle after single contractions. *NMR Biomed.* 2004; 17:392–398.
164. Potthast S, Schulte A, Kos S, Aschwanden M, Bilecen D. Blood Oxygenation Level-Dependent MRI of the Skeletal Muscle during Ischemia in Patients with Peripheral Arterial Occlusive Disease. *RöFo - Fortschritte auf dem Gebiet der Röntgenstrahlen und der Bildgeb. Verfahren*. 2009; 181:1157–1161.
165. Sanchez OA, Copenhaver EA, Elder CP, Damon BM. Absence of a significant extravascular contribution to the skeletal muscle BOLD effect at 3 T. *Magn. Reson. Med.* 2010; 64:527–35.
166. Lebon V, Carlier P, Brillault-Salvat C, Leroy-Willig A. Simultaneous measurement of perfusion and oxygenation changes using a multiple gradient-echo sequence: application to human muscle study. *Magn. Reson. Imaging*. 1998; 16:721–29.
167. Krüger G, Kastrup A, Glover GH. Neuroimaging at 1.5 T and 3.0 T: Comparison of oxygenation-sensitive magnetic resonance imaging. *Magn. Reson. Med.* 2001; 45:595–604.
168. Donahue KM, Van Kylen J, Guven S, El-Bershawi A, Luh W-M, Bandettini PA, Cox RW, Hyde JS, Kissebah AH. Simultaneous gradient-echo/spin-echo EPI of graded ischemia in human skeletal muscle. *J. Magn. Reson. Imaging*. 1998; 8:1106–1113.
169. Versluis B, Backes WH, Van Eupen MGA, Jaspers K, Nelemans PJ, Rouwet E V, Teijink JAW, Mali WPTM, Schurink G-W, Wildberger JE, Leiner T. Magnetic Resonance Imaging in Peripheral Arterial Disease Reproducibility of the Assessment of Morphological and Functional Vascular Status. *Invest. Radiol.* 2011; 46:11–24.
170. Regensteiner JG, Wolfel EE, Brass EP, Carry MR, Ringel SP, Hargarten ME, Stamm ER, Hiatt WR. Chronic changes in skeletal muscle histology and function in peripheral arterial disease. *Circulation*. 1993; 87:413–21.
171. Yamamoto K, Taniguchi R, Hosaka A, Hoshina K, Okamoto H, Shigematsu K, Miyata T. Fate of the asymptomatic contralateral limb after initial intervention for ipsilateral critical limb ischemia. *Int. Angiol.* 2013; 32:526–31.
172. Slade JM, Towse TF, Gossain V V, Meyer RA. Peripheral microvascular response to muscle contraction is unaltered by early diabetes but decreases with age. *J. Appl. Physiol.* 2011; 111:1361–71.
173. Janssen I, Heymsfield SB, Wang ZM, Ross R, Bassey E, Harries U, Baumgartner R, Koehler K, Gallagher D, Romero L, Heymsfield S, Ross R, Garry P, Lineman R, Baumgartner R, Waters D, Gallagher D, Morley J, Garry P, Bemben M, Massey B, Bemben D, Misner J, Boileau R, Beneke R, Neuerburg J, Bohnodrf K, Bevier W, Wiswell R, Pyka G, Kozak K, Newhall K, Marcus R, Borkan G, Hults D, Gerzof S, Robbins A, Silbert C,

Clarys J, Martin A, Drinkwater D, Clement F, Cohn S, Vartsky D, Yasumura S, Sawitsky A, Zanzi I, Vaswani A, Ellis K, Engstrom C, Loeb G, Reid J, Forrest W, Avruch L, Evans W, Flegg J, Lakatta E, Forbes G, Forbes G, Welle S, Frontera W, Meredith C, O'Reilly K, Knuttgen H, Evans W, Gallagher D, Heymsfield S, Gallagher D, Visser M, Meersman R De, Sepúlveda D, Baumgartner R, Pierson R, Harris T, Heymsfield S, Goodpaster B, Kelley D, Ho K, Evans W, Blizzard R, Veldhuis J, Merriam G, Somojlik E, Furlanetto R, Rogol A, Kaiser D, Thorner M, Kehayias J, Fiatarone M, Zhuang H, Roubenoff R, Lexell J, Downham D, Sjostrom M, Lukaski H, Maughan R, Watson J, Weir J, et al. Skeletal muscle mass and distribution in 468 men and women aged 18-88 yr. *J. Appl. Physiol.* 2000; 89:81–8.

174. Olive J, DeVan A, McCully K. The effects of aging and activity on muscle blood flow. *Dyn. Med.* 2002; 1:2.

175. Galbán CJ, Maderwald S, Stock F, Ladd ME. Age-related changes in skeletal muscle as detected by diffusion tensor magnetic resonance imaging. *J. Gerontol. A. Biol. Sci. Med. Sci.* 2007; 62:453–8.

176. Zuo CS, Sung Y-H, Simonson DC, Habecker E, Wang J, Haws C, Villafuerte RA, Henry ME, Dobbins RL, Hodge RJ, Nunez DJR, Renshaw PF. Reduced T2* values in soleus muscle of patients with type 2 diabetes mellitus. *PLoS One*. 2012; 7:e49337.

177. Simons JP, Goodney PP, Nolan BW, Cronenwett JL, Messina LM, Schanzer A. Failure to achieve clinical improvement despite graft patency in patients undergoing infrainguinal lower extremity bypass for critical limb ischemia. *J. Vasc. Surg.* 2010; 51:1419–1424.

178. Carsten CG, Taylor SM, Langan EM, Crane MM. Factors associated with limb loss despite a patent infrainguinal bypass graft. *Am. Surg.* 1998; 64:33-7-8.

179. Dietzek AM, Gupta SK, Kram HB, Wengerter KR, Veith FJ. Limb loss with patent infra-inguinal bypasses. *Eur. J. Vasc. Surg.* 1990; 4:413–7.

180. Rutherford RB. Presidential address: Vascular surgery- Comparing outcomes. *J Vasc Surg*. 1996; 23:5–17.

181. Fisher CM, Burnett A, Makeham V, Kidd J, Glasson M, Harris JP. Variation in measurement of ankle-brachial pressure index in routine clinical practice. *J. Vasc. Surg.* 1996; 24:871–875.

182. White MJ, Thornton JS, Hawkes DJ, Hill DLG, Kitchen N, Mancini L, McEvoy AW, Razavi R, Wilson S, Yousry T, Keevil SF. Design, operation, and safety of single-room interventional MRI suites: practical experience from two centers. *J. Magn. Reson. Imaging*. 2015; 41:34–43.

183. Truwit CL, Hall WA. Intraoperative magnetic resonance imaging-guided neurosurgery at 3-T. *Neurosurgery*. 2006; 58:ONS-338-45; discussion ONS-345-6.

184. Walcher T, Manzke R, Hombach V, Rottbauer W, Wöhrle J, Bernhardt P. Myocardial perfusion reserve assessed by T2-prepared steady-state free precession blood oxygen level-dependent magnetic resonance imaging in

comparison to fractional flow reserve. *Circ. Cardiovasc. Imaging*. 2012; 5:580–6.

185. Tara L. Haas PGLH-TYRLT. Exercise Training and Peripheral Arterial Disease. *Compr. Physiol.* 2012; 2:2933.

186. Robbins JL, Jones WS, Duscha BD, Allen JD, Kraus WE, Regensteiner JG, Hiatt WR, Annex BH, Andersen P, Saltin B, Askew C, Green S, Walker P, Kerr G, Green A, Williams A, Febbraio M, Bartoli V, Dorigo B, Bauer T, Brass E, Nehler M, Barstow T, Hiatt W, Bergstrom J, Brass E, Hiatt W, Brass E, Hiatt W, Green S, Clyne C, Weller R, Bradley W, Silber D, O'Donnell T, Callow A, Duscha B, Annex B, Green H, Pippen A, Kraus W, Duscha B, Kraus W, Keteyian S, Sullivan M, Green H, Schachat F, Pippen A, Brawner C, Blank J, Annex B, Gardner A, Skinner J, Cantwell B, Smith L, Gardner A, Skinner J, Cantwell B, Smith L, Green S, Hammarsten J, Bylund-Fellenius A, Holm J, Schersten T, Krotkiewski M, Hellige G, Ensink F, Baller D, Prennschutz-Schutzenau H, Sigmund-Duchanova H, Zipfel J, Henriksson J, Nygaard E, Andersson J, Eklof B, Hepple R, Mackinnon S, Goodman J, Thomas S, Plyley M, Hiatt W, Regensteiner J, Hargarten M, Wolfel E, Brass E, Hiatt W, Regensteiner J, Wolfel E, Carry M, Brass E, Hiatt W, Wolfel E, Regensteiner J, Brass E, Hirsch A, Haskal Z, Hertzer N, Bakal C, et al. Relationship between leg muscle capillary density and peak hyperemic blood flow with endurance capacity in peripheral artery disease. *J. Appl. Physiol.* 2011; 111:81–6.

187. Halperin JL. Evaluation of patients with peripheral vascular disease. *Thromb. Res.* 2002; 106:V303–V311.

188. Levy BI, Schiffrin EL, Mourad J-J, Agostini D, Vicaut E, Safar ME, Struijker-Boudier HAJ. Impaired tissue perfusion: a pathology common to hypertension, obesity, and diabetes mellitus. *Circulation*. 2008; 118:968–76.

189. Conley JE. Collateral Arterial Circulation in the Legs. *Arch. Surg.* 1960; 81:348.

190. Lawall H, Bramlage P, Amann B. Stem cell and progenitor cell therapy in peripheral artery disease. A critical appraisal. *Thromb. Haemost.* 2010; 103:696–709.

191. Regensteiner JG, Wolfel EE, Brass EP, Carry MR, Ringel SP, Hargarten ME, Stamm ER, Hiatt WR. Chronic changes in skeletal muscle histology and function in peripheral arterial disease. *Circulation*. 1993; 87:413–21.

192. Partovi S, Aschwanden M, Jacobi B, Schulte AC, Walker UA, Staub D, Imfeld S, Broz P, Benz D, Zipp L, Jaeger KA, Takes M, Robbin MR, Huegli RW, Bilecen D. Correlation of muscle BOLD MRI with transcutaneous oxygen pressure for assessing microcirculation in patients with systemic sclerosis. *J. Magn. Reson. Imaging*. 2013; 38.

193. Wacker CM, Hartlep AW, Pfleger S, Schad LR, Ertl G, Bauer WR. Susceptibility-sensitive magnetic resonance imaging detects human myocardium supplied by a stenotic coronary artery without a contrast agent. *J. Am. Coll. Cardiol.* 2003; 41:834–40.

194. Bernhardt P, Manzke R, Bornstedt A, Gradinger R, Spiess J, Walcher D,

Rasche V, Hombach V. Blood oxygen level-dependent magnetic resonance imaging using T2-prepared steady-state free-precession imaging in comparison to contrast-enhanced myocardial perfusion imaging. *Int. J. Cardiol.* 2011; 147:416–9.

195. Pijls NHJ, de Bruyne B, Peels K, van der Voort PH, Bonnier HJRM, Bartunek J, Koolen JJ. Measurement of Fractional Flow Reserve to Assess the Functional Severity of Coronary-Artery Stenoses. *N. Engl. J. Med.* 1996; 334:1703–1708.
196. Lin W, Paczynski RP, Celik A, Hsu CY, Powers WJ. Effects of acute normovolemic hemodilution onT2* - weighted images of rat brain. *Magn. Reson. Med.* 1998; 40:857–864.
197. Lin W, Paczynski RP, Celik A, Hsu CY, Powers WJ. Experimental Hypoxemic Hypoxia: Effects of Variation in Hematocrit on Magnetic Resonance T2*-Weighted Brain Images. *J. Cereb. Blood Flow Metab.* 1998;1018–1021.
198. Guensch DP, Nadeshalingam G, Fischer K, Stalder AF, Friedrich MG. The impact of hematocrit on oxygenation-sensitive cardiovascular magnetic resonance. *J. Cardiovasc. Magn. Reson.* 2016; 18:42.